# Integrated monitoring and structural analysis strategies for the study of large historical construction. Application to Mallorca cathedral

TESIS DOCTORAL

tesis doctoral realizada por:
Ahmed Elyamani Ali Mohamed

dirigida por:
Pere Roca i Fabregat

Barcelona, febrero de 2015

Universitat Politècnica de Catalunya
Departament d´Enginyeria de la Construcció

# CHAPTER 6

# UPDATING OF MALLORCA CATHEDRAL NUMERICAL MODEL

## 6.1 Introduction

In this chapter the updating process of the numerical model of Mallorca cathedral is presented. The attempts made to obtain a best matching between the experimental modal parameters and the numerical ones are addressed. The model updating process has been aimed at improving the model by adjusting some of its input data, for instance, the moduli of elasticity of different materials, the boundary conditions and the influence of the adjacent buildings. The objective has been to obtain a more realistic model that maybe used with confidence in the structural assessment of the cathedral.

## 6.2 Description of the initial FE model

A detailed description of the initial FE model and its mesh can be found at (Martínez, 2007). Here, only a brief description is given with focus on meaningful issues to the current study. The different parts of the cathedral (naves' vaults, arches, columns, walls, buttresses and filling above vaults) were modeled using solid elements consisting of four-node three-side isoparametric solid pyramid. These elements represented approximately 95% of the mesh. The remaining 5% represented the vaults of the apse modeled using three-node triangular isoparametric curved shells. At the base, the three components of the displacement were restrained. The model included 149248 nodes and 491851 elements with total of 490789 degrees of freedom. Some views of the model are shown in Figure 6.1. Among the materials that compose the building, four characteristic materials, already described in chapter 3, are considered in the model. The corresponding properties, refer to chapter 3, are summarized in Table 6.1 . Referring to the last column of Table 6.1, it can be seen that properties of material 1 are expected to be the most influential on the global behavior since it represents three quarters of the total weight of the building. On the other hand, the properties of materials number 3 and 4 are expected to have less effect since they represent together less than 5% of the cathedral weight.

From the model views, it can be noticed that not all parts of the cathedral were modeled. The lateral chapels' vaults and the longitudinal wall connecting all the buttresses were not modeled. Based on the visual inspection (carried out before creating the model) the tower and the two adjacent buttresses were noticed to be connected from the ground level up to level 17m. Above this level up to the buttress top, a narrow separation joint was noticed, Figure 6.2, which suggested that the tower is not connected to the buttresses. However, behind this joint, the tower and the buttresses might be connected.

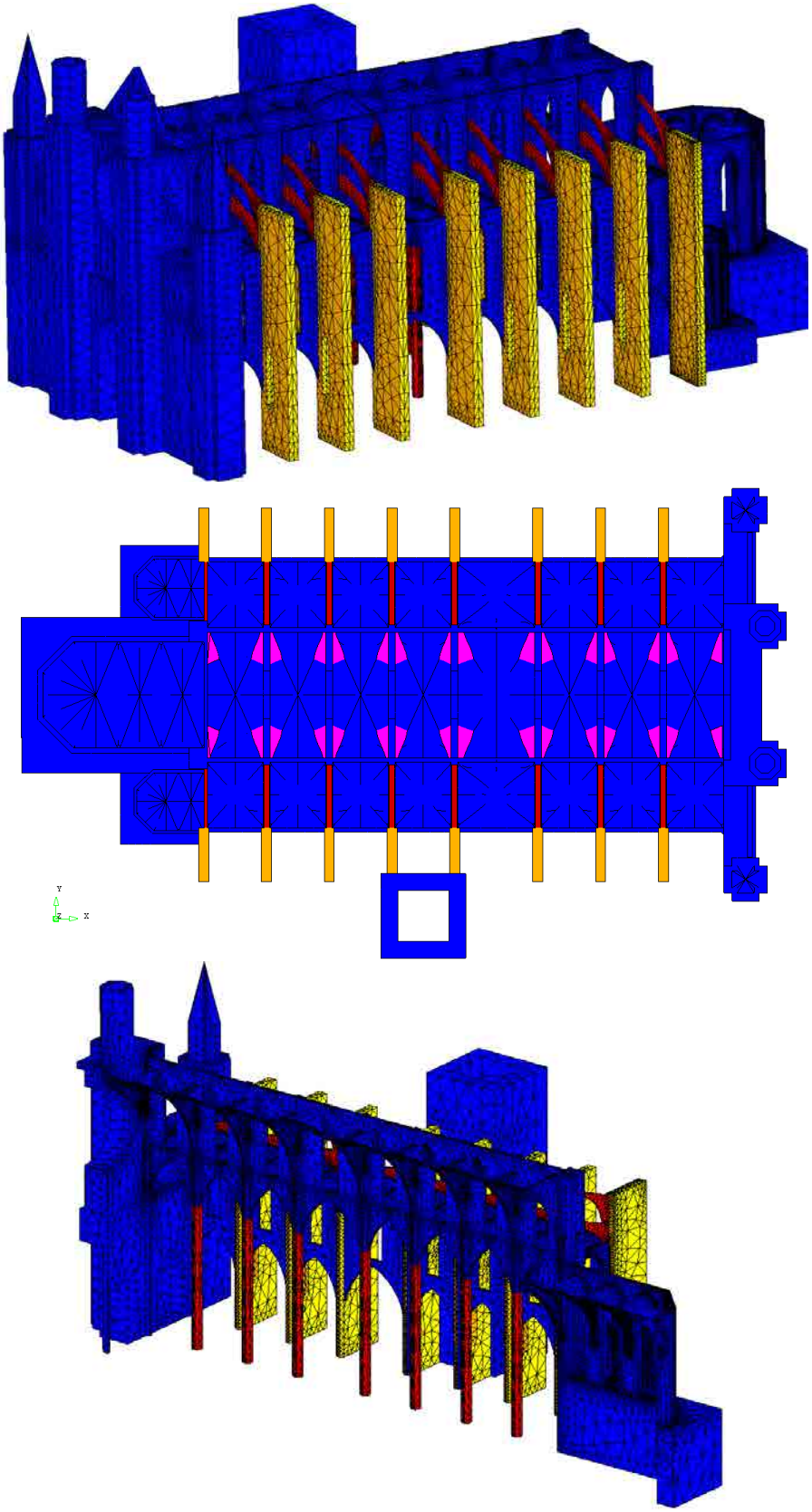

*Figure 6.1. Views of the FE model: complete model (top); plan showing filling above vaults in magenta (center); and longitudinal section (bottom).*

*Table 6.1. Properties of different materials in the FE model.*

| No. & color | Structural parts | Young's Modulus (MPa) | Density (kg/m³) | Poisson's ratio | Total weight of parts / Total weight of cathedral |
|---|---|---|---|---|---|
| 1 | Entire cathedral except the following | 3816 | 2100 | 0,2 | 74 % |
| 2 | Buttresses | 3600 | 2100 | 0,2 | 22 % |
| 3 | Columns and flying arches | 15264 | 2400 | 0,2 | 3 % |
| 4 | Filling over the vaults | 1908 | 2000 | 0,2 | 1 % |

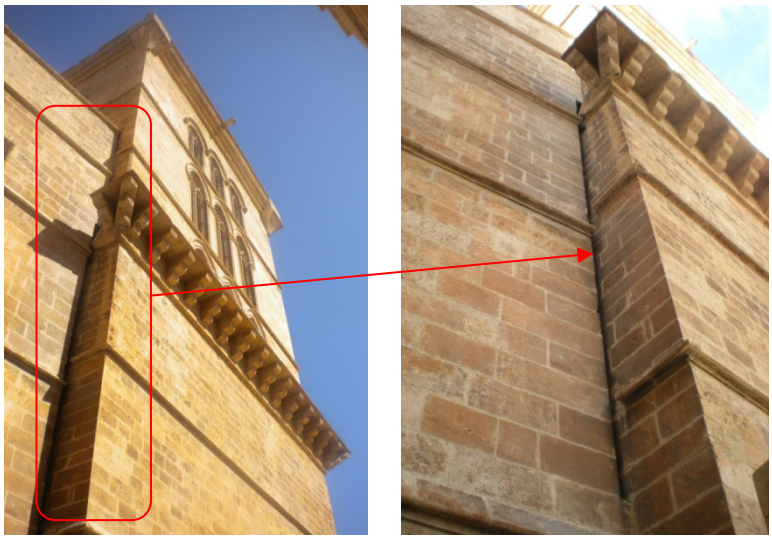

*Figure 6.2. View to the tower-buttress relation (left); and zoom to the separation (right).*

## 6.3 Initial correlation of experimental and numerical modal parameters

The experimental frequencies and mode shapes obtained from the dynamic identification tests and their numerical counterparts were compared using the frequency discrepancy ($D_f$) and the Modal Assurance Criteria (MAC), previously presented in chapter 2. To correlate the experimental and the numerical mode shapes, it was possible to base first on the visual comparison followed by the calculation of the MAC values to have a quantitative measurement of the visual correlation. Also, the closeness between the

experimental and the numerical natural frequencies provided a clear tool for the correlation.

As described in chapter 4, the dynamic identification process allowed the identification of eight experimental modes. The frequencies of all of them were estimated to an acceptable level of accuracy and the mode shapes of modes number 2, 3and 4 only were characterized in a reliable way. The numerical modes (chapter 4, Figure 4.1) and the experimental modes (chapter 4, Figs. 4.15 to 4.22) were correlated. The experimental mode 1 had a combination of longitudinal and transversal movements; therefore, it was associated with the numerical modes 1 and 2. The experimental mode 2 was matched with the numerical mode 1 only because both had a clear longitudinal shape. Similarly, the experimental mode 4and the numerical mode2were matched because of their predominant transversal shape. The numerical modes related to the tower (number 3 and 4) were not matched with any of the experimental ones, since no information was obtained about the tower mode shapes. Also, there was a clear difference in the frequencies values between the numerical modes 3 and 4 and the identified experimental ones. The experimental mode 5 was associated with the numerical modes number 5,6 and 7 to find the best match since it had near frequency value to all of them. The experimental modes number 6 and 7 were correlated to numerical modes number 8 and 9 respectively because they had very close frequency values. Finally, the experimental mode number 8 was correlated to the numerical mode number 10.

The $D_f$ and MAC values for the previous comparisons are summarized in Tables 6.2 and 6.3, respectively. Regarding the comparison of the experimental and the numerical frequencies it can be seen that there was a slight difference between $D_f$ values when considering the sets of “all” or “selected” setups. The definitions of these two sets have been presented in chapter 4. The reason is that the experimental frequencies slightly changed between both sets, as previously mentioned in chapter 4. This was not the case for MAC index. For some modes there was an important difference between the mode shape vectors obtained from the sets of “selected” or “all” setups. For instance, it was clear for the case of experimental mode 2that when considering the set of all setups, very low values were found. On the contrary, when considering only the set of “selected” setups, higher values were obtained. This finding indicated the importance to check well which setups were able to best estimate the mode shape to form a realistic experimental vector, and to exclude those setups that could contaminate the experimental mode shape vector.

*Table 6.2. $D_f$ values for correlation of initial FE model with experimental frequencies.*

| Method | Setups set | Mode type and ID. | | | | | | | | | | |
|---|---|---|---|---|---|---|---|---|---|---|---|---|
| | | Exp. Num. | 1 1 | 1 2 | 2 1 | 3 1 | 4 2 | 5 5 | 5 6 | 5 7 | 6 8 | 7 9 | 8 10 |
| FDD | selected | | 11,1 | 39,3 | 11,3 | 15,5 | 1,5 | 0,9 | 0,1 | 9,0 | 1,7 | 1,7 | 0,4 |
| SSI-cov/ref | all | | 9,3 | 37,0 | 11,4 | 15,9 | 1,0 | 0,8 | 0,1 | 9,1 | 2,5 | 1,0 | 0,7 |
| | selected | | - | - | 11,0 | 16,2 | 1,0 | 1,4 | 0,6 | 8,5 | - | - | - |
| SSI-data/ref | all | | 8,9 | 36,5 | 12,1 | 16,1 | 1,0 | 0,9 | 0,1 | 9,0 | 1,2 | 0,5 | 0,9 |
| | selected | | - | - | 12,3 | 16,0 | 0,9 | 1,4 | 0,6 | 8,5 | - | 1,3 | - |
| pLSCF | all | | 10,9 | 39,0 | 11,2 | 15,8 | 1,0 | 1,0 | 0,2 | 8,9 | 1,6 | 0,6 | 1,1 |
| | selected | | - | - | 10,8 | 15,9 | 1,1 | 1,0 | 0,2 | 8,8 | 1,6 | 1,4 | 1,0 |

*Table 6.3. MAC values for correlation of initial FE model with experimental modes.*

| Method | Setups set | Mode type and ID. | | | | | | | | | | |
|---|---|---|---|---|---|---|---|---|---|---|---|---|
| | | Exp. Num. | 1 1 | 1 2 | 2 1 | 3 1 | 4 2 | 5 5 | 5 6 | 5 7 | 6 8 | 7 9 | 8 10 |
| FDD | selected | | 0,56 | 0,03 | 0,52 | 0,49 | 0,69 | 0,20 | 0,10 | 0,0 | 0,49 | 0,08 | 0,47 |
| SSI-cov/ref | all | | 0,36 | 0,05 | 0,07 | 0,01 | 0,70 | 0,27 | 0,01 | 0,0 | 0,27 | 0,33 | 0,55 |
| | selected | | - | - | 0,89 | 0,62 | 0,72 | 0,03 | 0,01 | 0,01 | - | - | - |
| SSI-data/ref | all | | 0,16 | 0,10 | 0,04 | 0,02 | 0,69 | 0,25 | 0,01 | 0,0 | 0,07 | 0,28 | 0,24 |
| | selected | | - | - | 0,85 | 0,77 | 0,74 | 0,11 | 0,21 | 0,20 | - | 0,67 | - |
| pLSCF | all | | 0,01 | 0,01 | 0,08 | 0,05 | 0,69 | 0,11 | 0,13 | 0,01 | 0,53 | 0,26 | 0,27 |
| | selected | | - | - | 0,88 | 0,79 | 0,73 | 0,03 | 0,04 | 0,0 | 0,60 | 0,14 | 0.36 |

In Table 6.4 the best correlated pair of numerical-experimental modes and the corresponding $D_f$ and MAC values are shown. The two experimental mode shapes that were estimated to a good level of accuracy, i.e., modes 2 and 4 (refer to table 4.12 in chapter 4) have good MAC values 0,89 and 0,74 respectively. This indicated the accuracy of the FE model and its ability to reproduce the real structure. The low MAC values for other modes can be explained because of the difficulty of identifying the corresponding experimental modes as previously discussed in chapter 4. For all modes, except first one, the values of $D_f$ were very low which showed the good distribution of masses and stiffness in the FE model. However, for the first numerical mode, which was a global longitudinal one, the high $D_f$ value (11%) suggested that in the longitudinal direction of the cathedral, the real stiffness was larger than that simulated by the model.

Table *6.5*shows the comparison between the numerical natural frequencies and the experimental ones obtained from the dynamic monitoring system. The $D_f$ values were higher than those for the dynamic identification. As mentioned in chapter 5, the average temperature of the entire monitoring period was much higher than that for the dynamic tests, thus resulted in higher frequencies and $D_f$ values.

*Table 6.4. Best correlated numerical and experimental modes and corresponding Df and MAC values.*

| | | | | | | | |
|---|---|---|---|---|---|---|---|
| Numerical mode ID. | | 1 | 2 | 5 | 8 | 9 | 10 |
| Frequency (Hz) | | 1,270 | 1,592 | 1,924 | 2,269 | 2,414 | 2,638 |
| Experimental mode ID. | | 2 | 4 | 5 | 6 | 7 | 8 |
| Frequency (Hz) | | 1,427 | 1,578 | 1,939 | 2,234 | 2,446 | 2,656 |
| $D_f$ | | 11,0 | 0,9 | 0,8 | 1,6 | 1,3 | 0,7 |
| MAC | | 0,89 | 0,74 | 0,27 | 0,60 | 0,67 | 0,55 |
| Best Result | Method | SSI-cov/ref | SSI-data/ref | SSI-cov/ref | pLSCF | SSI-data/ref | SSI-cov/ref |
| | Setups | Selected | Selected | All | Selected | Selected | All |

*Table 6.5. Comparison between initial FE model frequencies and mean frequencies obtained from the dynamic monitoring system.*

| | | | | | | |
|---|---|---|---|---|---|---|
| Numerical mode ID. | 1 | 2 | 5 | 8 | 9 | 10 |
| Frequency (Hz) | 1,270 | 1,592 | 1,924 | 2,269 | 2,414 | 2,638 |
| Experimental mode ID. | 2 | 4 | 5 | 6 | 7 | 8 |
| Frequency (Hz) | 1,496 | 1,631 | 1,988 | 2,353 | 2,593 | 2,797 |
| $D_f$ | 15,1 | 2,4 | 3,2 | 3,6 | 6,9 | 5,7 |

## 6.4 Model updating procedure

The dynamic identification tests were oriented to capture the global behavior of the cathedral. There were two modes that represented this behavior and were accurately identified. Those were the 1st numerical associated with the 2nd experimental (1Num-2Exp) which was a pure longitudinal mode, and the 2nd numerical associated with the 4th experimental (2Num-4Exp) which was a transversal mode. Consequently, the updating process could be uncoupled so that the 1Num-2Exp mode and the 2Num-4Exp modes could be used to adjust the model in the longitudinal and the transversal directions, respectively. For these modes, Figure 6.3 compares the experimental and the numerical normalized modal displacements (in the X,Y and Z directions) at each dynamic tests' measurement point for the three zones of the cathedral—corresponding to the south,

central and north naves. The places of the points in the tests can be consulted in chapter 4, Figure 4.2.

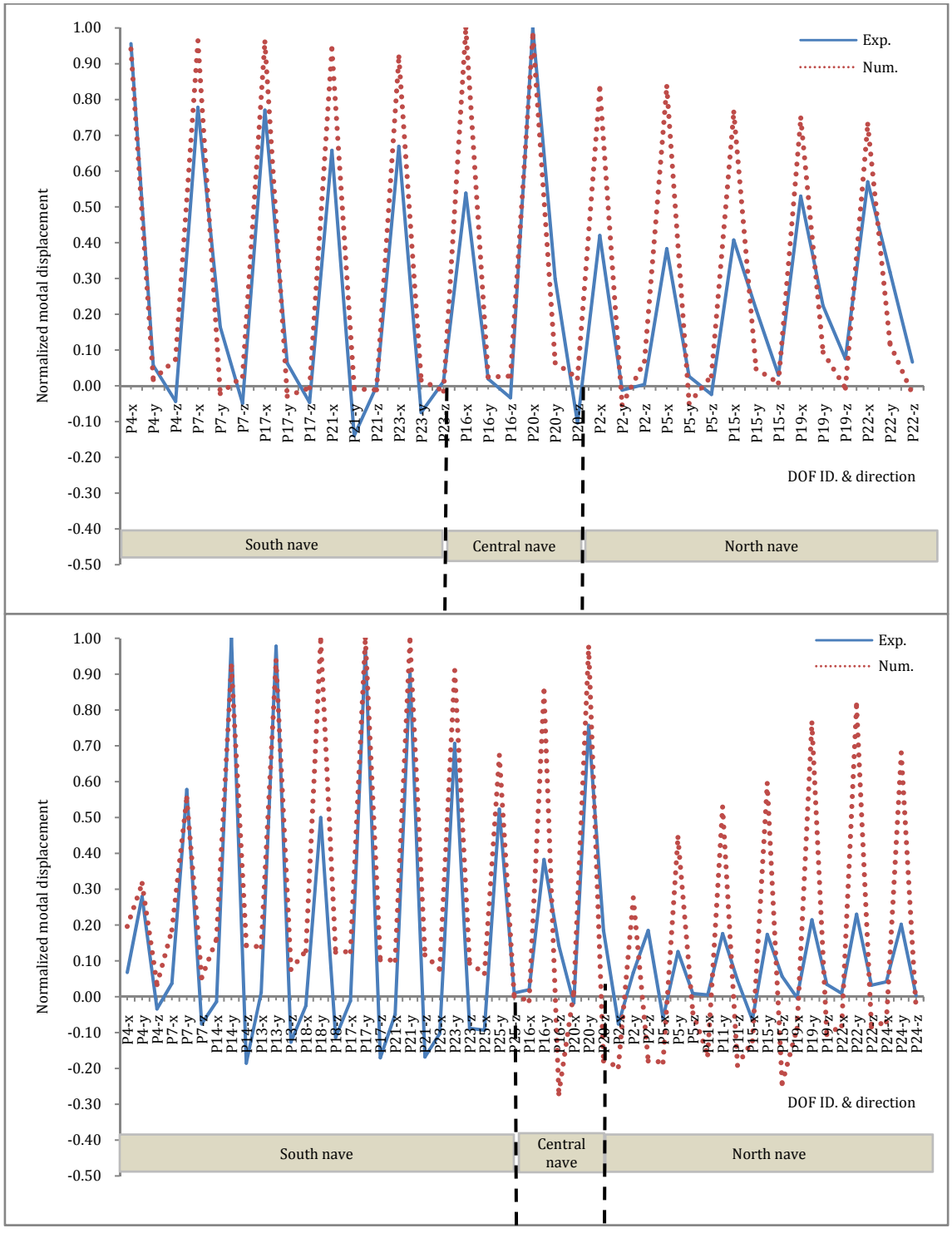


*Figure 6.3. Comparison between mode shapes of 1Num-2Exp (top); and 2Num-4Exp (bottom).*

This comparison allowed better understanding of the correlation between the experimental and the numerical mode shapes and helped in showing the parts of the FE

model that needed updating. As can be noticed in Figure 6.3, from the plot of 1Num-2Exp mode (numerical mode 1 associated with experimental mode 2), it appeared that the numerical-experimental correlation was good for the Y and Z directions. Instead, for the X direction, the model was not well matched with the dynamic tests. This finding beside the high difference between the numerical and experimental frequencies previously pointed out (with $D_f$=11%) raised the need for an updating by adding the missed walls that connected the buttresses. As a consequence, the numerical frequency might increase and became closer to the experimental one.

For the 2Num-4Exp mode, it was possible to note that the north nave showed the lowest correlation in the transversal Y direction. Therefore, it was worth trying to connect the tower with the adjacent buttresses and see the effect. Connecting the tower with the full height of the buttresses might increase the stiffness in the transversal direction. Finally, in the cathedral's structural configuration the buttresses were the main elements providing stiffness in the transversal direction. Accordingly, the modulus of elasticity of their masonry might have significant influence on this mode shape.

Finally, as previously stated in chapters 3 and 4, there was a major crack between the third and the fourth bays. Modeling this crack might also have an influence on the numerical modal parameters. For sake of clarity, the methodology previously described is schematically represented in Figure 6.4. Next, the discussion of the updating process is limited to the modal parameters that were satisfactory experimentally identified, i.e. the frequencies of all modes and the mode shapes of the modes 1Num-2Exp and 2Num-4Exp.

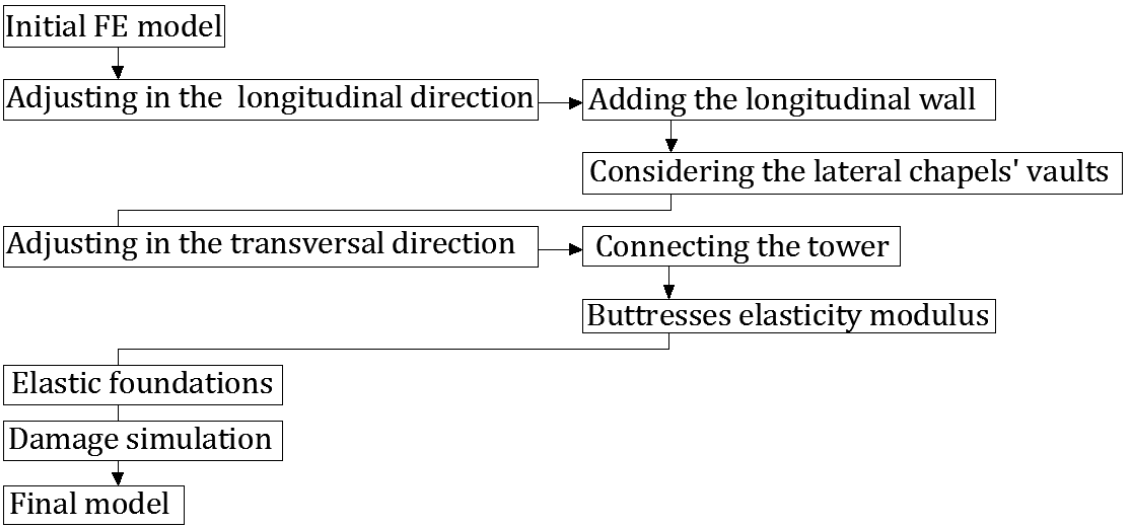


*Figure 6.4. Followed procedure in updating the numerical model.*

### 6.4.1 Adjusting in the longitudinal direction

#### 6.4.1.1 Adding the longitudinal wall

The longitudinal wall connecting all the buttresses was added to the model. The height and the thickness of that wall were obtained from the available drawings. It was given the properties of the material constituted most of the cathedral (material 3 in Table 6.1). It was found that the cathedral stiffness increased and therefore all the modes' frequencies increased, see Table 6.6. Successfully, the $D_f$ of the 1Num-2Exp mode was decreased from 11% to 6,8%. For the rest of the modes, the $D_f$ increased. The highest increase was noticed for the mode 8Num-6Exp. This mode was a local mode in which the two buttresses at the triumphal arch bay were the clearly moving elements. In Figure 6.5 it can be noticed that two more adjacent buttresses showed movement due to the connection introduced by the wall, thus resulting in increasing the frequency. Adding the wall was not so influential on the shapes of any of the first two modes and no significant changes were noticed in the MAC values. Figure 6.6 shows the case of the 1Num-2Exp mode.

*Table 6.6. Comparing the numerical and experimental modes after adding the longitudinal wall.*

| Mode ID. | 1Num-2Exp | 2Num-4Exp | 5Num-5Exp | 8Num-6Exp | 9Num-7Exp | 10Num-8Exp |
|---|---|---|---|---|---|---|
| Num. Frequency (Hz) | 1,330 | 1,668 | 1,986 | 2,516 | 2,592 | 2,732 |
| $D_f$ | 6,8 | 5,7 | 2,4 | 12,6 | 7,4 | 2,9 |
| MAC | 0,89 | 0,71 | 0,24 | 0,30 | 0,80 | 0,55 |

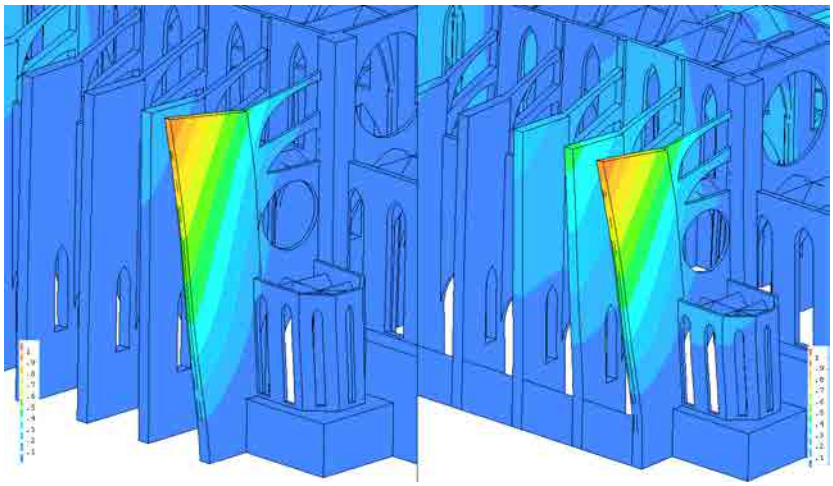

*Figure 6.5. Mode 8: before adding the wall (left); and after adding it (right).*

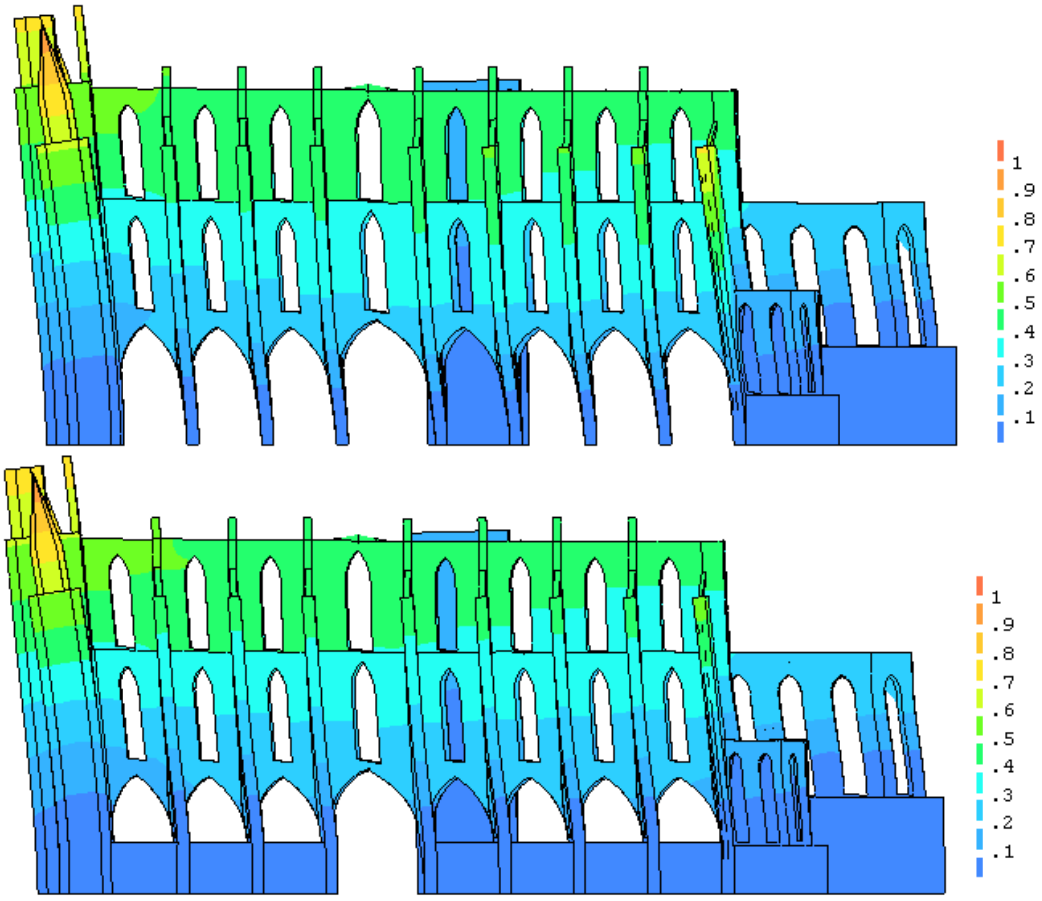


*Figure 6.6. Comparison between 1Num-2Exp mode shape before (top) and after (bottom) adding the longitudinal wall between buttresses.*

#### 6.4.1.2 Considering the lateral chapels' vaults

As mentioned, the vaults of the lateral chapels had not been initially modeled. Therefore, at the level of the vaults springs were added, in a simplified way, to model their effect. All springs had the same stiffness. For any spring, the stiffness was varied from 1E+01 to 1E+06t/m with a step value of 1E+01 t/m. It was noticed that the frequency of the first numerical mode became near to the experimental one in the range from 1E+03 to 1E+04, Figure 6.7 (a). Therefore, three smaller values of 1,25E+03, 2,50E+03 and 5E+03 were tried. It was noticed the lowest $D_f$ value obtained when a spring stiffness of 1,25E+03 t/m was used, Figure 6.7 (b).

In Table 6.7 the $D_f$ and MAC values of all modes are shown. As seen, The $D_f$ of the mode 1Num-2Exp was reduced significantly from that of the previous updating step. However, the $D_f$ of the rest of the modes also increased. Negligible changes in the MAC values of all modes were noticed.

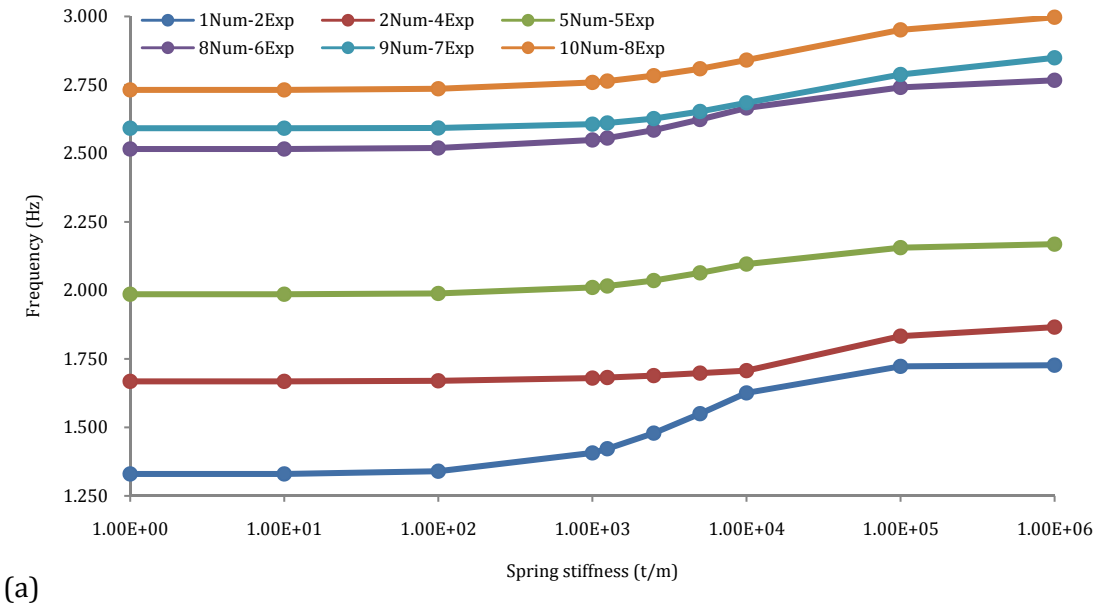


(a)

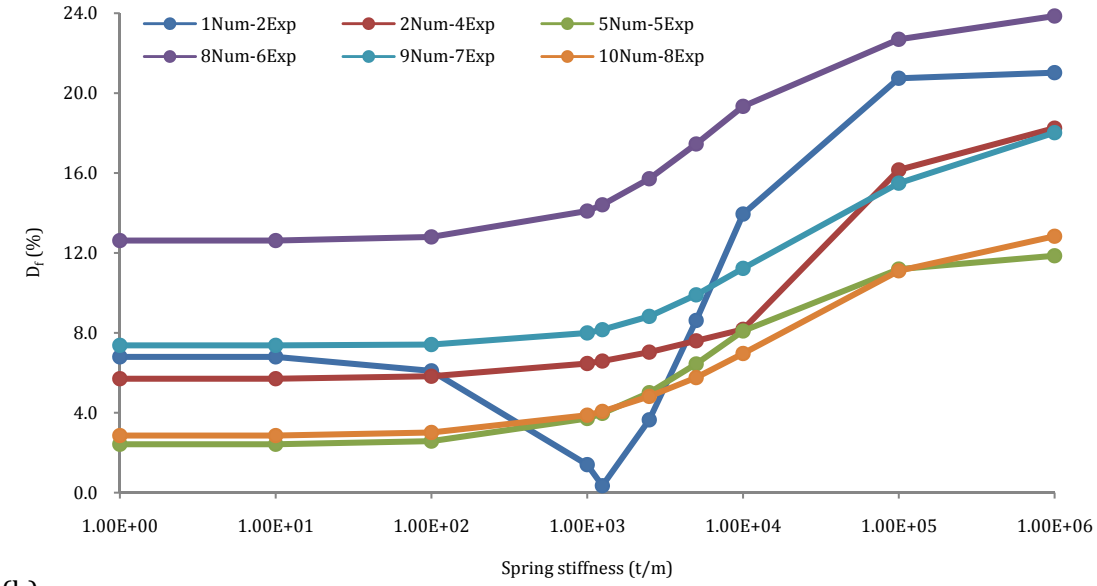


(b)

*Figure 6.7. The effect of lateral chapels' vaults: (a) on frequencies; and (b) on $D_f$.*

*Table 6.7. Comparing the numerical and experimental modes after considering the effect of the lateral chapels' vaults.*

| Mode ID. | 1Num-2Exp | 2Num-4Exp | 5Num-5Exp | 8Num-6Exp | 9Num-7Exp | 10Num-8Exp |
|---|---|---|---|---|---|---|
| Num. Frequency (Hz) | 1,422 | 1,682 | 2,016 | 2,556 | 2,611 | 2,764 |
| $D_f$ | 0,4 | 6,6 | 4,0 | 14,4 | 8,2 | 4,1 |
| MAC | 0,88 | 0,73 | 0,20 | 0,26 | 0,78 | 0,54 |

### 6.4.2 Adjusting in the transversal direction

#### 6.4.2.1 Modifying the tower-cathedral connection

The tower was connected to the full height of the adjacent buttresses aiming at increasing the lateral stiffness that would decrease the north nave modal displacement, hence, improving the match with the experimental mode shape. Nevertheless, the new connection did not reduce the north nave modal displacement. It was noticed only a reduction in the tower modal displacement. Also, the two modes of the tower (numerical modes 3 and 4) manifested increase in frequency from 1,726 and 1,888 to 1,955 and 2,025 Hz, respectively. No improvement in the MAC value of the 2Num-4Exp mode, but on the contrary, the frequency increased to 1,726 Hz which became more far than the experimental one. An increase in $D_f$ for all modes was also noticed, see Table 6.8. Thus, this model tuning was not considered and the tower-cathedral connection returned to its original assumed state.

*Table 6.8. Comparing the numerical and experimental modes after connecting tower with full height of adjacent buttresses.*

| Mode ID. | 1Num-2Exp | 2Num-4Exp | 5Num-5Exp | 8Num-6Exp | 9Num-7Exp | 10Num-8Exp |
|---|---|---|---|---|---|---|
| Num. Frequency (Hz) | 1,435 | 1,726 | 2,161 | 2,578 | 2,621 | 2,801 |
| $D_f$ | 0,5 | 9,4 | 11,4 | 15,4 | 8,6 | 5,5 |
| MAC | 0,89 | 0,74 | 0,13 | 0,15 | 0,80 | 0,53 |

#### 6.4.2.2 Adjusting the elasticity modulus of the buttresses

In this trial a gradual reduction in the modulus of elasticity of the buttresses was followed from 95% to 70% of the original value. In Figure 6.8, the relation between the used reduction factor and the $D_f$ of all the modes is shown. As can be noticed, reducing the modulus of elasticity of the buttresses resulted in reducing the $D_f$ for all the modes, except for the mode 1Num-2Exp. The reduction factor of 75% was considered as an optimized value. At which, four out of the six modes had low $D_f$ values between 0,5 and 2,1 and the other two modes had Df values of 6,4 and 10,9 as summarized in Table 6.9. Negligible changes were noticed in the MAC values for all the modes.

*Table 6.9. Comparing the numerical and experimental modes after reducing the modulus of elasticity of the buttresses.*

| Mode ID. | 1Num-2Exp | 2Num-4Exp | 5Num-5Exp | 8Num-6Exp | 9Num-7Exp | 10Num-8Exp |
|---|---|---|---|---|---|---|
| Num. Frequency (Hz) | 1,404 | 1,611 | 1,974 | 2,478 | 2,569 | 2,669 |
| $D_f$ | 1,6 | 2,1 | 1,8 | 10,9 | 6,4 | 0,5 |
| MAC | 0,88 | 0,75 | 0,16 | 0,29 | 0,77 | 0,54 |

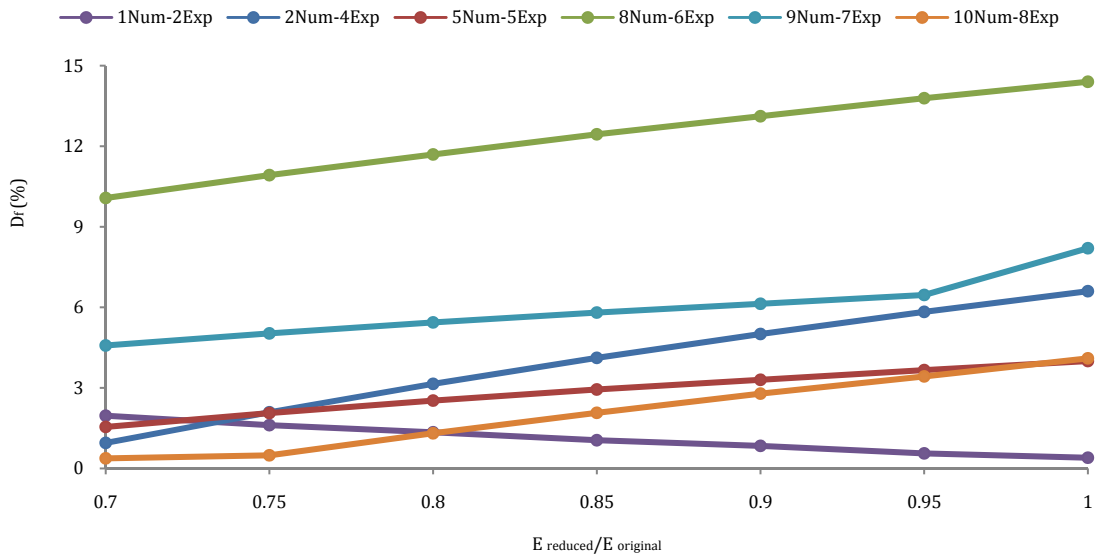


*Figure 6.8. Finding the optimized ratio for reducing elasticity modulus of the buttresses.*

### 6.4.3 Using elastic foundations

The foundations were modeled using elastic springs in the vertical direction (Z) and in the horizontal directions (X and Y). The horizontal stiffnesses of any spring were assumed equal in the X and Y directions and were taken as a ratio from the spring vertical stiffness. As previously presented in chapter 3, most of the cathedral foundations were built on conglomerate rock and only a few of them were built on filling (see section 3.4.6). Therefore, two groups of springs were used, the first one represented the foundations on rock and the second one represented the foundations on filling.

The initial vertical stiffness of any spring assigned to any node was calculated as the product of the soil modulus of subgrade reaction and the tributary area of the node. The modulus of subgrade reactions were taken as 1E10N/m$^3$ for the rock and 1E7N/m$^3$ for the filling, guided by the recommendations given in the soil investigation report (Ingeniería de Sondeos S.A., 2002). The initial average vertical spring stiffness in the rock zone was

6,89E9 N/m and in the filling zone was 5,51E6 N/m. The horizontal stiffness of any spring was taken initially as 10% of the vertical stiffness.

In the updating process, three variables were changed (1) the vertical stiffness of the springs defined for the rock zone, (2) the vertical stiffness of the springs defined for the filling zone, (3) the ratio between the horizontal and the vertical spring stiffness. It should be noted that when changing a variable the other two variables were kept constant.

It was noticed that the second variable was the most pronouncing one on the dynamic behavior. As can be noticed in Figure 6.9, when using the initial value of this variable, and for all modes, the $D_f$ values increased significantly and the MAC values decreased significantly because of the excess flexibility of the cathedral at the filling zone. When increasing it with two orders of magnitude, the $D_f$ values improved for almost all the modes and the MAC values retrieved the values of the previous updating step (adjusting the modulus of elasticity of buttresses).

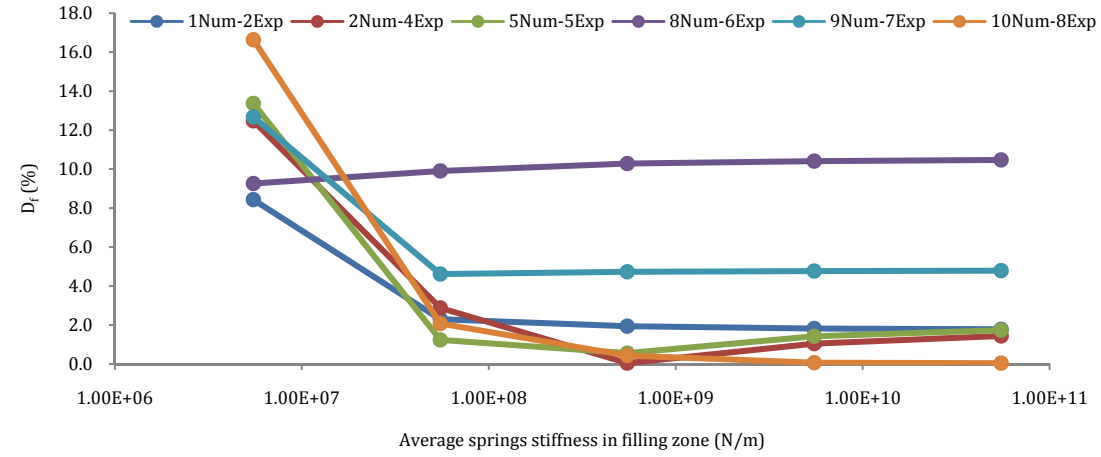


(a)

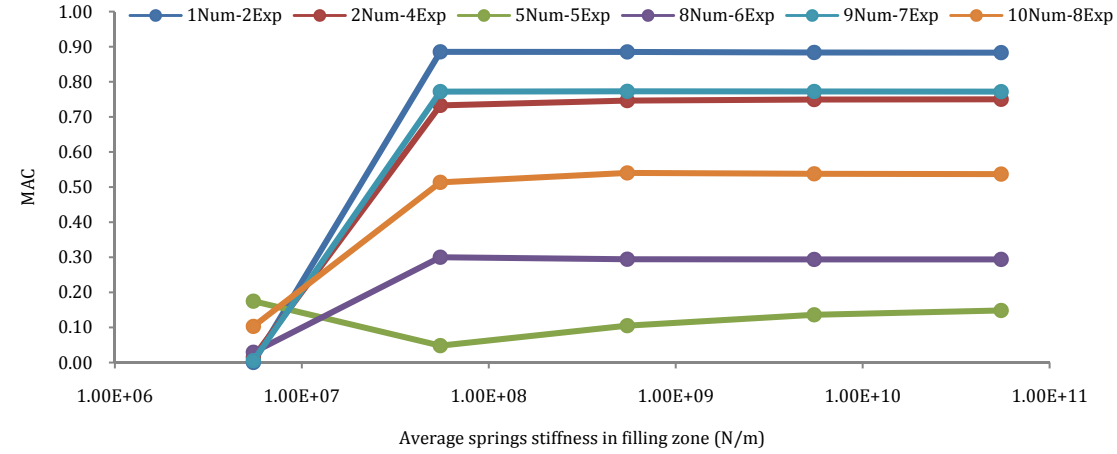


(b)

*Figure 6.9. Effect of changing the average spring stiffness in the filling zone on: (a) $D_f$; and (b) MAC.*

For the first variable, increasing the initial value with two orders of magnitude, improved slightly the $D_f$ values. For the last variable when using values more than 10%, no changes occurred in the $D_f$ and MAC values for all modes. Summarizing, the best values for the average spring stiffness in the rock zone was 6,89E11 N/m and in the filling zone was 5,51E8 N/m and the horizontal stiffness was 10% of the vertical stiffness for any spring in the two zones. Table 6.10 reports the matching after using the elastic foundations. As can be noticed, all the frequencies slightly decreased from the previous updating step and this improved the matching, in particular, for the modes 2Num-4Exp and 5Num-5Exp.

*Table 6.10. Comparing the numerical and experimental modes after using elastic foundations.*

| Mode ID. | 1Num-2Exp | 2Num-4Exp | 5Num-5Exp | 8Num-6Exp | 9Num-7Exp | 10Num-8Exp |
|---|---|---|---|---|---|---|
| Num. Frequency (Hz) | 1,399 | 1,577 | 1,950 | 2,464 | 2,562 | 2,645 |
| $D_f$ | 1,9 | 0,1 | 0,6 | 10,3 | 4,7 | 0,4 |
| MAC | 0,89 | 0,75 | 0,11 | 0,29 | 0,77 | 0,54 |

### 6.4.4 Damage simulation

The last updating trial was to simulate the damage experienced by the cathedral. Among the most significant damage was the cracking that can be seen in many places as previously discussed in chapter 3. One of the significant cracks is the one located between the third arch and the fourth vault from the west façade, Figure 6.10. It was previously monitored for a period of about five years and proved to be active with a rate of 1cm/century (Godde, 2009).


*Figure 6.10. Photos for the crack between third arch and fourth vault. In the left photo a zoom is made to the static monitoring sensor.*

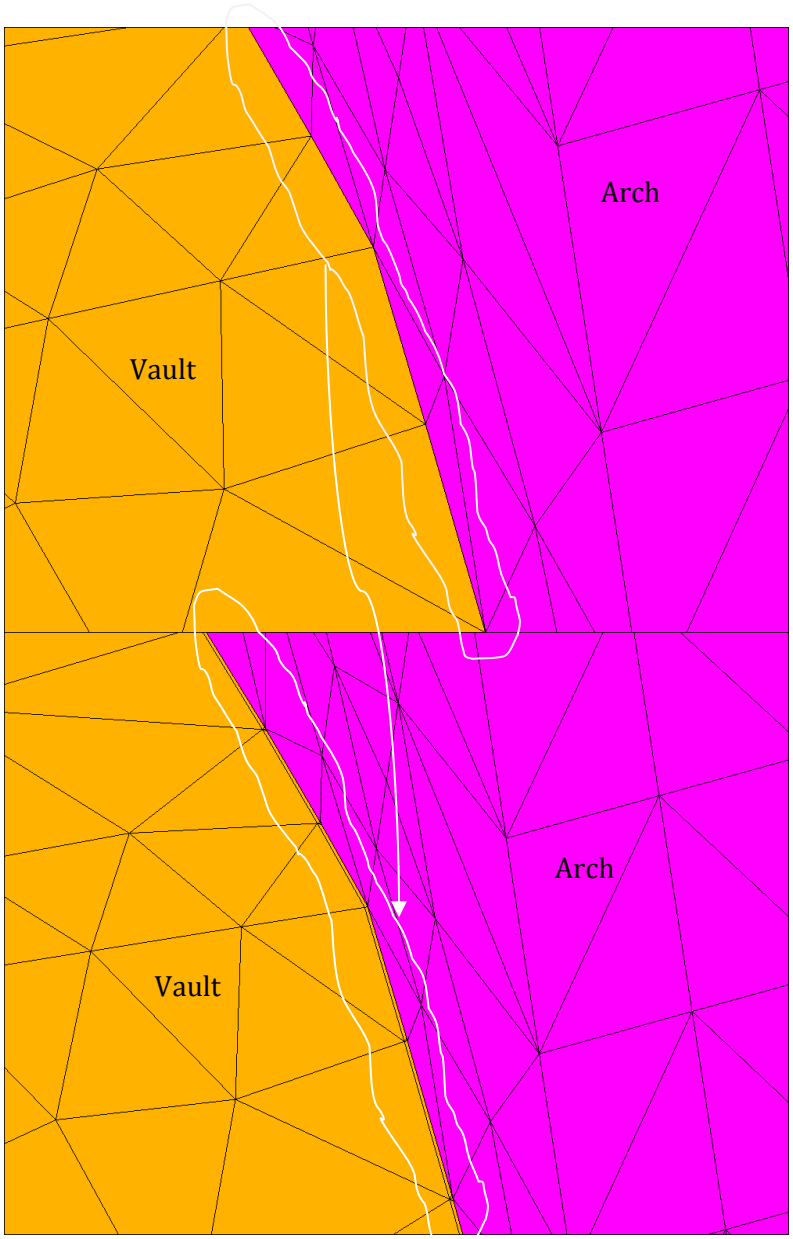


*Figure 6.11. The numerical modeling of the crack by doubling the nodes. Before simulating the crack (top); and after simulating the crack (bottom).*

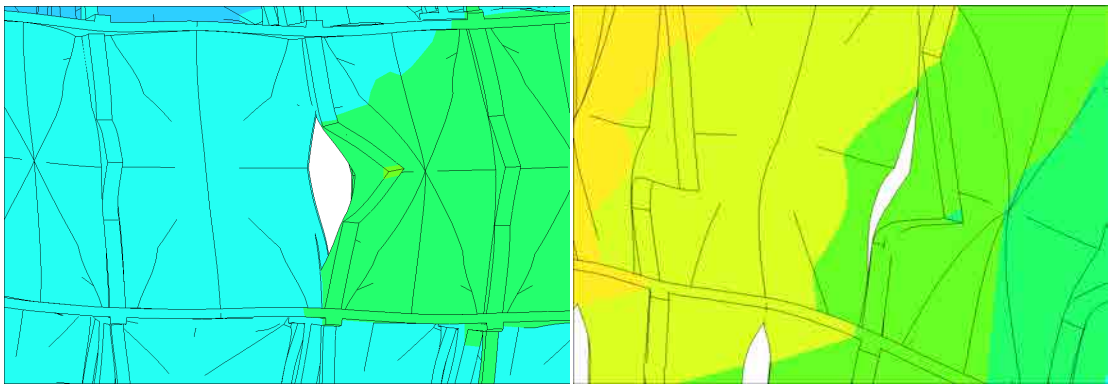

*Figure 6.12. Zoom at the crack location in the first mode (left); and the second mode (right).*

To simulate the crack in the numerical model, a separation between the arch and the vault was made by doubling the nodes located at their contact line. At the contact line, the nodes belonging to the arch mesh were kept and new nodes were defined for the vault mesh, as shown in Figure 6.11. The arch original nodes and the vault new nodes had the same X and Z coordinates, but in the Y direction they were spaced 1 mm. This modeling approach allowed to reproduce the crack effect as can be seen in Figure 6.12 for the first two numerical modes.

Due to the large size of the model, this local crack did not show any significant effect neither on the natural frequencies nor on the mode shapes. The same values for $D_f$ and MAC of the previous updating step were obtained with the cracked model.

### 6.4.5 Final FE model after updating

Finishing with the updating process, the model of the section 6.4.3was considered as the final one. Table 6.11 summarizes the comparison in terms of $D_f$ and MAC values between the final model and the dynamic identification as well as the dynamic monitoring. Comparing with the dynamic identification frequencies, the final model showed good $D_f$ values around 2% or less for four out of the six modes. Three from these four modes were global modes; those are: 1Num-2Exp; 2Num-4Exp and 10Num-8Exp. The two modes that exhibit relatively high $D_f$ values were local ones. This in turn showed the good ability of the model to reproduce the real global dynamic behavior of the cathedral. Regarding the MAC values, the two reliable experimental modes number 2 and 4 were in good correlation with their numerical counterpart number 1 and 4with MAC values of 0,89 and 0,75 respectively. The MAC values for other modes were not significant because of their poor experimental identification.

*Table 6.11. Comparing the numerical frequencies with the dynamic tests and the dynamic monitoring frequencies.*

| Mode ID. | | 1Num-2Exp | 2Num-4Exp | 5Num-5Exp | 8Num-6Exp | 9Num-7Exp | 10Num-8Exp |
|---|---|---|---|---|---|---|---|
| Num. Frequency (Hz) | | 1,399 | 1,577 | 1,950 | 2,464 | 2,562 | 2,645 |
| Dynamic tests | Frequency (Hz) | 1,427 | 1,578 | 1,939 | 2,234 | 2,414 | 2,656 |
| | $D_f$ | 1,9 | 0,1 | 0,6 | 10,3 | 4,7 | 0,4 |
| Dynamic monitoring | Frequency (Hz) | 1,496 | 1,631 | 1,988 | 2,353 | 2,593 | 2,797 |
| | $D_f$ | 6,5 | 3,3 | 1,9 | 4,7 | 1,2 | 5,4 |

The comparison of the frequencies of the final model with those of the dynamic monitoring showed a good agreement with half of the modes had a $D_f$ value around 3% or less and the other half had a $D_f$ value around 6% or less, with average of 3,8% when considering all the modes. This result showed clearly that the final model was improved with respect to the initial one and could be used in the following phases in the structural assessment process.

The first ten mode shapes of the final model are plotted in Figure 6.13. When comparing those modes with their initial counterpart plotted in Figure 4.1 of chapter 4, it can be noticed that the modes 1,2,3,7 and 10 kept their initial shapes as their MAC values were near 1. The remaining modes exhibited changes. The first updating step was behind these changes because this step resulted in connecting all the buttresses together which subsequently changed the buttresses' movement and thus changed the full mode shapes.

Figure 6.14 compares the experimental frequencies and the frequencies of the initial and the final models. It can be noticed for the first two modes that negligible changes occurred in the MAC values. For the initial model, the frequencies of five modes were very near to the experimental frequencies (their dots laid on the 45° line). For the final model, the frequencies of four modes laid on the 45° line. The important gain from updating the initial model is in the reduction of the $D_f$ of the first mode from 11,0% to only 1,9% while keeping the same MAC value. This mode was the one with the highest mass participation factor among all modes (about 60% in longitudinal direction). However, for the local modes number 8 and 9 the $D_f$ values increased from 1,6 and 1,3 to 10,3% and 4,7%, respectively.

The change in the $D_f$ and MAC values after each updating step is shown in Figure 6.15. It can be seen that the first two updating steps increased the $D_f$ for all modes except the 1Num-2Exp mode. The step of reducing the modulus of elasticity of the buttresses improved all modes except 1Num-2Exp. In addition, this step uniformed the $D_f$ value for all the modes (except 8Num-6Exp and 9Num-7Exp) at about 2%. The MAC values of the modes 1Num-2Exp and 2Num-4Exp did not suffer from significant changes during the updating process.

An evaluation of the initial correlation (Tables 6.2 and 6.3) was carried out by recalculating the $D_f$ and MAC values between the experimental modes and their counterpart numerical ones as summarized in Tables 6.11 and 6.12. It can be noticed that the initial correlation was correct and no changes in any of the initial correlation decisions were required.

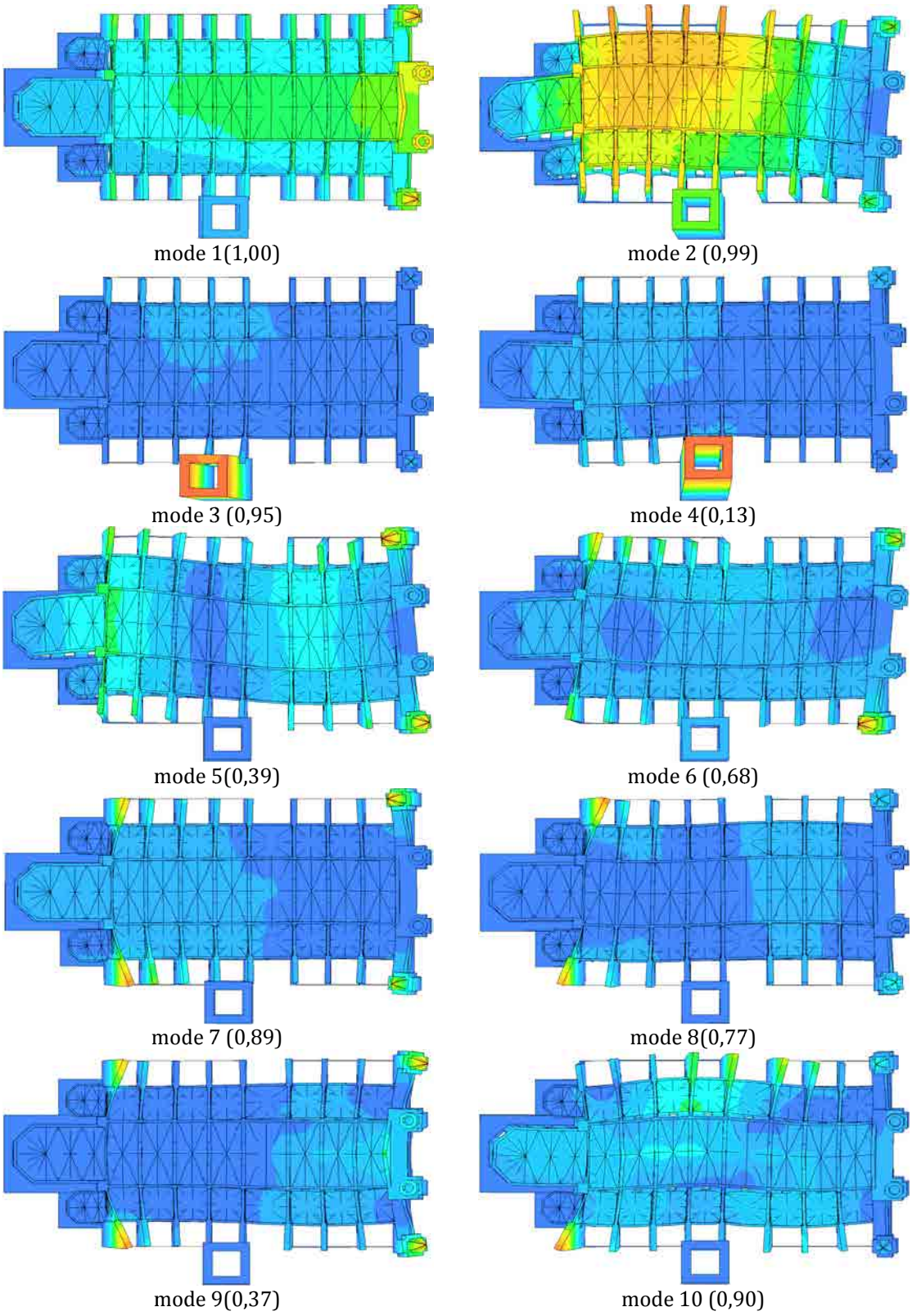


*Figure 6.13. The first ten mode shapes after updating. In parentheses MAC value between the initial and the final models.*

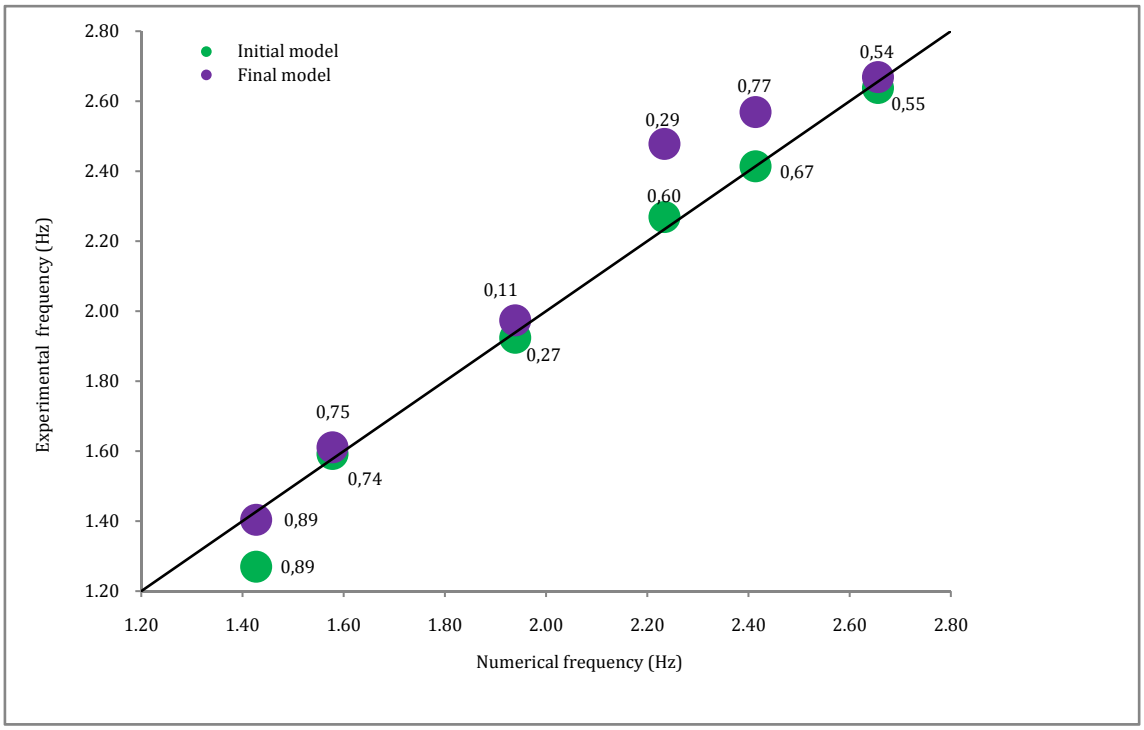


*Figure 6.14. Comparison between the experimental frequencies and the frequencies of the initial and the final models, the MAC values are shown beside the dots.*

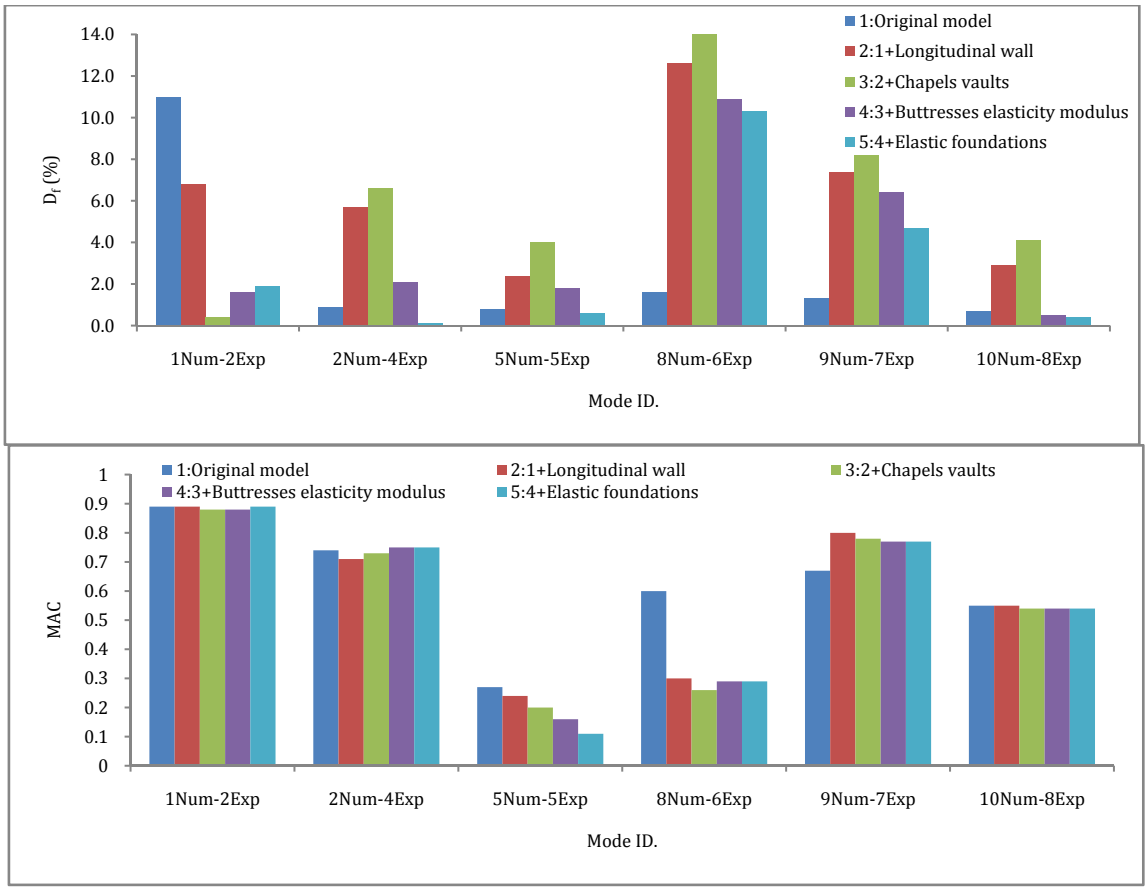


*Figure 6.15. The changes in $D_f$ (top); and MAC (bottom) with the updating steps.*

*Table 6.12. Confirmation of the initial correlation using $D_f$ values .*

| Method | Setups set | Mode type and ID. | | | | | | | | | | |
|---|---|---|---|---|---|---|---|---|---|---|---|---|
| | | Exp. Num. | 1 1 | 1 2 | 2 1 | 3 1 | 4 2 | 5 5 | 5 6 | 5 7 | 6 8 | 7 9 | 8 10 |
| FDD | selected | | 22,4 | 38,0 | 2,2 | 6,9 | 0,5 | 0,4 | 5,2 | 17,9 | 10,4 | 6,5 | 0,2 |
| SSI-cov/ref | all | | 20,4 | 35,7 | 2,4 | 7,4 | 0,1 | 0,6 | 5,3 | 18,1 | 11,3 | 5,8 | 0,4 |
| | selected | | - | - | 1,9 | 7,7 | 0,0 | 0,1 | 4,7 | 17,4 | - | - | - |
| SSI-data/ref | all | | 20,0 | 35,3 | 3,2 | 7,6 | 0,1 | 0,4 | 5,2 | 17,9 | 9,9 | 5,2 | 0,7 |
| | selected | | - | - | 3,4 | 7,5 | 0,1 | 0,1 | 4,7 | 17,4 | - | 6,1 | - |
| pLSCF | all | | 22,2 | 37,7 | 2,1 | 7,3 | 0,1 | 0,4 | 5,1 | 17,9 | 10,3 | 5,3 | 0,8 |
| | selected | | - | - | 1,7 | 7,4 | 0,1 | 0,3 | 5,1 | 17,8 | 10,3 | 6,2 | 0,8 |

*Table 6.13. Confirmation of the initial correlation using MAC values.*

| Method | Setups set | Mode type and ID. | | | | | | | | | | |
|---|---|---|---|---|---|---|---|---|---|---|---|---|
| | | Exp. Num. | 1 1 | 1 2 | 2 1 | 3 1 | 4 2 | 5 5 | 5 6 | 5 7 | 6 8 | 7 9 | 8 10 |
| FDD | selected | | 0,54 | 0,06 | 0,50 | 0,45 | 0,71 | 0,00 | 0,16 | 0,02 | 0,39 | 0,01 | 0,43 |
| SSI-cov/ref | all | | 0,33 | 0,07 | 0,05 | 0,00 | 0,71 | 0,16 | 0,00 | 0,01 | 0,25 | 0,13 | 0,54 |
| | selected | | - | - | 0,89 | 0,62 | 0,72 | 0,13 | 0,06 | 0,02 | - | - | - |
| SSI-data/ref | all | | 0,13 | 0,12 | 0,03 | 0,01 | 0,71 | 0,02 | 0,05 | 0,01 | 0,02 | 0,03 | 0,22 |
| | selected | | - | - | 0,84 | 0,76 | 0,75 | 0,21 | 0,00 | 0,19 | - | 0,77 | - |
| pLSCF | all | | 0,01 | 0,01 | 0,06 | 0,03 | 0,71 | 0,01 | 0,18 | 0,05 | 0,36 | 0,03 | 0,24 |
| | selected | | - | - | 0,88 | 0,77 | 0,75 | 0,08 | 0,06 | 0,02 | 0,29 | 0,12 | 0,30 |

## 6.5 Conclusions

The chapter presented the updating process of the numerical model of Mallorca cathedral. The process aimed at improving the initial model in order to attain a higher level of confidence in the following phases of the seismic assessment of the cathedral.

In an initial step, the experimental and numerical modes were correlated. Half of the experimental modes were easily correlated with their numerical counterparts and the other half had to be tried with many numerical modes. The numerical modes that showed the lowest $D_f$ and the highest MAC values were initially correlated with their experimental correspondent.

The updating process was uncoupled so that the longitudinal direction was first adjusted and then the transversal one. In the longitudinal direction, it was found that adding the longitudinal wall that connects all the buttresses and also introducing the effect of the lateral chapels' vaults improved the model. In the transversal direction, adjusting the elasticity modulus of the buttresses improved the model. Using elastic foundations instead of rigid ones, improved the matching of the numerical and experimental frequencies. The simulation of the damage did not help in matching the numerical and the experimental results.

This page is intentionally left blank.

# CHAPTER 7

# SEISMIC ASSESSMENT OF MALLORCA CATHEDRAL

## 7.1 Introduction

This chapter discusses the phase of the seismic assessment of Mallorca cathedral. For that purpose, different analysis methods were used. Nonlinear static (pushover) analysis was firstly carried out. To reveal the dependency of results on the input material properties, a sensitivity analysis was performed. Then, the numerical results were compared with the results of the kinematic limit analysis as a way to cross check the seismic safety assessment. For evaluation of the seismic performance of the cathedral, the N2 method was employed. Although for such a large historical structure, the nonlinear time-history (dynamic) analysis seemed to be very time consuming, an attempt to perform this type of advanced analysis was carried out. The results and conclusions of this phase were the base for the seismic strengthening intervention proposals.

## 7.2 Constitutive model and properties of materials

To simulate the nonlinear behavior of the masonry, both cracking (tensile regime) and crashing (compressive regime) were considered. Tensile regime was modeled using smeared cracking, in specific, multi-directional fixed crack model. In this model cracking was specified as a combination of tension cut-off (Figure 7.1 a), tension softening (Figure 7.1-b), and shear retention. Compressive regime was modeled using isotropic plastic Drucker-Prager model.

Some of the properties of the materials have been already mentioned in chapter 6, Table 6.1. In Table 7.1 the rest of the used properties of materials are presented. The compressive strength $f_c$ of the first three materials were taken as found by González and Roca (2003) who carried out compressive tests on samples of the stone. For the filling material a low compressive strength was assumed. The values of the ultimate crack strain $\varepsilon_u^{cr}$ were assumed so that the four materials had near tensile fracture energies.

For all the materials, the tensile strength $f_t$ was assumed as 5% of $f_c$, the shear retention factor was taken as 0,01 and the two angles of internal friction and dilatancy were assumed equal (associated plasticity) with a value of 10°. Those values were reasonably assumed based on studies on similar historical construction.

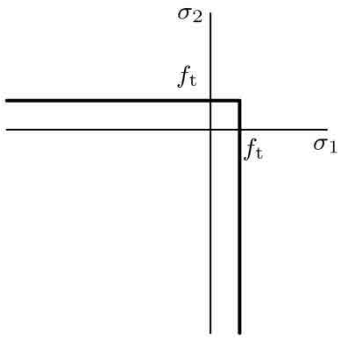


σ1 and σ2 are the two-dimensional principal stresses.

*(a)*

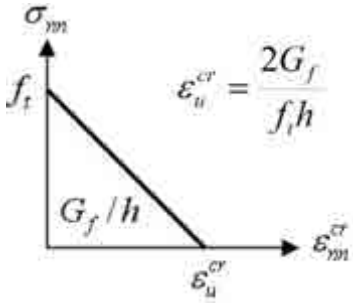


Gf is the fracture energy in tension, $\varepsilon_u^{cr}$ is the ultimate crack strain, h is the crack band width taken as the cubic root of the element volume.

*(b)*

*Figure 7.1. Representation of (a) tension cut-off and (b) tension softening (DIANA, 2009).*

*Table 7.1. Properties of the different materials in the FE model.*

| Material No. & structural elements | (1) All the cathedral except the following | (2) Buttresses | (3) Columns and flying arches | (4)Filling over vaults |
|---|---|---|---|---|
| $f_c$ (MPa) | 2 | 2 | 8 | 1 |
| $\varepsilon_u^{cr}$ (%) | 0,40 | 0,43 | 0,10 | 0,81 |

## 7.3 Characterization of the seismic demand

The seismic demand was characterized using two codes: the Spanish code for seismic design (NCSE-02, 2002) and the Eurocode 8 (EC-08) (CEN, 2004).

### 7.3.1 Characterization of the seismic demand according to NCSE-02

The Spanish code defines the seismic calculations acceleration ($a_c$) as:

$a_c = S\ \rho\ a_b$ *Equation 7.1*

where:

- $a_b$ is the basic seismic acceleration. The code value of 0,04g is used (mentioned in annex 1 for Palma de Mallorca zone).

- ρ is a coefficient considers the importance of the building and it considers tacitly the return period. ρ =1 and 1,3 for 475 and 975 years respectively.

- S is the coefficient of the soil amplification. It is calculated from one of the following three expressions:

For $\rho\, a_b \leq 0{,}1g$ $$S = \frac{C}{1{,}25}$$ *Equation 7.2*

For $0{,}1g < \rho\, a_b < 0{,}4g$ $$S = \frac{C}{1{,}25} + 3{,}33\left(\rho \cdot \frac{a_b}{g} - 0{,}1\right)\left(1 - \frac{C}{1{,}25}\right)$$ *Equation 7.3*

For $0{,}4g \leq \rho\, a_b$ $$S = 1{,}0$$ *Equation 7.4*

In the above expressions C is the soil coefficient which equals 1,6 for the soil underneath the cathedral because it is considered a soil of type III with shear wave velocity between 200 and 400 m/s. More details about the cathedral's foundation soil were discussed in chapter 3. S is calculated as 1,28 for the two considered return periods.

Substituting the values of S, $a_b$ and ρ in Equation 7.1, the acceleration $a_c$ becomes equal to 0,051g and 0,067g for 475 and 975 years, respectively.

Then to determine the response spectrum, $a_c$ is multiplied by the normalized elastic spectrum of the code which has three branches defined by:

If $T < T_A$ $$\alpha\,(T) = 1 + 1{,}5 \cdot T/T_A$$ *Equation 7.5*

If $T_A \leq T \leq T_B$ $$\alpha\,(T) = 2{,}5$$ *Equation 7.6*

If $T > T_B$ $$\alpha\,(T) = K \cdot C/T$$ *Equation 7.7*

where:

α (T) is the value of the normalized response spectrum for 5% critical damping. T is the fundamental period of the structure in seconds. K is the coefficient of contribution, takes the value of 1 (annex 1 for the zone of Palma de Mallorca). TA and TB are calculated by means of the following equations: TA = K·C/10=0,16 s, and TA = K·C/2,5=0,64 s. The two response spectra are shown in Figure 7.2.

### 7.3.2 Characterization of the seismic demand according to EC-08

The Eurocode 8 (CEN, 2004) defines the horizontal response spectrum $S_e$ (T) of the horizontal component of the seismic action by the following expressions:

$0 \leq T \leq T_B: S_e(T) = a_g \cdot S \cdot [1 + \frac{T}{T_B} \cdot (\eta \cdot 2{,}5 - 1)]$ *Equation 7.8*

$T_B \leq T \leq T_C: S_e(T) = a_g \cdot S \cdot \eta \cdot 2{,}5$ *Equation 7.9*

$T_C \leq T \leq T_D: S_e(T) = a_g \cdot S \cdot \eta \cdot 2{,}5 \frac{T_C}{T}$ *Equation 7.10*

$T_D \leq T \leq 4s: S_e(T) = a_g \cdot S \cdot \eta \cdot 2{,}5 \cdot \left[\frac{T_C \cdot T_D}{T^2}\right]$ *Equation 7.11*

where

- $S_e$ (T) is the elastic response spectrum;

- T is the vibration period of a linear single-degree-of-freedom system;

- $a_g$ is the design ground acceleration on type A ground ($a_g = \gamma_1.a_{gR}$. $\gamma_1$ is the importance factor and $a_{gR}$ is the reference peak ground acceleration on type A ground);

- $T_B$ is the lower limit of the period of the constant spectral acceleration branch;

- $T_c$ is the upper limit of the period of the constant spectral acceleration branch;

- $T_D$ is the value defining the beginning of the constant displacement response range of the spectrum;

- S is the soil factor;

- η is the damping correction factor with a reference value of η = 1 for 5% viscous damping.

$a_{gR}$ is 0,04g as defined in NCSE-02. The reference return period of the EC-08 is 475 years for which the $\gamma_1$ =1, so $a_g$ =0,04g. For 975 years return period, $\gamma_1$ is calculated from the relation given in item 2.1(4) of the code: $\gamma_1 \sim (475/975)^{-1/3} = 1{,}27$, so $a_g$ =0,051g. The soil type is B, so S = 1.2; $T_B$ = 0.15 sec; $T_C$ = 0.5 sec; and $T_D$ = 2 sec. Figure 7.2 shows the two response spectra.

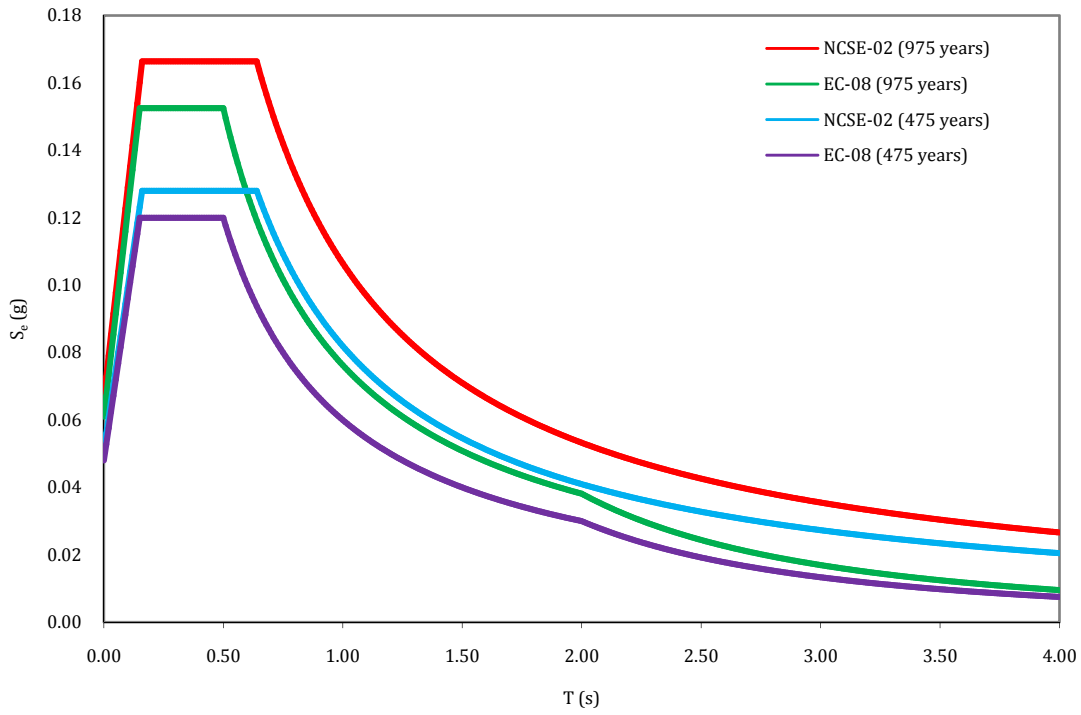


*Figure 7.2. The elastic response spectrum Se (g) using the Eurocode 8 (EC8) and the Spanish code NCSE-02.*

## 7.4 Nonlinear static analysis

### 7.4.1 Introduction

In the nonlinear static (pushover) analysis a monotonically increasing horizontal load was applied under constant gravity load. The horizontal load distribution adopted was a uniform load proportional to the structural elements' masses. The cathedral was subjected to the seismic loads in the longitudinal (X-direction) and the transversal (Y-direction) considering both the positive and the negative sings. The procedure is well known and is proposed by both of EC-08 and NCSE-02.

The structure showed different seismic capacities depending on the direction of the applied seismic forces whether transversal or longitudinal. In the transversal direction, the structure resisted seismic loads thanks to the stiffness of the eight frame-like structures composed by the piers, the diaphragmatic arches, the flying arches and the buttresses; the west façade and the stiff walls at the apse area. These frames showed large capacity when the forces were applied in its more resistant (in plane) direction, and thus the cathedral showed higher capacity. In the longitudinal direction, the loading of the buttresses and the façade occurred in the direction perpendicular to their plane therefore caused a lower seismic capacity.

For plotting a representative capacity curve of the structure, the choice of only a single control point that could represent the actual capacity was a challenging task. Therefore, four control points were selected. The first point was the center of gravity of the full cathedral (CG-cathedral), the second was the center of gravity of the naves' roof (CG-roof), the third was the point with the highest elevation (Top) which located at the top of the gable of the west facade, and finally the point with the maximum displacement (Max-D) in the direction under consideration. The seismic responses in each of the studied directions are discussed hereinafter.

### 7.4.2 The seismic response in the longitudinal (±X) direction

#### 7.4.2.1 In (+X) direction

The obtained capacity curve in this direction is presented in Figure 7.3. The point Top was found to be also the one with the highest displacement. It can be noticed that the curves' start point was not at zero displacement, because the gravity loads were applied first followed by the seismic loads. From the capacity curve, it was observed that the behavior was linear up to a load value of about 0,040g and the collapse occurred at 0,114g.

Four different points on the curves were selected to follow the collapse progression, those were the points from (a) to (d) as shown on the curve.

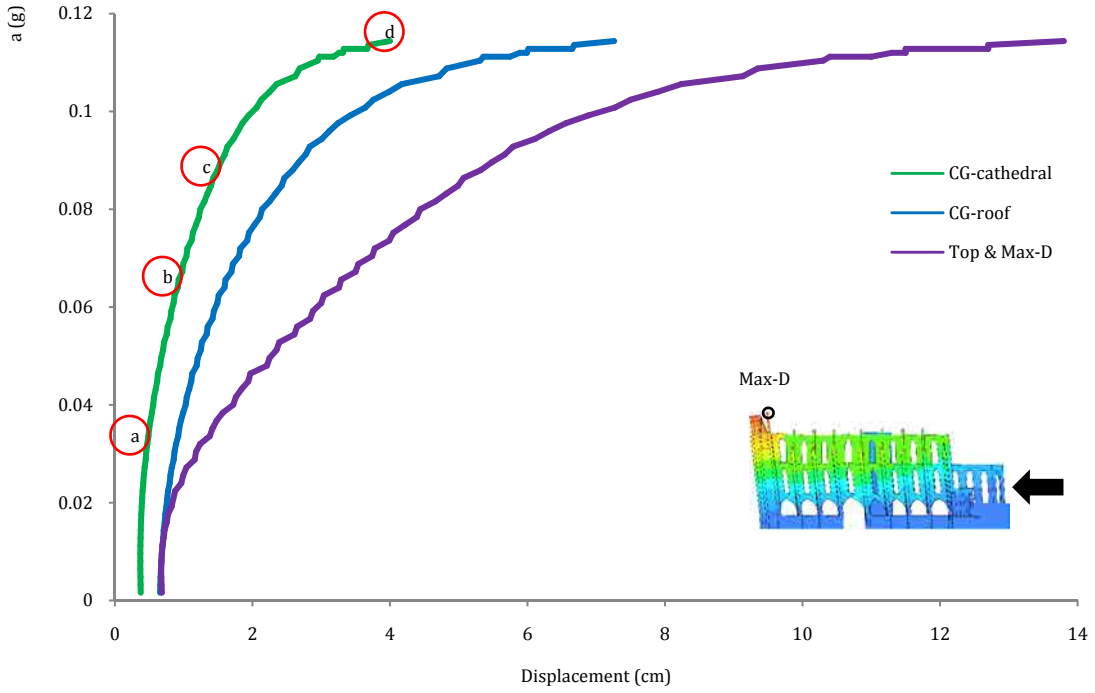


*Figure 7.3. Capacity curve for the seismic analysis in (+X) direction. The control point (Max-D) is shown in circle.*

The collapse progression was observed by following the damage experienced by the resisting structural elements in this direction, Figure 7.4. Those were the two frames consisting of the two upper clerestory walls supported on the columns, and the two frames consisting of the two lower clerestory walls supported on the buttresses. In addition, the apse's walls and the west and the east facades also provided the seismic resistance.

The cracks started at about 0,04g in the first bay of the upper and the lower clerestory walls due to the start of the west façade overturning (Figure 7.4 a). The cracks were diagonal and initiated from the top of the windows' openings. The cracks extend was larger for the case of the upper clerestory walls than that of the lower clerestory walls. No cracks could be seen in the other parts of the cathedral.

At 0,07g, the first bay of the upper clerestory walls was totally cracked above the windows' openings (Figure 7.4 b). Thus, the west façade lost its connection with these walls at the level of the top of the windows, and still connected at the level of the bottom of the windows. Diagonal cracks began to open at all the bays of the lower clerestory walls starting from the windows' openings. More cracks were observed at the top of the

windows' openings than those at the bottom. The bay with the largest span (fourth bay from the west façade) had cracks above and below the window's opening.

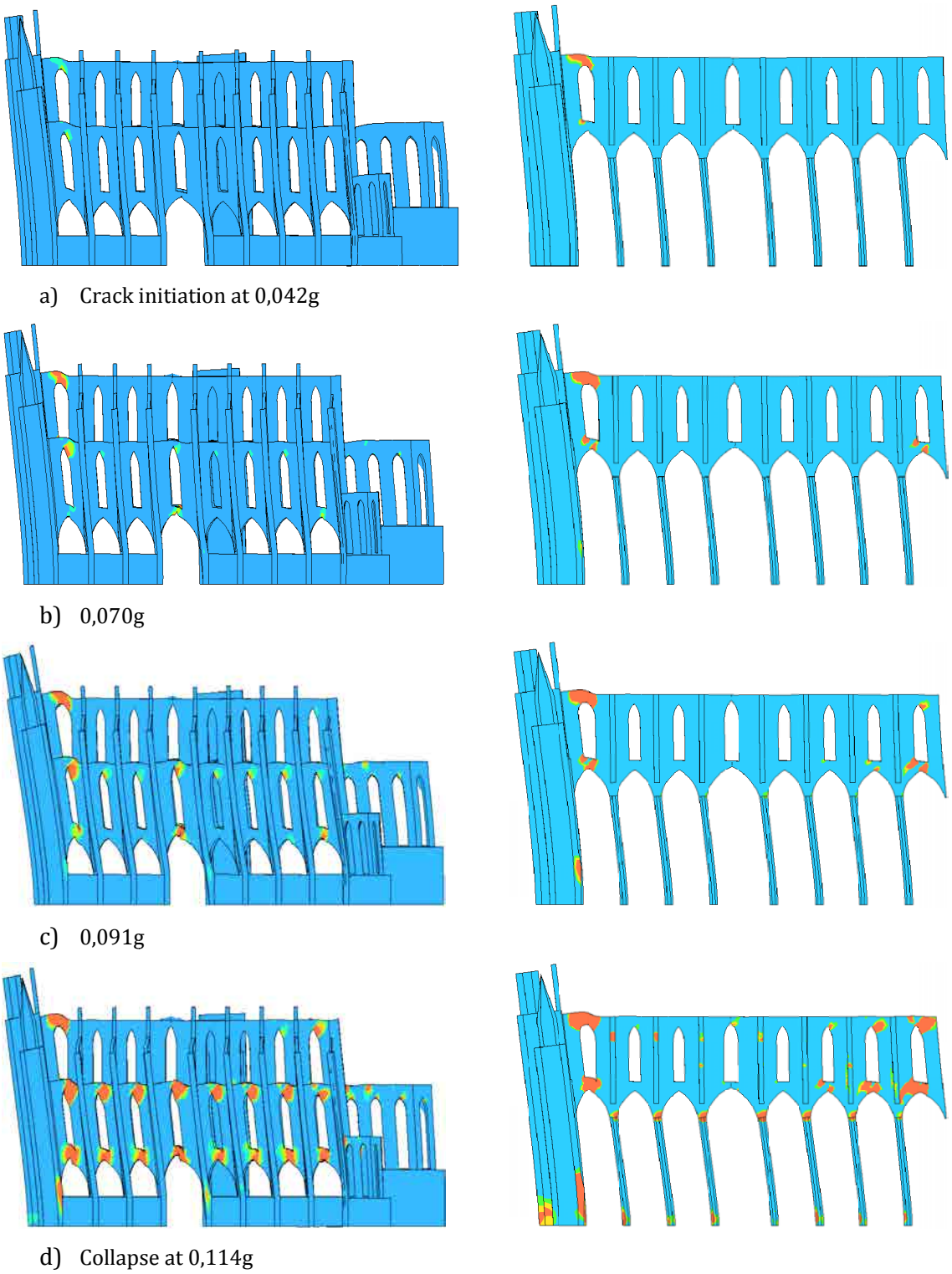

a) Crack initiation at 0,042g

b) 0,070g

c) 0,091g

d) Collapse at 0,114g

*Figure 7.4. Progress of damage in the two typical resisting frames: lower clerestory wall supported on buttresses (left); and upper clerestory wall supported on columns (right). Contour of maximum principal strain plotted on deformed mesh. Case of (+X).*

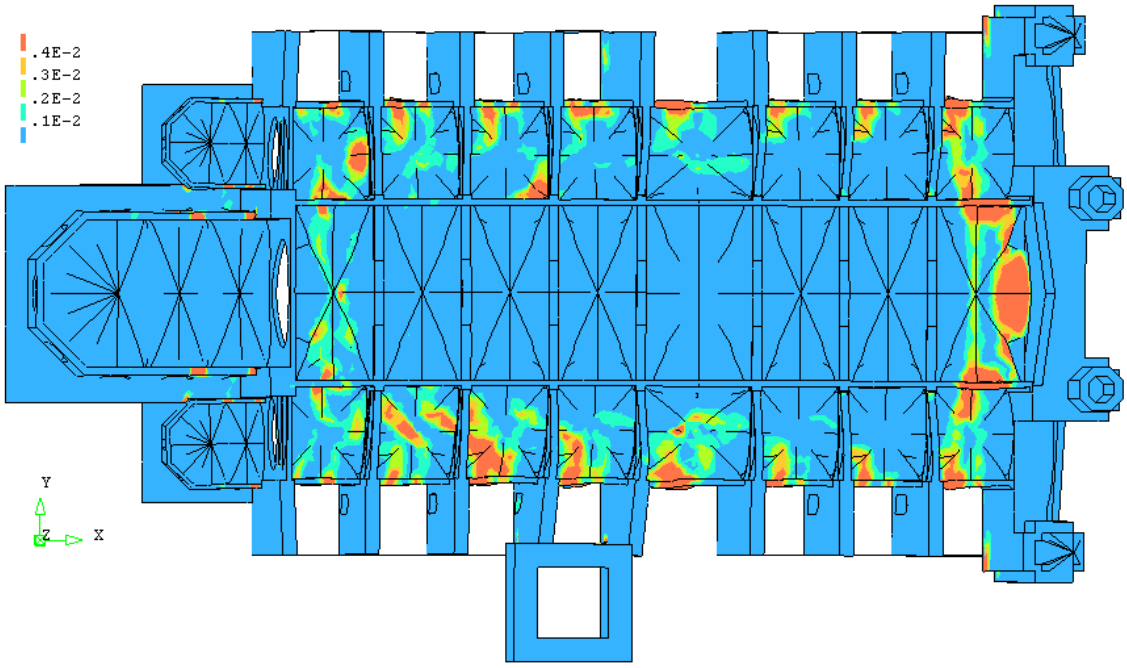


*Figure 7.5. Cracking pattern of vaults at collapse load. Contour of maximum principal strain plotted on deformed mesh. In red cracked areas. Case of (+X).*

The walls of the central chapel of the apse started to crack above the windows' openings. The lower clerestory walls (supported on the stiffer buttresses) were cracked in all bays, whereas the upper clerestory walls (supported on the less stiff columns) were cracked in one bay only.

The cracks observed at the previous loading stage extended more at 0,091g (Figure 7.4 c). The first bay of the lower clerestory walls was totally cracked above the windows' opening which increased the overturning of the west façade. The columns started to crack at its connections with the upper clerestory walls.

At collapse (Figure 7.4 d), the west façade completely overturned after losing all its connections with the rest of the cathedral. As the first bay of upper and lower clerestory walls were completely cracked around the windows' openings, and also the first bay of the vault of the main nave was cracked (Figure 7.5). The damage of the west façade is shown in Figure 7.6. As can be seen, it was concentrated near the base and at the top of the entrance column. It can be understood that the west facade moved like a rigid body that overturned out-of-plane. For the rest of the cathedral, all the bays of the lower clerestory walls cracked completely around the windows' openings. This showed that the buttresses were no longer connected together by the clerestory walls, as they sequentially lost their stability and overturned out-of-plane. The east façade lost its connections with the clerestory walls because their last bays were completely cracked around the windows'

opening. The Columns overturned after being cracked at the base and at their connections with the clerestory walls. There was a concentration of the damage at the connection between the tower and the two adjacent buttresses. At the choir area, the cracking occurred only around the large windows of the upper walls, while the massive lower walls did not show any damage.

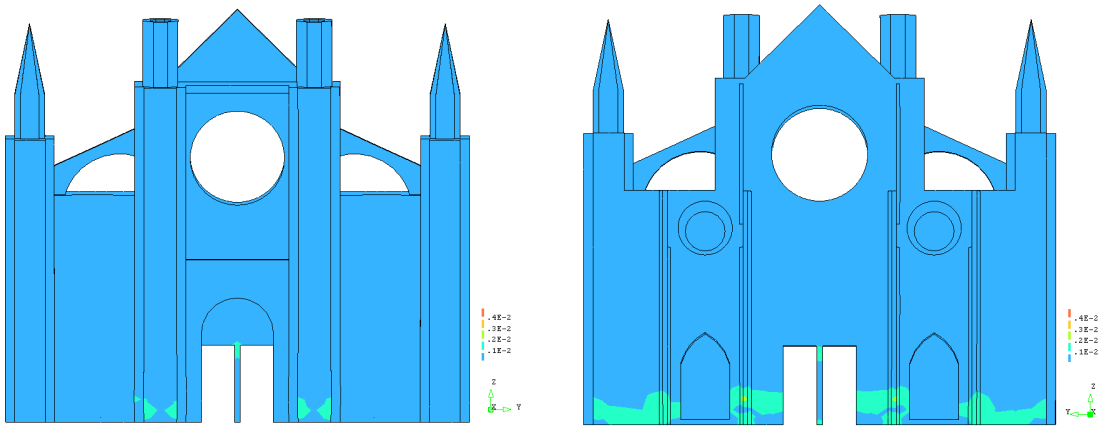

*Figure 7.6. Damage experienced by the west façade at collapse load. Case of (+X). From outside the cathedral (left) and from inside the cathedral (right). Contour of maximum principal strain plotted on deformed mesh.*

#### 7.4.2.2 In (–X) direction

This direction showed the lowest capacity among the four considered directions. The attained capacity was only 0,095g. Figure 7.7 shows the different capacity curves for the considered control points. The point Max-D was observed to be at the top of the most north buttress. The three marked points on the curves a, b and c were used to follow the collapse evolution as shown in Figure 7.8.

The cracking process started like the case of +X at about 0,04g. The first cracks appeared at the last bay of the lower clerestory walls due to the east façade's overturning. The cracks were diagonal and started from the top of the windows' opening. Cracks also appeared at the first bay of the same walls under the windows' openings, Figure 7.8 a. At 0,07g, with more overturning of the east façade more cracks opened at distinguished zones, these were all the bays of the lower clerestory walls above windows' openings, the first and the last bays of the upper clerestory walls above the windows' openings and at the connections of the columns with the clerestory walls.

At 0,095g the collapse occurred due to the overturning of the east façade after separation from the rest of the cathedral. The lower clerestory walls were diagonally cracked above and below windows' openings. The same was noticed for the first and the

last bays of the upper clerestory walls. After being cracked at their top, the columns lost their connections with the upper clerestory walls.

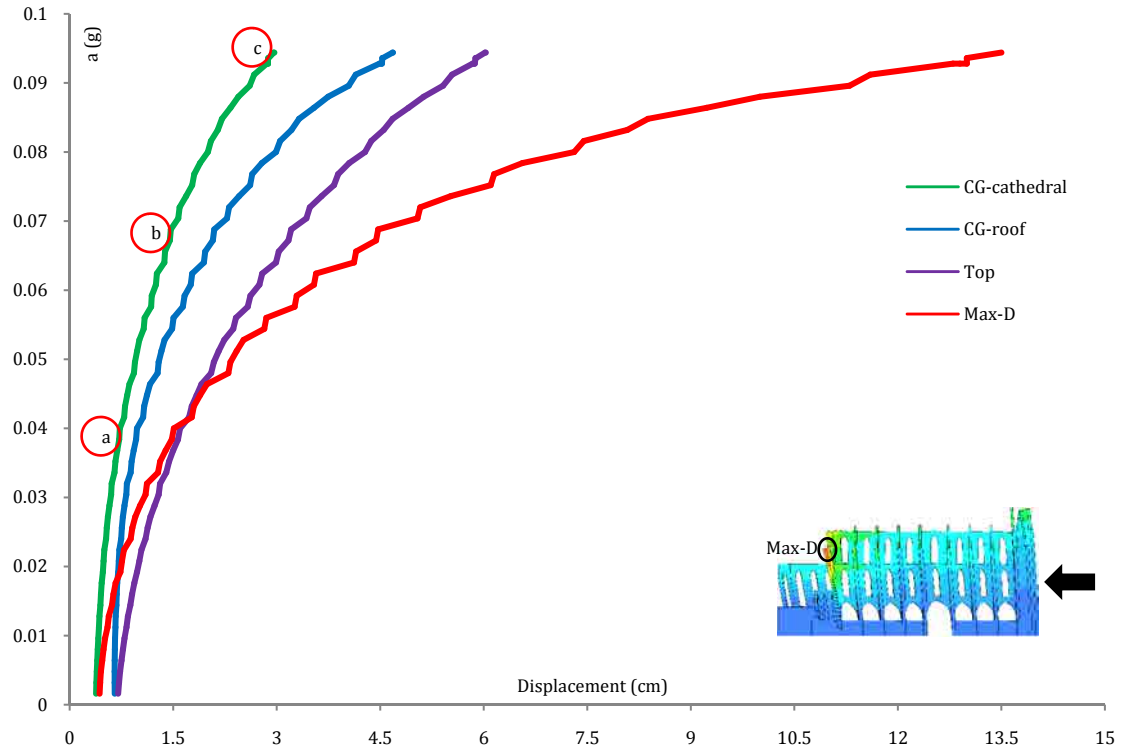


*Figure 7.7. Capacity curve for the seismic analysis in (-X) direction. The control point (Max-D) is shown in circle.*

Figure 7.9 shows the damage exhibited by east façade at collapse. Localized damages at some specific connections of the façade and the rest of the cathedral are clear. The connections with the upper and the lower clerestory walls are totally cracked (surrounded by black ellipses). The cracking is profound and is visible from the inside and the outside of the cathedral. The first location of cracking is at the connection between the springing of the arch of the first bay of the lower clerestory wall and the façade buttress. Since the seismic load is applied perpendicular to the plane of the buttress, it results in its rotation around its connection with the arch springing, causing cracking and separation. Another region showing a similar damage is the connection of the façade near the rose window with the very stiff wall of the choir. In this region damage seems to be caused by a pounding effect. Whereas the whole façade is suffering from out of plane bending, and significant deformation, the choir lateral walls are loaded in their plane and experience a much smaller deformation. In addition, due to the overturning of the buttresses, an initiation of a long diagonal crack is clear from inside the cathedral (surrounded by black

cloud in the figure). The crack starts from near the base and extends to near the lower flying arch. Two small cracks can be noticed above the two rose windows.

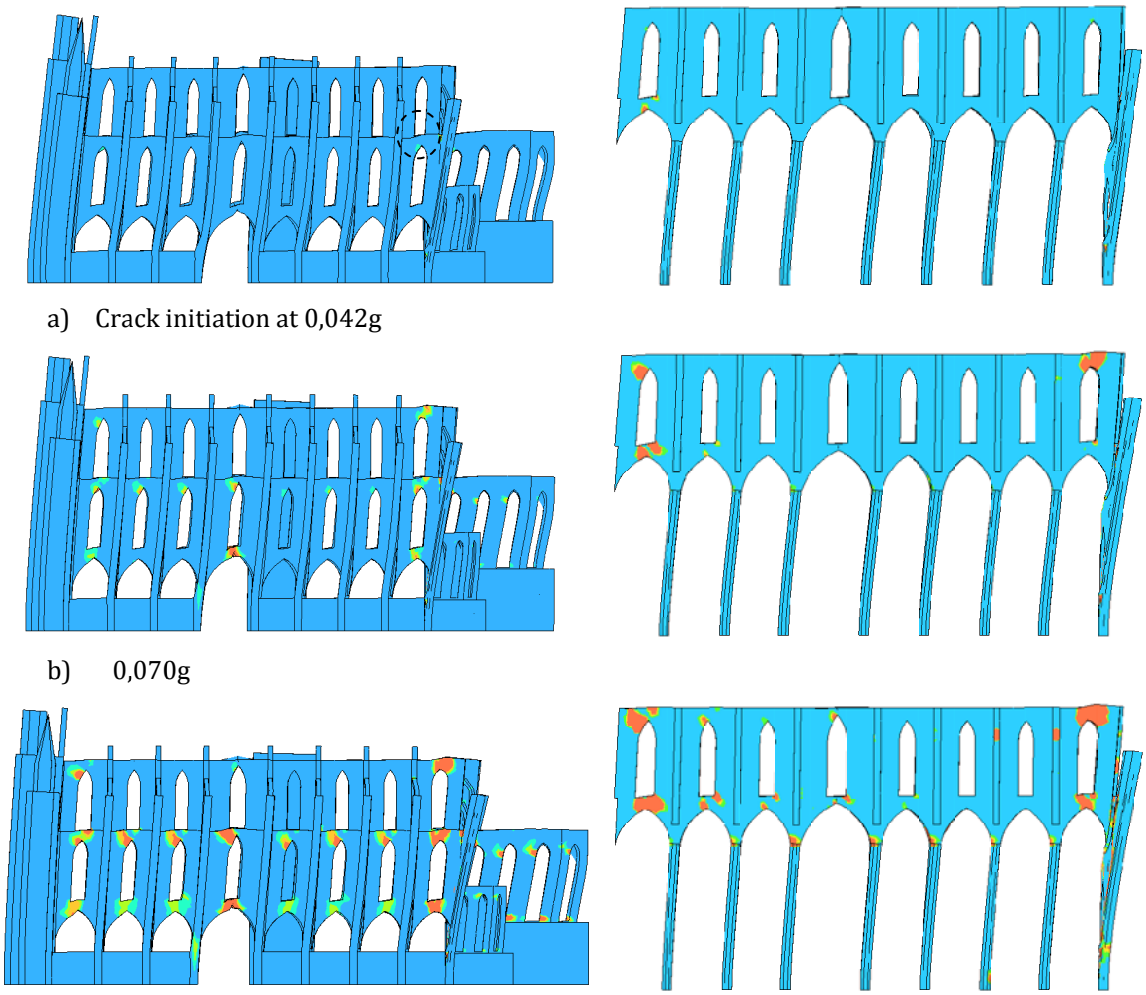

a) Crack initiation at 0,042g

b) 0,070g

c) Collapse at 0,095g

*Figure 7.8. Progress of damage in the two typical resisting frames: lower clerestory walls supported on buttresses (left); and upper clerestory walls supported on columns (right) Contour of maximum principal strain plotted on deformed mesh. Case of (-X).*

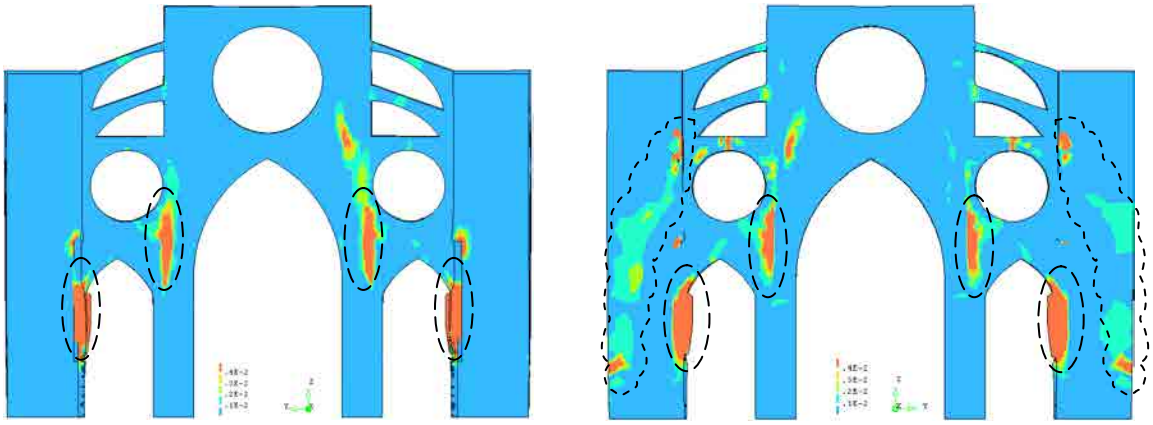

*Figure 7.9. Damage experienced by the east façade at collapse load. From outside the cathedral (left); and from inside the cathedral (right). Contour of maximum principal strain plotted on deformed mesh.*

#### 7.4.2.3 Comparison with the actual state of cracking in the cathedral

The damage patterns found by the numerical analysis were compared with the actual state of cracking in the cathedral to investigate if these cracks were of a seismic origin. Figure 7.10 reports the crack survey of the north and the south clerestory walls as can be seen from inside the cathedral. Some photos for some of the important cracks are shown in Figure 7.11. It was noticed that all the bays of the clerestory walls were cracked. The first four bays from the west façade showed more intensive cracking pattern when compared to the bays near the east façade. The bay with the longest span exhibited more cracks than the other bays.

Regarding the cracks shapes, two types could be noticed, the first were the diagonal cracks around the openings of the windows. The second were the vertical cracks between the walls and the supporting elements whether the columns or the buttresses. The diagonal cracks were near to those found by the pushover analysis so they perhaps related to the seismic history of the island of Mallorca.

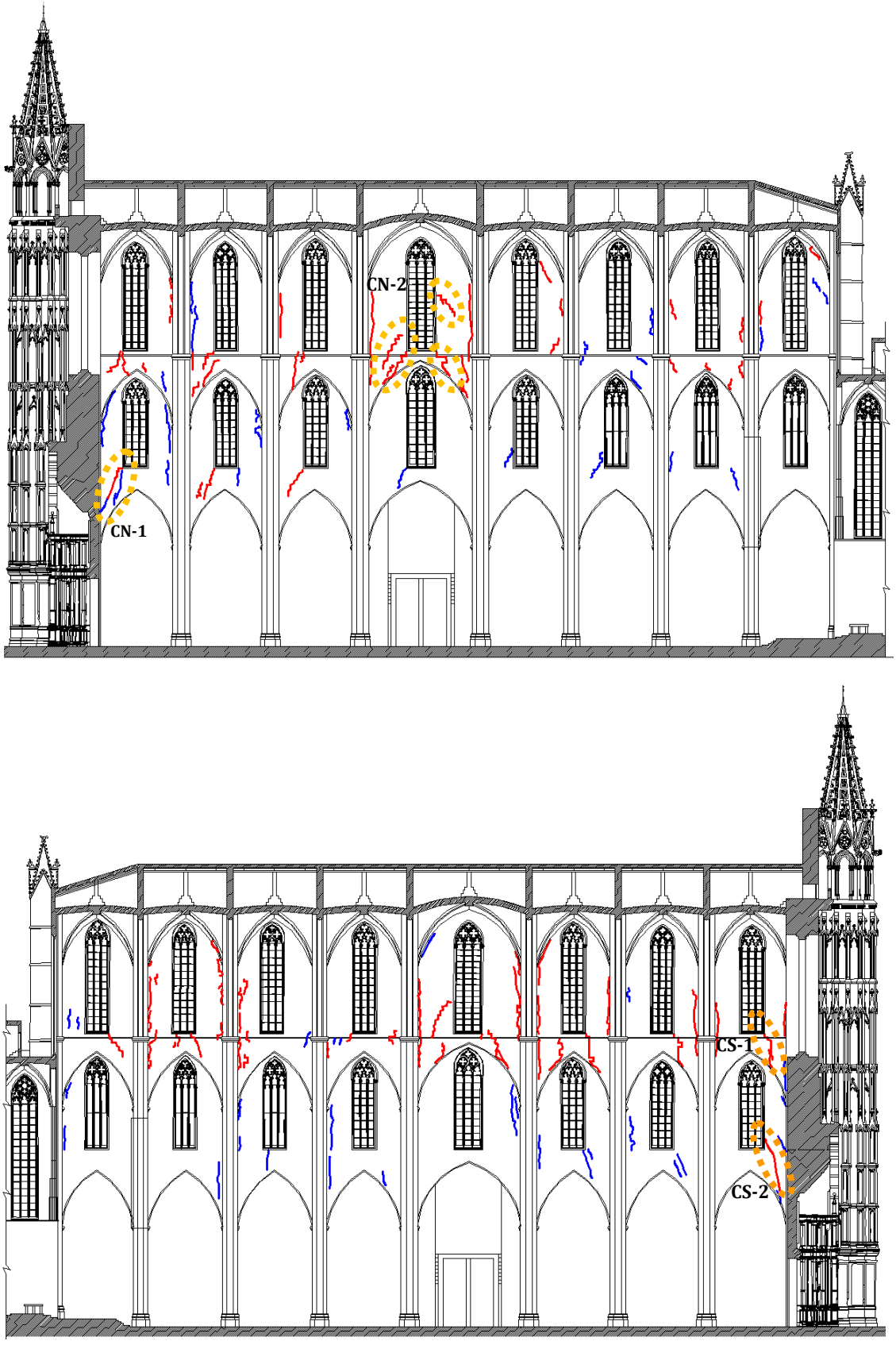


*Figure 7.10. Crack survey of north (top) and south (bottom) clerestory walls. Red cracks are wider than blue ones. Photos for cracks surrounded by circles are shown in the next figure.*

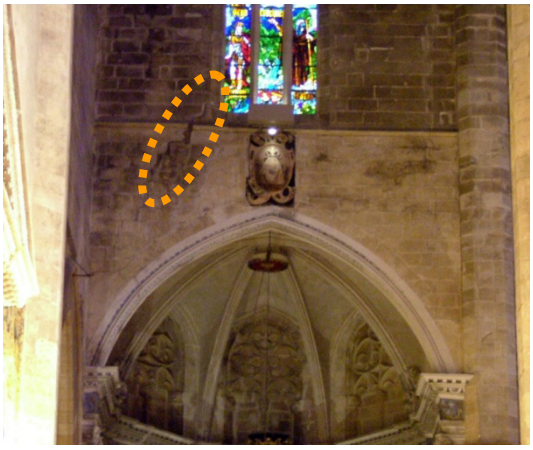

CN-1

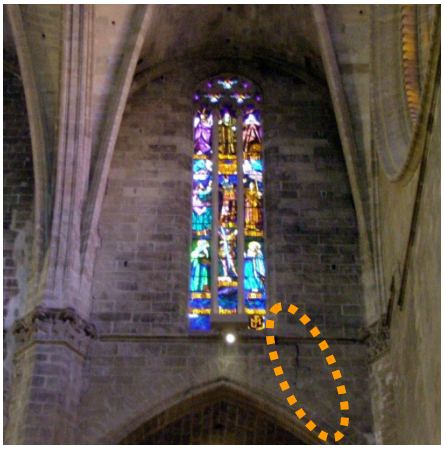

CS-1

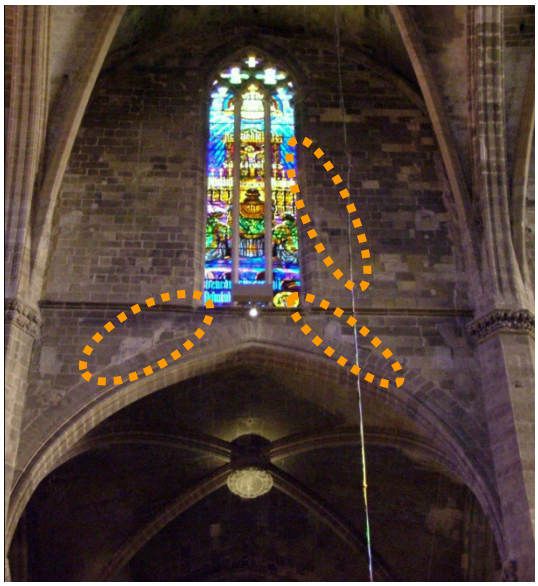

CN-2

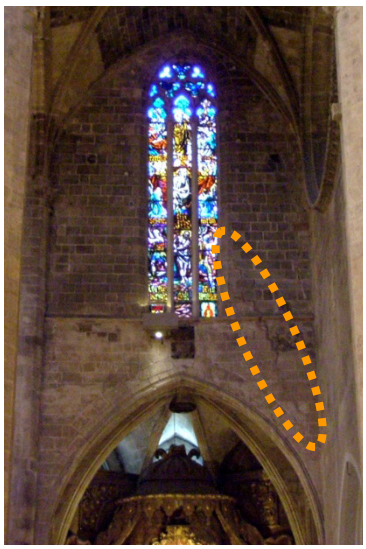

CS-2

*Figure 7.11. Photos from inside the cathedral for some of the cracks of the previous figure.*

### 7.4.3 The seismic response in the transversal (±Y) direction

#### 7.4.3.1 In (+Y) direction

In this direction the building showed a higher capacity (0,118g) than that in the longitudinal direction. Figure 7.12 shows the capacity curves. The point Max-D was found to be at the top of the fifth flying arch counting from the west façade.

The cathedral resisted the seismic loading thanks to seven frame-like structures. Each of them was composed by the columns supporting the diaphragmatic arch and the main nave vault which in turn were connected to the buttresses by the two batteries of the flying arches and the lateral naves' vaults. In addition to these frames, the west and the east facades, the tower and the stiff walls of the apse resisted the lateral loads.

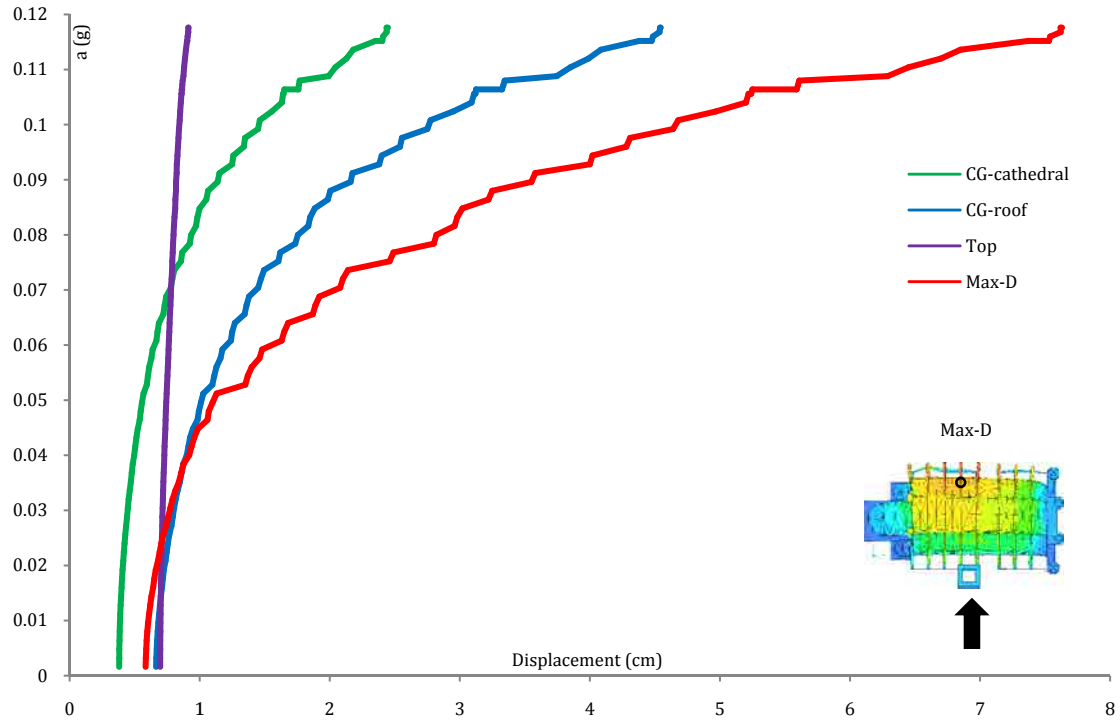


*Figure 7.12. Capacity curve for the seismic analysis in (+Y) direction. The control point (Max-D) is shown in plan.*

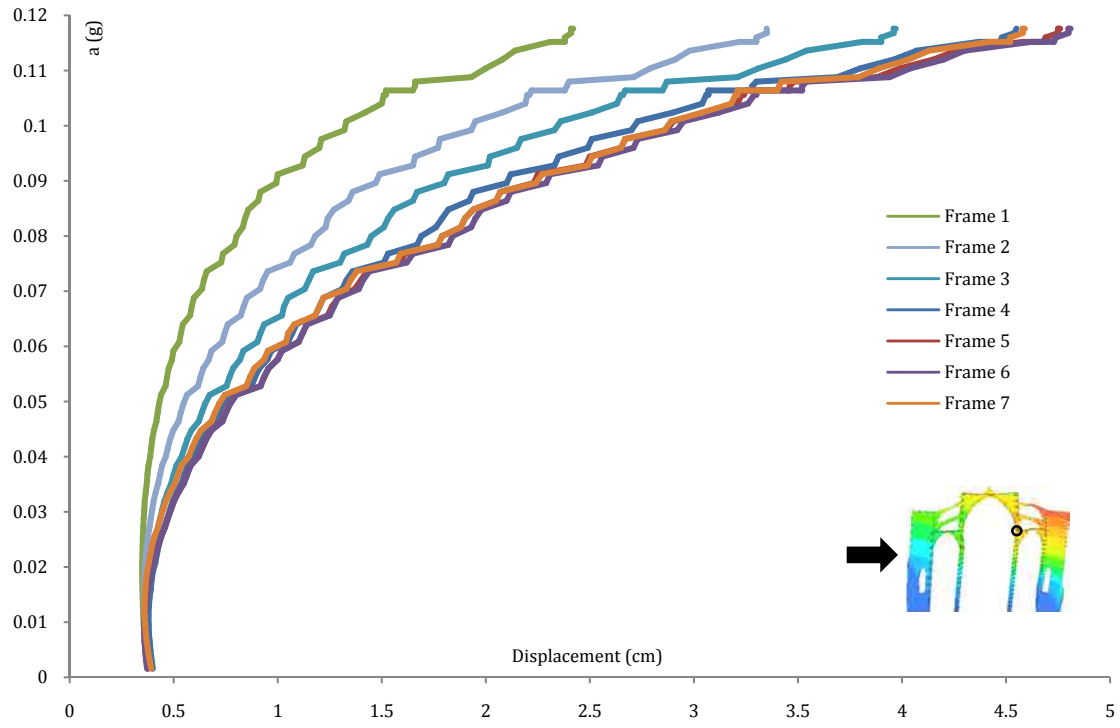


*Figure 7.13. Capacity curves for the seven typical frames. The control point is shown in circle. Case of pushover in +Y direction.*

The seven frames carried different portions of the seismic load depending on their location with respect to the center of rigidity of the whole cathedral, and depending also on their proximity from stiffer parts like the west façade. A comparison among the capacity curves of the seven frames is shown in Figure 7.13 for a control point located at the top of the south column, the frames counting started from the west facade. As can be noticed, the displacement of the control point increased when the frame location moved away from the west façade. The frames from 1 to 3 showed less displacement than the rest of the other frames due to the considerable resistance of the stiff west facade. The remaining four frames (from 4 to 7) showed alike capacity curves and the maximum displacements at collapse were in a narrow range from 4,5 to 4,8 cm.

To explain how the cathedral failed in this direction, the collapse mechanism of the typical bay number 2 was taken as a representative example. As expected in this type of Gothic cathedrals, a series of disconnections (hinges) between structural parts could be noticed with the increase in the applied lateral load until reaching collapse. This sequence of crack propagation is shown in Figure 7.14, in which, a capture was taken at each seismic load multiplier resulted in a crack initiation.

The hinge mechanism process started at a seismic load of 0,075g with the arising of four cracks at the top of the column, the upper flying arch, the top of the lateral nave's vault and the connection of the buttress with the longitudinal wall, being the largest damaged area at the flying arch. The following group of cracks started at 0,093g at the top of the lower flying arch, the bottom of the lateral nave's vault and the base of the buttress. One crack only initiated at 0,099g at the bottom of the lower north flying arch. At 0,102g a new crack appeared in the main nave vault followed by another one at the base of the buttress at 0,104g. The followed crack initiated at 0,106g at the top of the vault of the north lateral nave. Four cracks opened at the load factor of 0,109g, two at the north part of the bay, in specific, at the bottom of the upper flying arch and the connection of the lower flying arch with the main nave vault, the other two were at the south part at the connection of the lower flying arch with the main nave vault and just below the buttress window. Very near to collapse, at 0,114g, the base of the column was cracked.

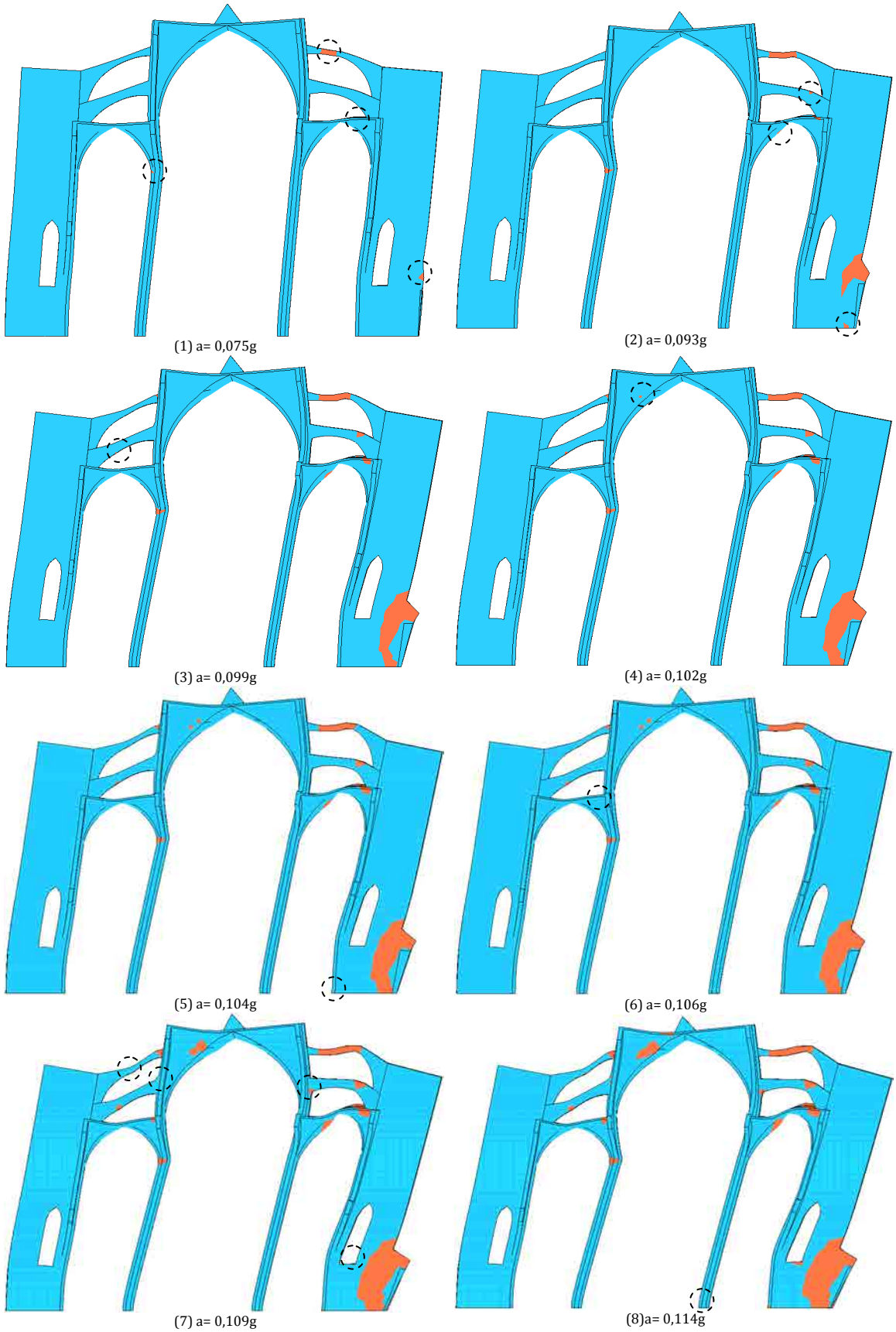


*Figure 7.14. From (1) to (8): arising cracking (in circle) and the associated seismic load factor. Cracking pattern in red plotted on deformed mesh.*

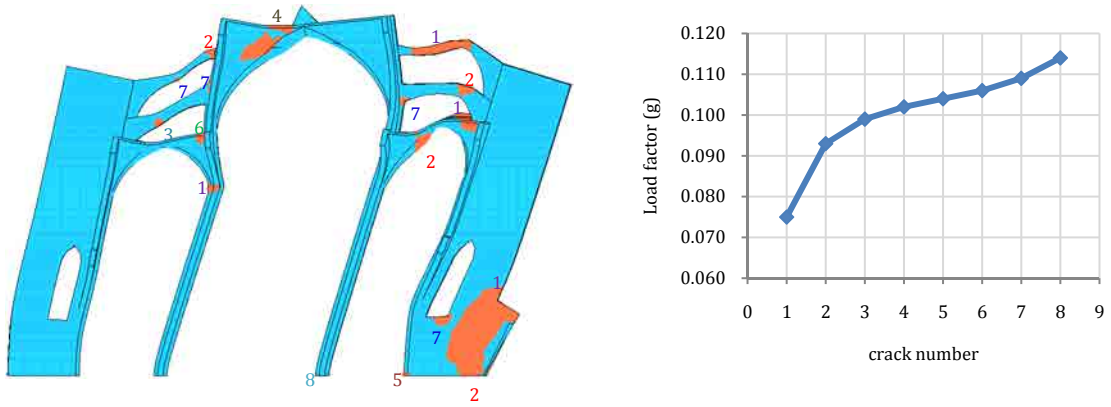


*Figure 7.15. Cracking pattern at collapse with sequence of cracking (left); and the seismic load factor of initiation of each crack (right).*

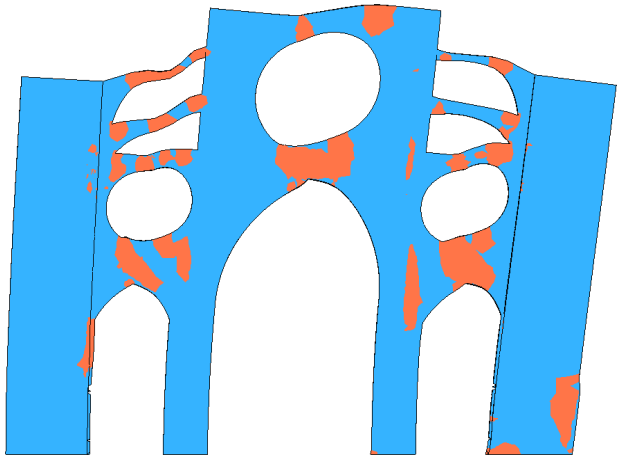

*Figure 7.16. Cracking pattern in red plotted on deformed mesh at collapse of the east facade.*

In Figure 7.15 the cracking pattern of the bay at collapse is shown (to the left) with the numbering of the previously discussed cracks and the corresponding seismic load multiplier (to the right). It is worth noticing that the cracks grew rapidly after the initiation of the second group of cracking. As can be noticed, the cracks from 3 to 8 initiated in a narrow load range between 0,099g to 0,114g. The first and the second group of cracks appeared at the slender column, the flying arches, the thin lateral nave vault and the buttress. Hence, it can be understood that for such type of Gothic cathedrals that the collapse initiated from the aforementioned framed slender elements.

In the same figure, it can be noticed that the damage in the buttress was influenced by the existing of the large window, as can be seen a diagonal crack could be tracked from just below the window down to the base. Nevertheless, the existence of the longitudinal wall interrupted this crack. As the longitudinal wall connected the buttresses together, hence they helped each other in carrying the seismic load. This made the damage to be

concentrated at the longitudinal wall-buttress connection, and the diagonal tension crack from the window to the base slightly decreased.

For the case of the east façade, Figure 7.16 shows the damaged areas at collapse. The cracks appeared at the same places previously described for a typical bay; in addition, large diagonal cracks were concentrated around the three big openings of the rose windows. As opposite to this façade, the west one did not show any signs of damage because the loading direction coincided with its very stiff in-plane direction.

### 7.4.3.2 In (-Y) direction

The resistance in this direction was the highest among all directions as can be seen in the capacity curve (Figure 7.17). In this figure the point Max-D was located at the top of the northern flying arch of the east façade. The capacity was 0,141g which was about 20% more than +Y direction. The existence of the tower as a strong support near the middle of the structure was the reason for the higher capacity. Figure 7.18 compares between the deformed shapes of the cathedral under the two cases of loading (±Y) using the same scale for the displacements and the deformed shapes. It shows the effect of the tower in reducing the displacements of -Y loading when compared with that of +Y.

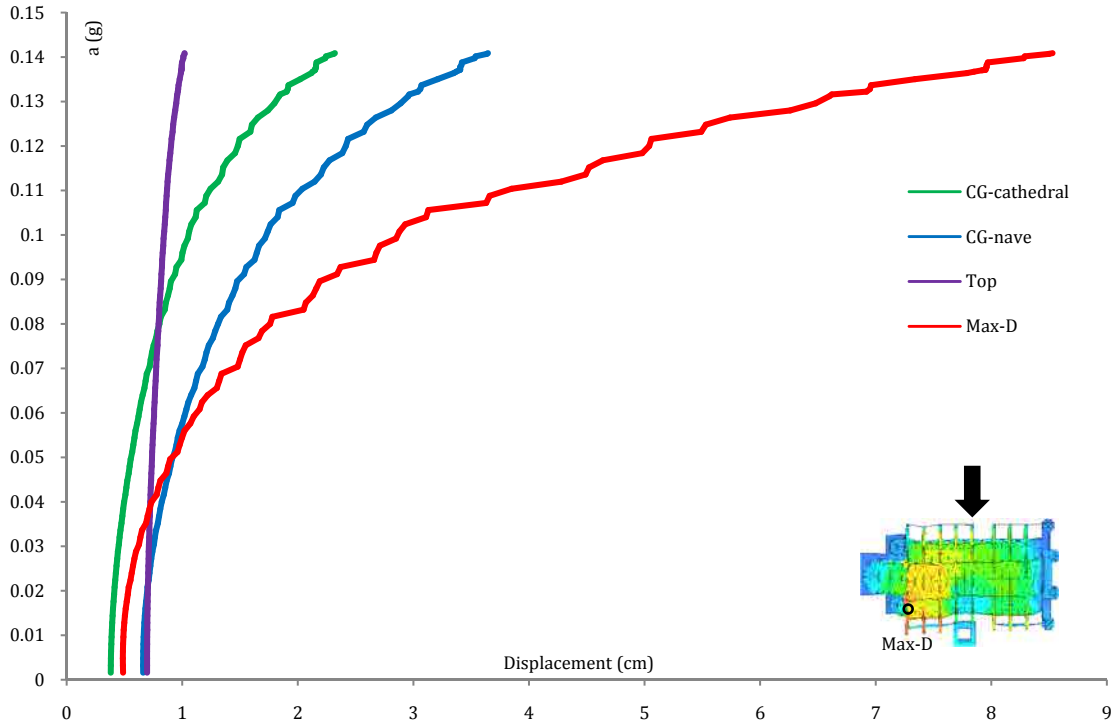


*Figure 7.17. Capacity curve for the seismic analysis in (-Y) direction. The control point (Max-D) is shown in circle.*

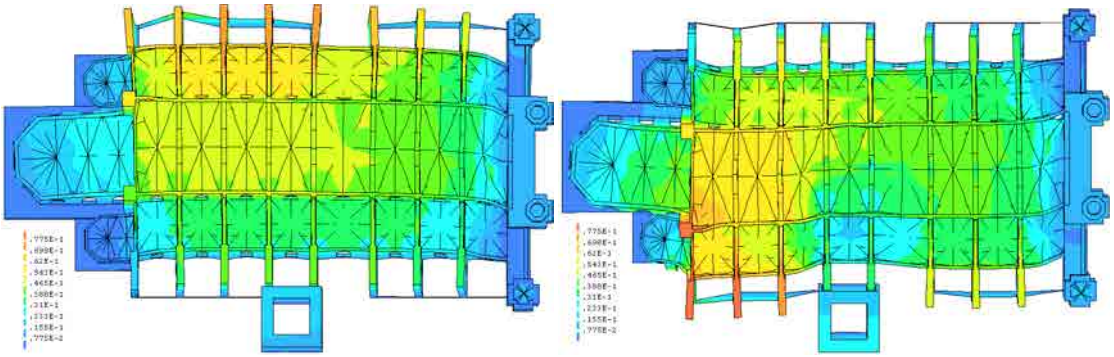

*Figure 7.18. Comparing deformations at collapse of case of +Y (left) with case of –Y (right).*

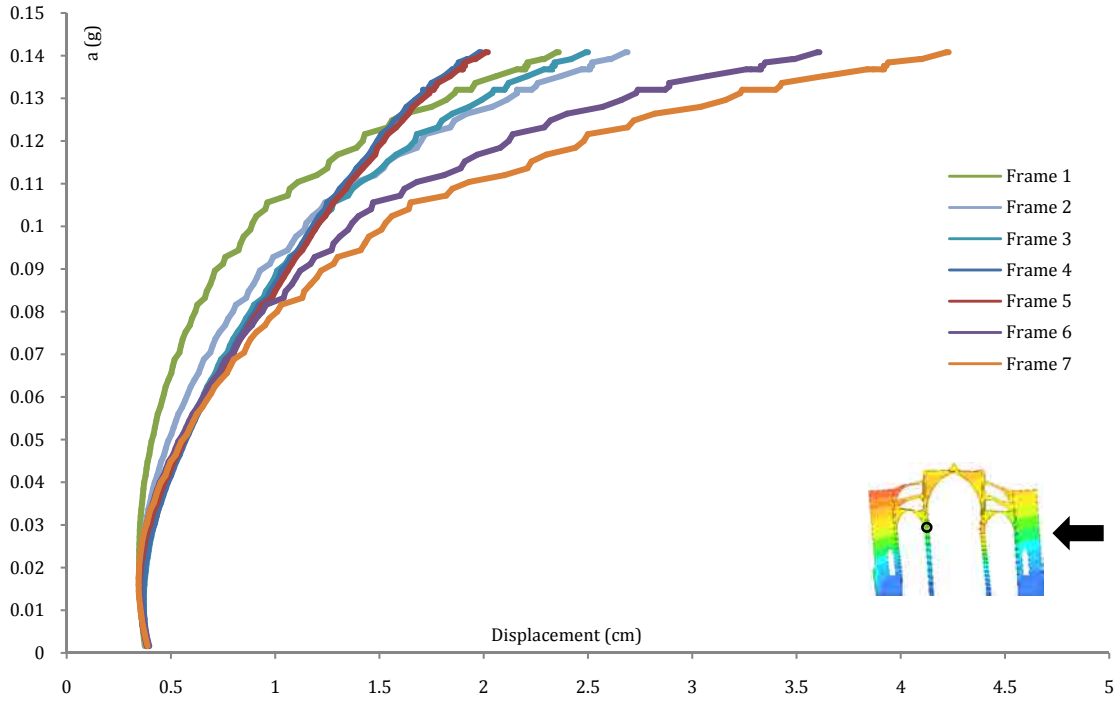


*Figure 7.19. Capacity curves for the seven typical frames. The control point is shown in circle.*

Similar to the case of +Y loading, a comparison among the seven bays was made, Figure 7.19. The two frames 4 and 5 which had the tower as a support showed the lowest displacement among all the frames. At collapse, the average displacement of the two frames 6 and 7 was two times of that of the frames 4 and 5. Like the case of +Y, the first three frames showed low displacement due to their proximity of the west façade.

Figure 7.20 shows the propagation of cracks in the typical frame number 2. The extrados of the northern lateral nave's vault and the top of the southern column were the first places to crack at 0,083g which was higher than the case of +Y (0,075g). Following, the northern buttress and the upper flying arch cracked at 0,094g. At 0,107g three cracks appeared at the lower battery of the northern and the southern flying arches.

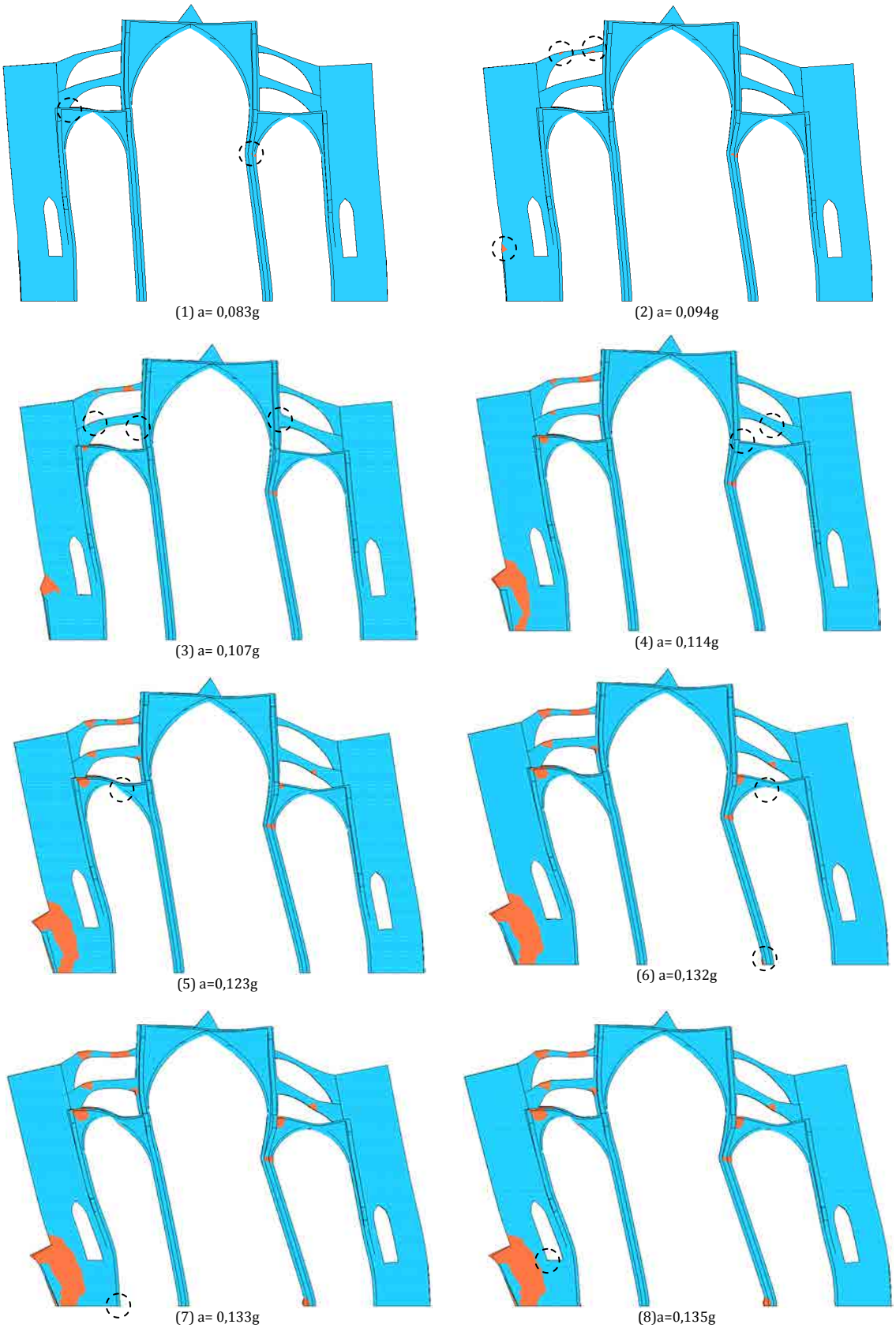


*Figure 7.20. From (1) to (8): arising cracking (in circle) and the associated seismic load factor. Cracking pattern in red plotted on deformed mesh.*

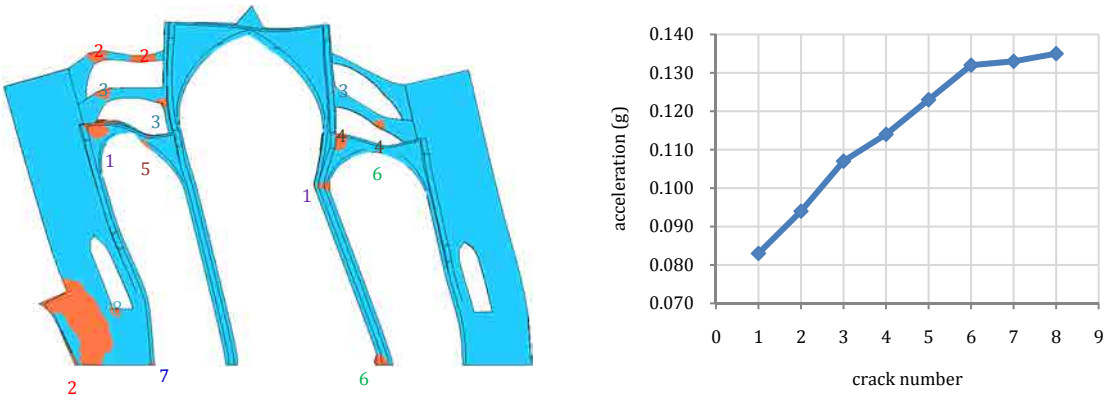


*Figure 7.21. Cracking pattern at collapse with sequence of cracking (left); and the seismic load factor of initiation of each crack (right).*

Another two cracks initiated at 0,114g at the southern lower flying arch and the extrados of the lateral nave's vault. The intrados of the northern lateral nave's vault cracked at 0,123g. At two near seismic loads (0,132g and 0,133g) the intrados of the southern lateral nave's vault, the base of the southern column and the base of the northern buttress were cracked. The last crack initiated at 0,135g at the bottom of the northern buttress' window.

The sequence of cracking with the associated seismic load factor is depicted in Figure 7.21. Comparing this case with the previous case of +Y, it could be noticed that a near sequence of structural elements' cracking was found. At first, the top of the column, the upper battery of flying arches, the extrados of lateral nave's vaults and the base of the buttress, and at last, the bases of the columns and the buttresses. In between, the lower battery of the flying arches, the extrados and the intrados of the lateral naves' vault cracked. An important difference between the two figures 7.15 and 7.21 (right) was the capability of the typical bay to resist after the initiation of the first crack in the case of –Y over a wider range of seismic loads from 0,094g to 0,135g. The collapse occurred at 0,141g, whereas in the case of +Y, a rapid cracking took place in a narrow range from 0,099g to 0,114g as previously mentioned. Another difference was the absence of the damage at the main nave's vault in case of –Y.

### 7.4.3.3 Comparison with the actual state of cracking in the cathedral

The analysis showed that some specific regions of the structural elements of the cathedral were vulnerable to damage under the seismic actions. Some currently visible cracks in the structure may be related to the previous seismic events that had already struck Mallorca Island, Figure 7.22 shows some examples. The diagonal crack around the rose window (Figure 7.22, a) is a typical crack due to seismic loading. Clemente (2006)

suggested that the crack in Figure 7.22-b resulted from creep effects; however, historic earthquakes might have contributed also in creating such damage. It can be noticed that the crack started at its top diagonally then continued vertically.

(a)

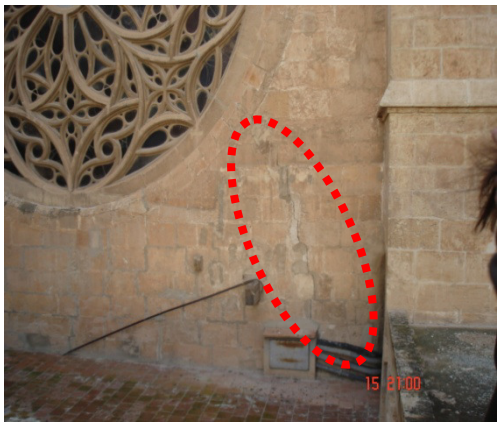

(b)

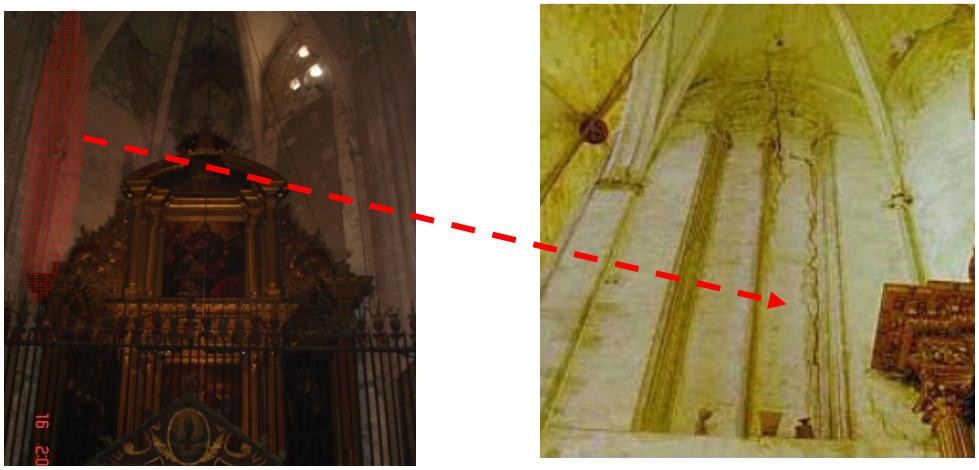

*Figure 7.22. Examples of damage possibly related to seismic events: (a) cracking around the middle rose window of the east façade; and (b) cracking at the south buttress of frame 3.*

### 7.4.3.4 Comparison with previous FE assessments on a typical bay

Some previous studies have been carried out on the seismic performance of the cathedral considering a typical bay as a representative of the full cathedral in the transverse direction. Here a comparison is made to discuss the creditability of such approach for the seismic assessment of large historical construction composed of a number of repeated typical bays. Obviously, analyzing only a typical bay instead of the full structure saves a lot of effort and time in the model creation, processing and analyzing results.

Figure 7.23 shows the damage pattern at collapse found by Roca et al. (2013). The authors analyzed a typical bay of Mallorca cathedral using the distributed and the localized damage models. A uniform pattern of lateral forces proportional to the mass was

used. Comparing the damage found by the 3D analysis (Figure 7.23) and the one herein presented, a good match in the locations of the hinges can be noticed. The difference that can be noticed is in the extent of damage. The left part (to the axis of symmetry) of the bay exhibited more damage in the analysis based on a typical bay than that found by the analysis of the full cathedral. This is probably due to the contribution of the west façade and the tower in the case of the 3D analysis.

Regarding the attained capacity, it ranged from 0,083g to 0,140g which was comparable to the one found by the 3D analysis of the full cathedral (0,118g and 0,141g). The variability found in the capacity depended on some factors like the adopted modeling approach for the typical bay whether 2D or 3D, the assumed value for the fracture energy in tension and the usage of the distributed or the localized damage models.

Based on this comparison, it can be understood that for such type of structures, analyzing only a typical bay could be a good approach to represent conservatively the seismic response of the full structure in the transverse directionin spite of the influence of other parts of the structure such as stiff façades and towers.

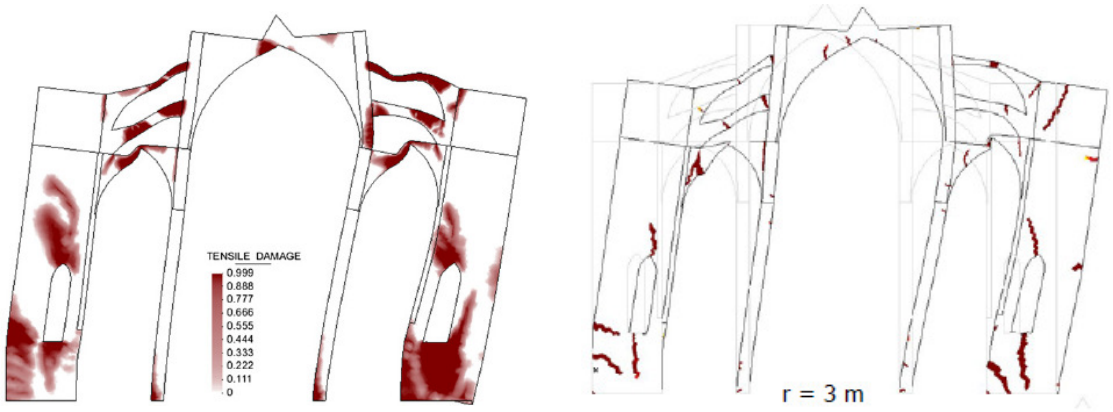


*Figure 7.23. Damage pattern from seismic analysis of a typical bay. Distributed damage model (left), localized damage model with (right). Source: Roca et al. ( 2013).*

### 7.4.4 Sensitivity analysis

A sensitivity analysis was carried out by varying the parameters that mostly influenced the behavior with the objective to investigate their effect on the seismic response of the cathedral. The values of the different mechanical properties of the defined materials in the FE model were changed and the new obtained capacities were compared with the reference model previously discussed. Due to the large size of the FE model and the required long computational time and hard drive storage capacity, only the weakest direction –X was evaluated.

The chosen values for the sensitivity analysis were the tensile strength $f_t$, the compressive strength $f_c$, the cracking strain $\varepsilon_u^{cr}$ and the modulus of elasticity E. When changing the mechanical properties of the materials, all the four materials defined in the model were changed together with the same ratio. In each trial only one parameter was changed keeping all the other parameters constant. Table 7.2 summarizes the tried values in the parametric study. When presenting the capacity curves, the control point Max-D was used.

*Table 7.2. Chosen values for the sensitivity analysis*.*

| The variable | Minimum | Maximum |
|---|---|---|
| Tensile strength ($f_t$) | $f_t$ =2,5% $f_c$ | $f_t$ = 10% $f_c$ |
| Compressive strength ($f_c$) | 0,75× $f_c$ | 2× $f_c$ |
| Ultimate crack strain ($\varepsilon_u^{cr}$) | $\varepsilon_u^{cr}$/10 | $\varepsilon_u^{cr}$ × 1000 |
| modulus of elasticity (E) | E/4 | E/2 |

* Refer to Table 7.1 for the reference values expressed here as symbols.

### 7.4.4.1 Tensile strength

The tensile strength of historical masonry is difficult to determine; however, it is known that it takes very low values. Here, two values were examined 2,5% and 10% of the compressive strength, in addition to the value of 5% of the compressive strength used for the reference model. As can be noticed in Figure 7.24 (left), a remarkable change in the capacity was associated with the change of the tensile strength.

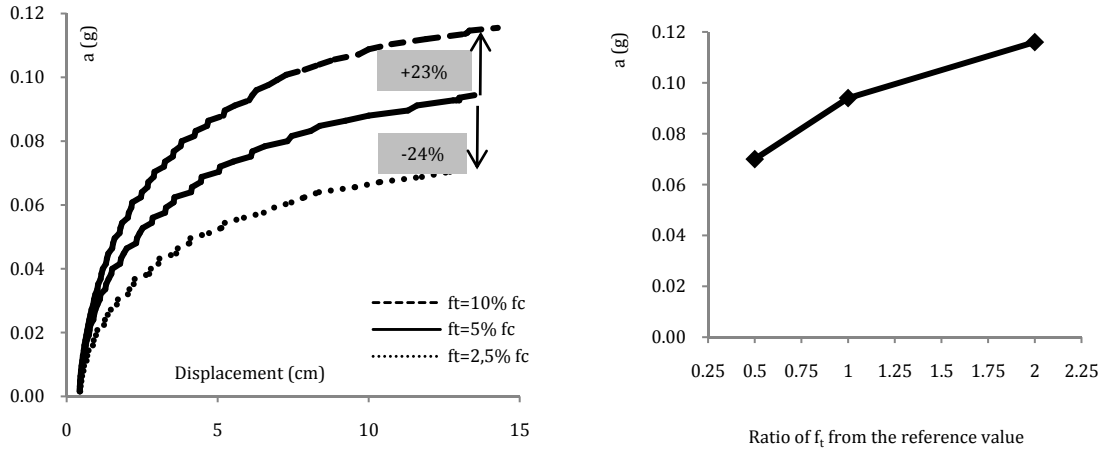


*Figure 7.24. Capacity curves varying $f_t$ (left); and change of the capacity with the change of $f_t$ ratio from the reference value (right).*

A reduction of about 24% was obtained when reducing the strength to the half of its reference value. An increase of about 23% was obtained when increasing the strength to the double of its reference value. Within the examined values, a linear trend between tensile strength and capacity could be noticed (Figure 7.24, right). Since the collapse was governed by the tensile cracking, this result was expected. For the examined values, the change in final displacement was not significant and the collapse mechanism remained the same.

#### 7.4.4.2 Compressive strength

The effect of decreasing this strength property was more pronounced than increasing it. When trying the half of the reference value, the cathedral was not able to bear its self-weight. The ability of the structure to bear its self-weight is essentially related to the compressive strength of its materials.

As shown in Figure 7.25 (left), when using 75% of the reference compressive strength, the capacity decreased by 23% and the final displacement decreased to about 50% of its reference value. Compared with the reference case, decreasing the compressive strength leaded the structure to suffer from higher ratio of stress/strength, so when applying the seismic load afterwards, the structure had less capacity to sustain it. In the same figure, it can be noticed that when increasing the compressive strength to the double of its reference value the capacity increased by only 6% with minor increase in final displacement. Since the collapse was not governed by the compressive failure (crushing), no benefit in strength was observed by increasing the compressive strengths.

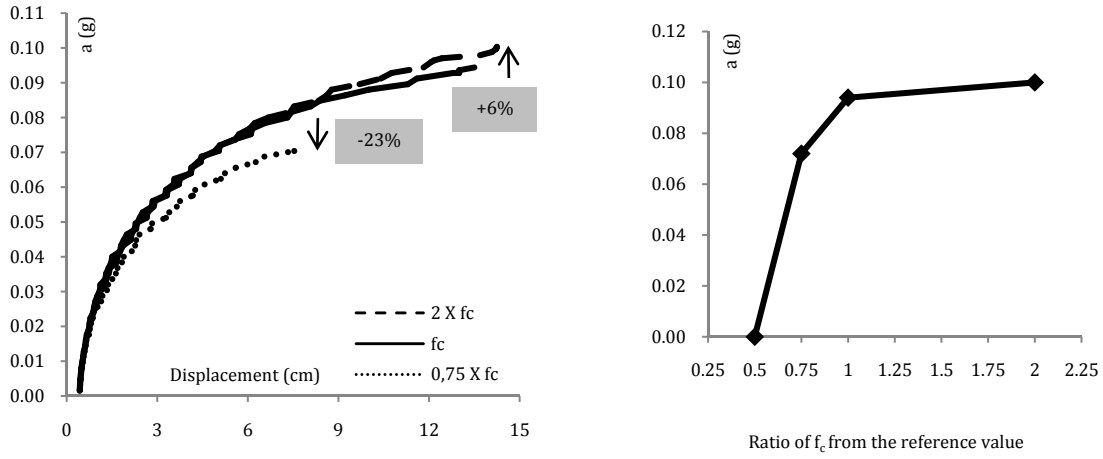


*Figure 7.25. Capacity curves varying $f_c$ (Left); and change of the capacity with the change of $f_c$ ratio from the reference value (right).*

Figure 7.25 (right) presents the relation between the investigated ratios of $f_c$ and the attained capacity. There was stability in the attained capacity when increasing the ratio from 1 to 2. This horizontal branch of the curve is expected to continue with higher ratios indicating the minor effect of increasing the compressive strength.

### 7.4.4.3 Ultimate crack strain

The ultimate crack strain and the fracture energy in tension $G_f$ were directly dependent. In the constitutive model used for defining the nonlinear tension softening behavior, it was possible to use either of $\varepsilon_u^{cr}$ or $G_f$ and the results were the same. Figure 7.26 (left) shows the obtained capacity curves when varying the ultimate crack strain. It can be seen that reducing this parameter by one order of magnitude resulted in a significant reduction in the capacity (about 60%) and the behavior was brittle. On the other side, the increase by one to three orders of magnitudes had slight influence on the capacity with an increase of about 4% only. For the same tensile strength and the crack bandwidth, increasing the ultimate crack strain leaded the material behavior to be like an elastic-perfect plastic behavior and no gain in the capacity was found Figure 7.26 (right).

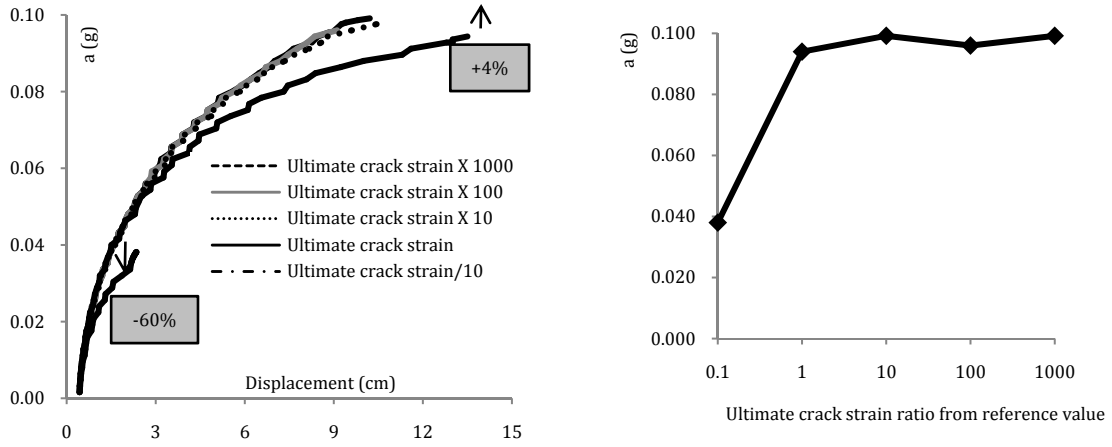


*Figure 7.26. Capacity curves varying $\varepsilon_u^{cr}$ (left); and change of the capacity with the change of $\varepsilon_u^{cr}$ ratio from the reference value (right).*

### 7.4.4.4 Modulus of elasticity (E)

For masonry structures, the modulus of elasticity can is conventionally estimated from the compressive strength using a simple expression: $E = factor.\ f_c$. The factor takes wide range of values from 550 to 1000 according to the used masonry design code. Referring to Table 7.1, it can be noticed that the adopted factor was about 1900 for all materials except for the buttresses which was about 1500. Therefore, two values of the elastic modulus were examined: E/2 and E/4. For the case of E/2, the factor was 750 for

the buttresses and 950 for the rest of the materials, and for the case of E/4 the factor was 375 and 475 for the buttresses and the rest of the materials, respectively.

Figure 7.27 shows the results of the sensitivity analysis of the modulus of elasticity. Reductions in the capacity about 17% and 37% were found when reducing E to one half and one quarter of its reference value, respectively. In addition, the nonlinear behavior started earlier when reducing E. In the reference case it started at about 0,04g, while it starts for less than 0,03g at E/2 and for about 0,02g for E/4. This could be attributed to the nonlinear geometrical effects.

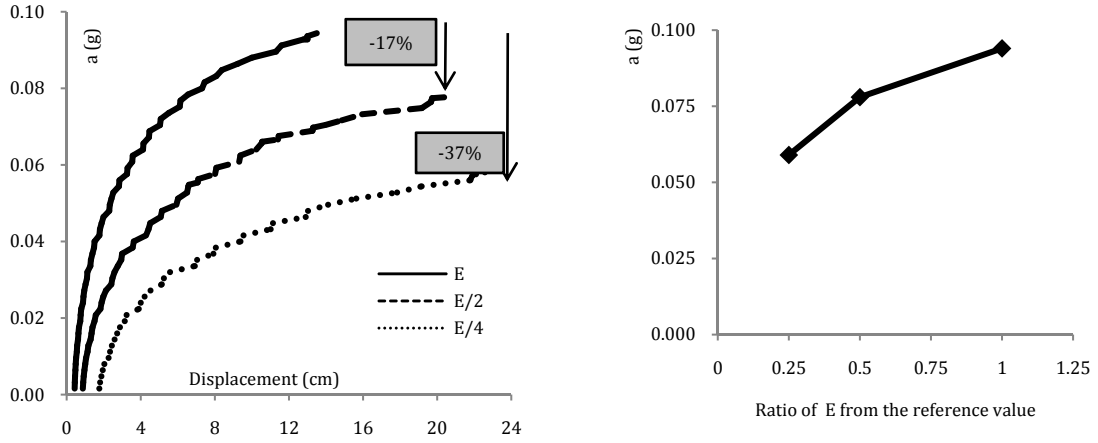


*Figure 7.27. Capacity curves varying the modulus of elasticity E (left); and change of the capacity with the change of E ratio from the reference value (right).*

## 7.5 Kinematic Limit analysis

Based on the collapse mechanisms found in the longitudinal direction by the pushover analysis, two collapse mechanisms were studied by the kinematic limit analysis technique. As discussed, for both cases of ±X direction, the overall collapse occurred due to the overturning of the west and the east façades.

For the +X direction, the west façade overturning was considered, Figure 7.28 (a). For the -X direction, Figure 7.28 (b) shows the damage pattern of the east façade at collapse, in which, the cracked areas show the possible locations of the hinges. In Figure 7.28 (c), the deformed shape at collapse is shown with indication to the hinges at which the equilibrium of the full mechanism was considered. The mechanism involved the overturning of the whole façade accompanied with the half of the adjacent bay. The two buttresses overturned around the top of the lower perpendicular apse's wall, whereas, the rest of the mechanism overturned around the top of the higher apse's wall.

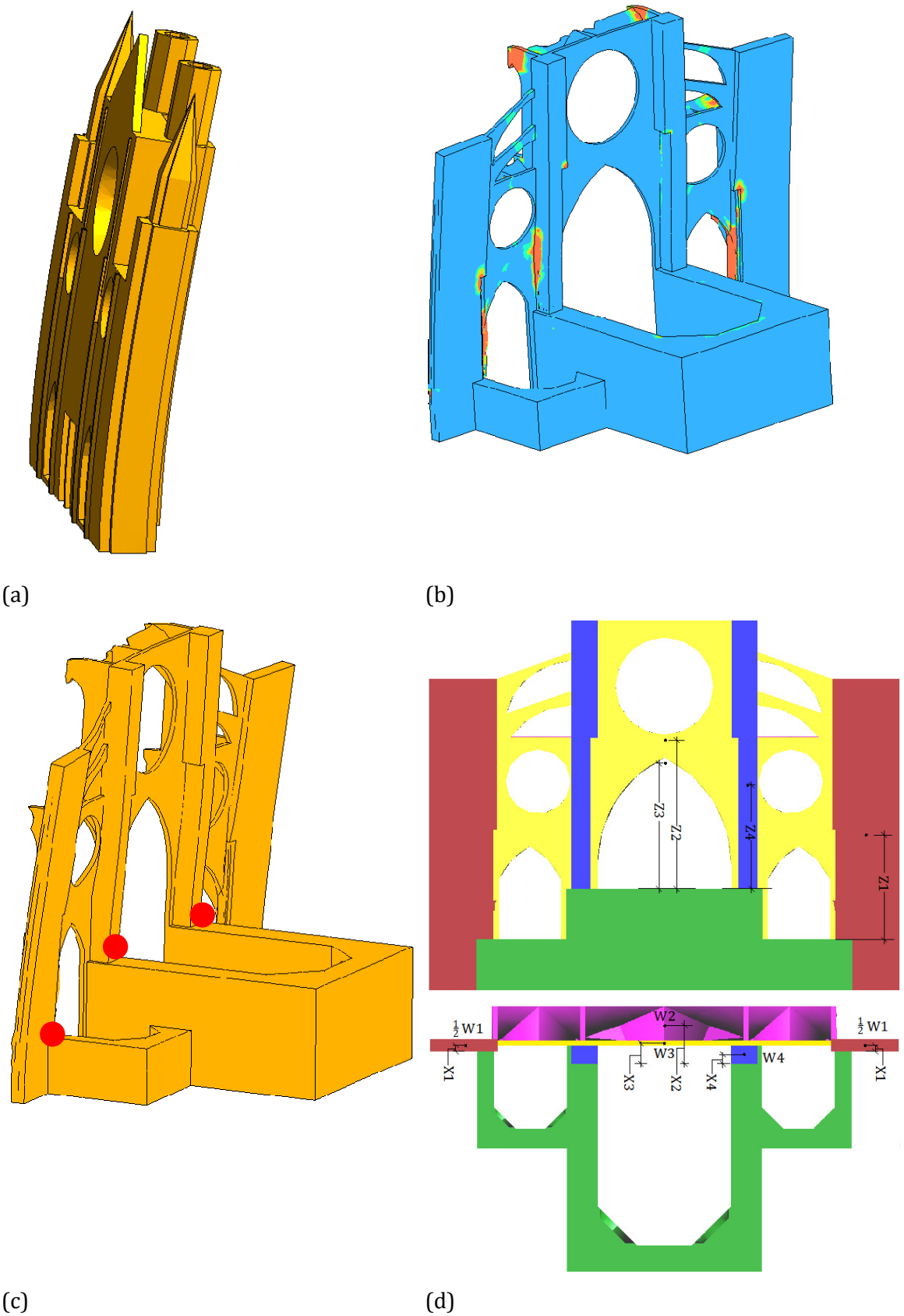


*Figure 7.28: (a) The west façade mechanism. The east façade mechanism: (b) cracked areas at collapse (in red) as deduced from the pushover analysis; (c) red circles show locations of hinges; and*

*(d) lever arms for the macro-block weights and the seismic forces.*

The lever arms for the weights and the corresponding horizontal seismic forces are shown in Figure 7.28 (d). In the two Tables 7.3 and 7.4, the weights, lever arms and virtual displacements used in calculating the spectral accelerations are summarized. The equations of calculations and the definition of those parameters were previously introduced in chapter 2. The found capacities were 0,144g and 0, 118g for the –X and +X directions, respectively. Those values were near to the capacities obtained by the pushover analysis.

*Table 7.3. Weights, lever arms and virtual displacements of the west and east facades mechanisms.*

| Façade | Part | Description | Weight (ton) | X (m) | Z (m) | δ(m) |
|---|---|---|---|---|---|---|
| West | W | Full facade | 26676 | 3,05 | 21,19 | 0,57 |
| East | W1 | Two buttresses | 1894 | 0,75 | 12,25 | 0,58 |
| | W2 | Half of the adjacent bay | 389 | 4,20 | 18,50 | 0,42 |
| | W3 | Triumphal arch and flying arches | 2356 | 1,95 | 13,20 | 0,50 |
| | W4 | Two column-like masses | 1256 | 0,60 | 9,90 | 0,50 |

*Table 7.4. The calculated parameters for the two mechanisms.*

| Façade | $\alpha_o$ | M* (Kg) | e*(m/s²) | $a_0^*$ |
|---|---|---|---|---|
| West | 0,144 | 2719270 | 1,000 | 0,144g |
| East | 0,118 | 5362 | 0,988 | 0,118g |

## 7.6 Nonlinear dynamic analysis

### 7.6.1 Dynamic seismic loading

The EC-08 (CEN, 2004) gives two choices for the representation of the seismic action as time-history ground acceleration, the first is the use of artificial accelerograms and the second is the use of recorded accelerograms. The two approaches were used and in the following are presented and compared.

#### 7.6.1.1 Artificial accelerograms

For Mallorca cathedral site, using the software SeismoArtif (SeismoArtif, 2013) seven artificial accelerograms were defined for each case of the response spectra of EC-08 (CEN, 2004) and NCSE-02 (NCSE-02, 2002) considering the two return periods of 475 and 975 years. The accelerograms were compatible with the spectra and were adapted to its frequency contents as required by the considered codes.

Figure 7.29 shows as an example one time-history for each code and return period. The four time-histories had the same time length about 7,5 seconds and they differed in the maximum PGA value and the significant time duration.

The comparison between the four cases in terms of the average PGA and the average significant duration of the seven records is shown in Figure 7.30. For the two considered return periods, the average PGA's of the time-histories of the NCSE-02 were higher than those of the EC-08. This was consistent with the spectra of the two codes (previously presented in Figure 7.2). Regarding the significant duration, for all cases it changes in narrow range from about 4,05 to 4.27 seconds.

Figure 7.31 plots the average spectra of the seven accelerograms of the four cases with comparison with the codes spectra and the upper (+10%) and the lower (-10%) limits. As can be noticed for the four cases, the first branch of the spectrum was slightly higher than the upper limit, the second branch was aligned with the upper limit and the third branch was contained with the upper and lower limits.

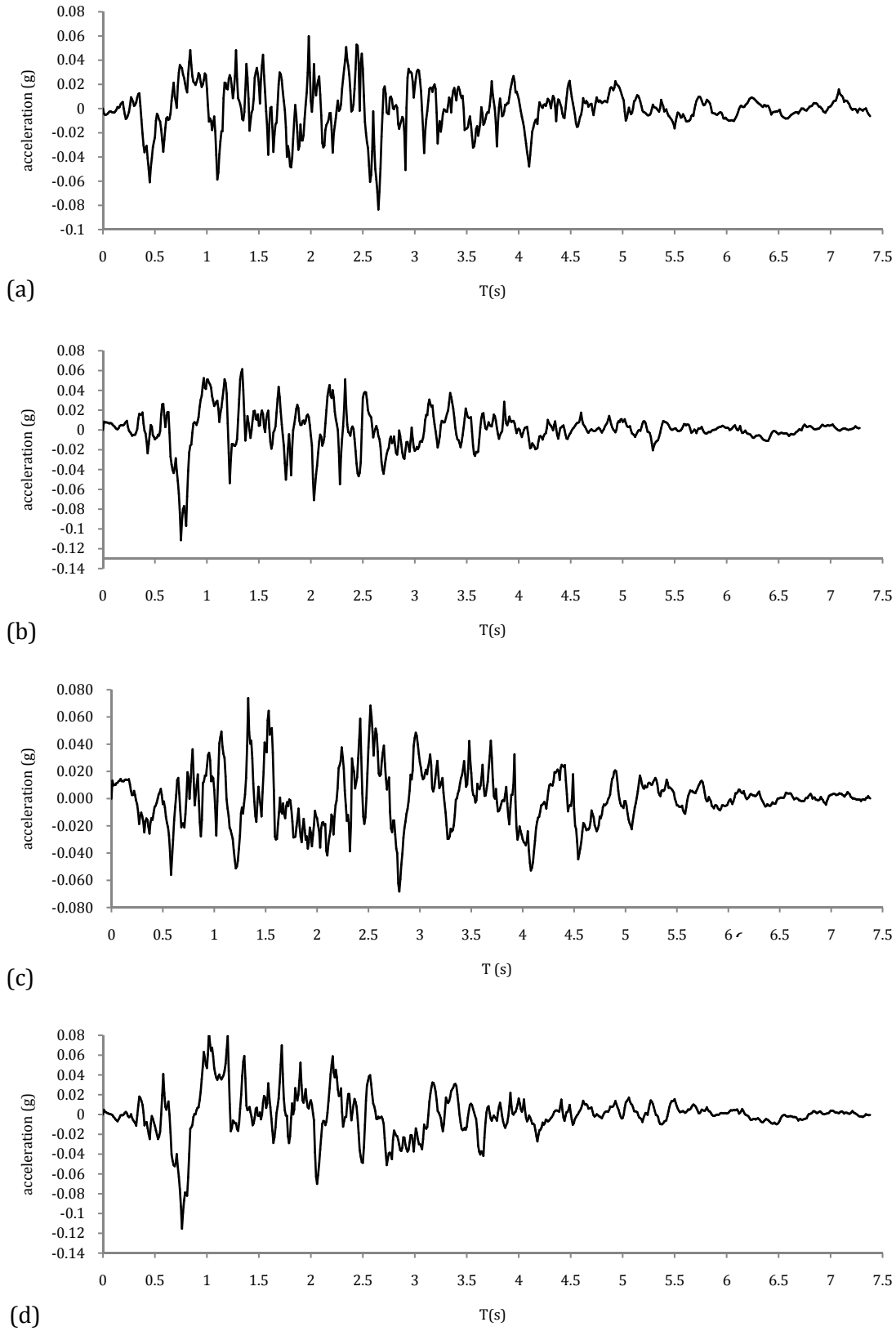


*Figure 7.29. Artificial time-histories compatible with: (a) EC-08 (475 years); (b) EC-08 (975 years); (c) NCSE-02 (475 years); and (d) NCSE-02 (975 years).*

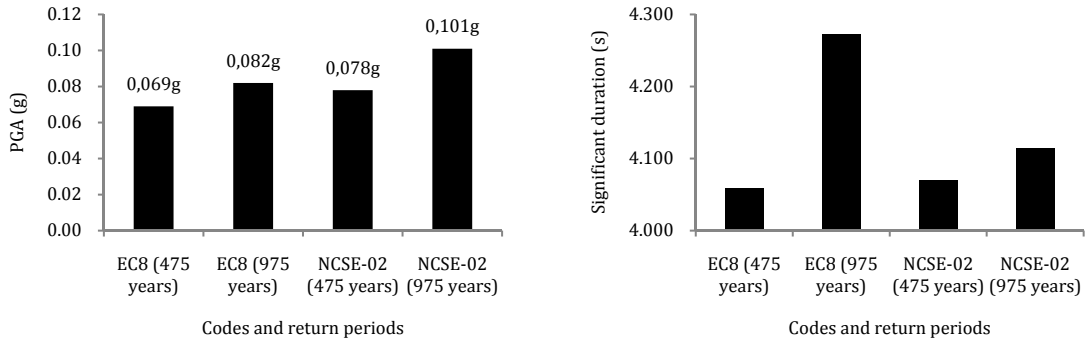


*Figure 7.30. Comparison between artificial time-histories of considered codes and return periods: average PGA (left) and significant duration (right).*

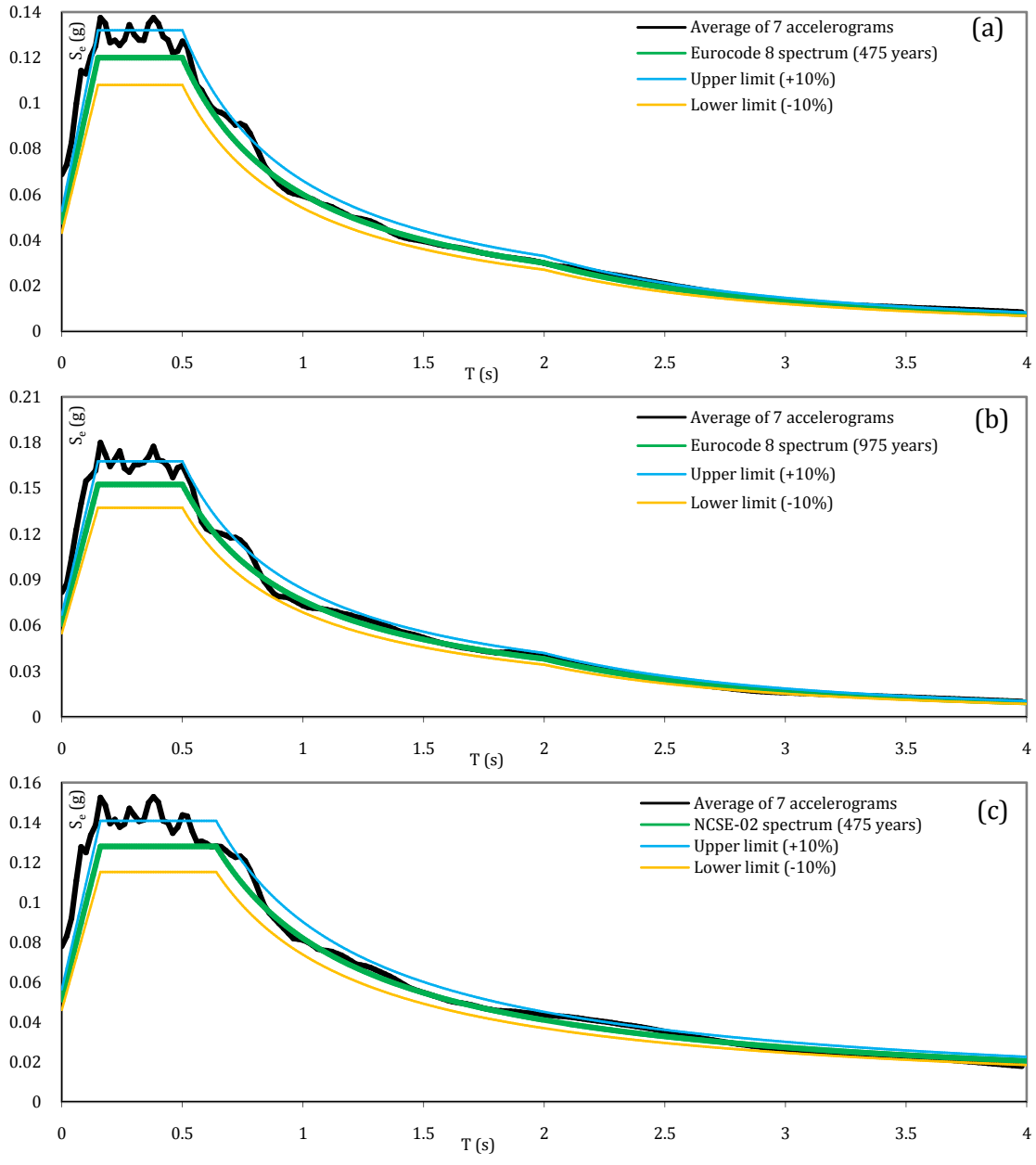

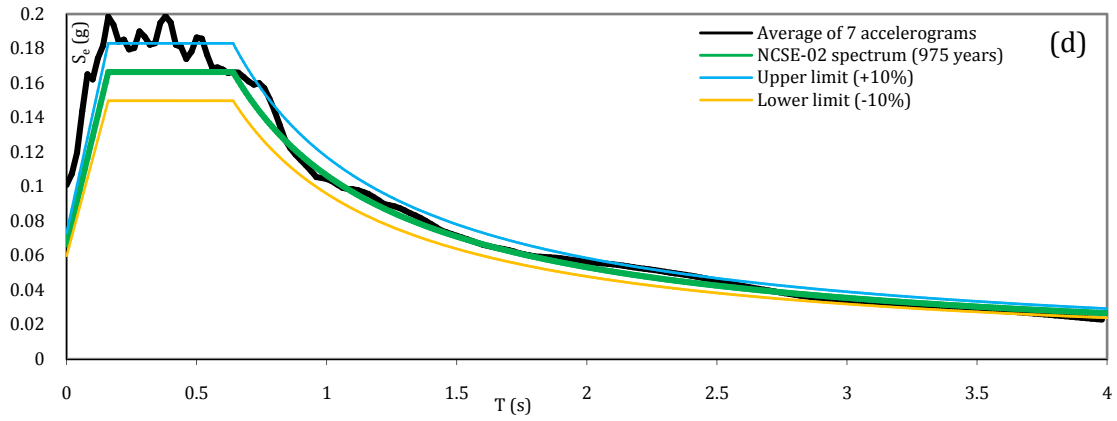


*Figure 7.31. Spectra of the four cases using SeismoArtif : (a) Eurocode 8 (475 years); (b) Eurocode 8 (975 years); (c)NCSE-02 (475 years); and (d) NCSE-02 (975 years).*

### 7.6.1.2 Real records accelerograms

The software REXEL v 3.5 (Iervolino et al. 2010) was used to find a compatible set of real records which their average spectrum is matched with the code spectrum. Each set was formed by seven real records. The records were selected from the European Strong-motion Database (http://www.isesd.cv.ic.ac.uk).

Table 7.5 reports the set of the seven earthquakes for each code and return period. The earthquake component and the station are mentioned in the table because for the same earthquake different PGA can be encountered depending on the direction of the earthquake component and the registration station. The highest PGA was not more than 0,101g which seemed reasonable for a low-to-moderate seismic intensity site of Mallorca Island.

A comparison between the averages PGA of the four combinations is depicted in Figure 7.32. As opposed to SeismoArtif, no information about the significant duration of the records was given by REXEL. Some examples of the real records are shown in Figure 7.33. The average spectra of the seven real records of the four cases in comparison with the codes spectra and the upper (+10%) and the lower (-10%) limits are plotted in Figure 7.34. For the two return periods of EC-08, the average spectra were within the limits or slightly higher than the upper limit. On the other side, for NCSE-02, the average spectra were slightly lower than the lower limit for periods more than 2 s and 2,5 s for 475 and 975 years, respectively. However, these spectra were still suitable since the periods of interest for Mallorca cathedral were from T=0,7 s or less, where 0,7 s was the period of the first mode.

*Table 7.5. Details of the combination of earthquake records compatible with the spectrum of each code and return period.*

| Code (return period) | Earthquake name (component direction-station) | Date | $M_w$ | PGA(g) |
|---|---|---|---|---|
| EC-08 (475) | Umbria Marche aftershock (y-ST228) | 03/04/1998 | 5,1 | 0,046 |
| | Friuli (x-ST15) | 06/05/1976 | 6,5 | 0,052 |
| | Izmit (y-ST574) | 17/08/1999 | 7,6 | 0,042 |
| | Izmit (y-ST2572) | 17/08/1999 | 7,6 | 0,063 |
| | Montenegro (y-ST70) | 15/04/1979 | 6,9 | 0,058 |
| | Montenegro (aftershock) (y-ST77) | 24/05/1979 | 6,2 | 0,055 |
| | Gulf of Akaba (y-ST2898) | 22/11/1995 | 7,1 | 0,091 |
| EC-08 (975) | Almiros aftershock (y-ST1300) | 11/08/1980 | 5,2 | 0,072 |
| | Izmit (x-ST766) | 17/08/1999 | 7,6 | 0,086 |
| | Ano Liosia (x-ST1141) | 07/09/1999 | 6,0 | 0,085 |
| | Ano Liosia (x-ST1255) | 07/09/1999 | 6,0 | 0,087 |
| | Friuli (aftershock) (x-ST28) | 15/09/1976 | 6,0 | 0,066 |
| | Manjil (x-ST190) | 20/06/1990 | 7,4 | 0,068 |
| | Ano Liosia (y-ST1257) | 07/09/1999 | 6,0 | 0,086 |
| NCSE-02 (475) | Almiros aftershock (x- ST1300) | 11/08/1980 | 5,2 | 0,072 |
| | Izmit (y- ST766) | 17/08/1999 | 7,6 | 0,099 |
| | Montenegro (x- ST63) | 09/04/1979 | 5,4 | 0,071 |
| | Ano Liosia (x- ST1255) | 07/09/1999 | 6,0 | 0,087 |
| | Friuli (x- ST14) | 06/05/1976 | 6,5 | 0,064 |
| | Paliouri (x- ST1329) | 10/04/1994 | 5,1 | 0,062 |
| | Izmit (y- ST779) | 17/08/1999 | 7,6 | 0,076 |
| NCSE-02 (975) | Izmit (x-ST766) | 17/08/1999 | 7,6 | 0,086 |
| | Ano Liosia (x-ST1141) | 07/09/1999 | 6,0 | 0,085 |
| | Patras (y-ST178) | 22/12/1988 | 4,9 | 0,101 |
| | Aigion (y-ST1331) | 15/06/1995 | 6,5 | 0,093 |
| | Ano Liosia (y-ST1101) | 07/09/1999 | 6,0 | 0,109 |
| | Umbria Marche aftershock (y-ST265) | 14/10/1997 | 5,6 | 0,082 |
| | Izmit (x-ST556) | 17/08/1999 | 7,6 | 0,092 |

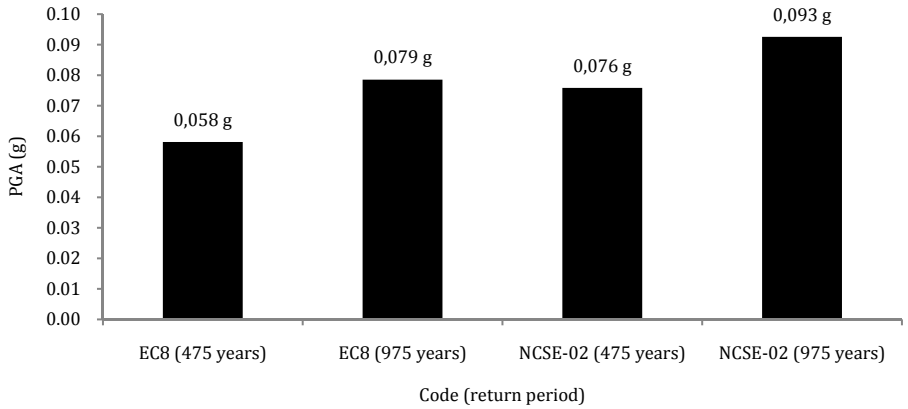


*Figure 7.32. The average PGA of each combination of real records compatible with each code and return period.*

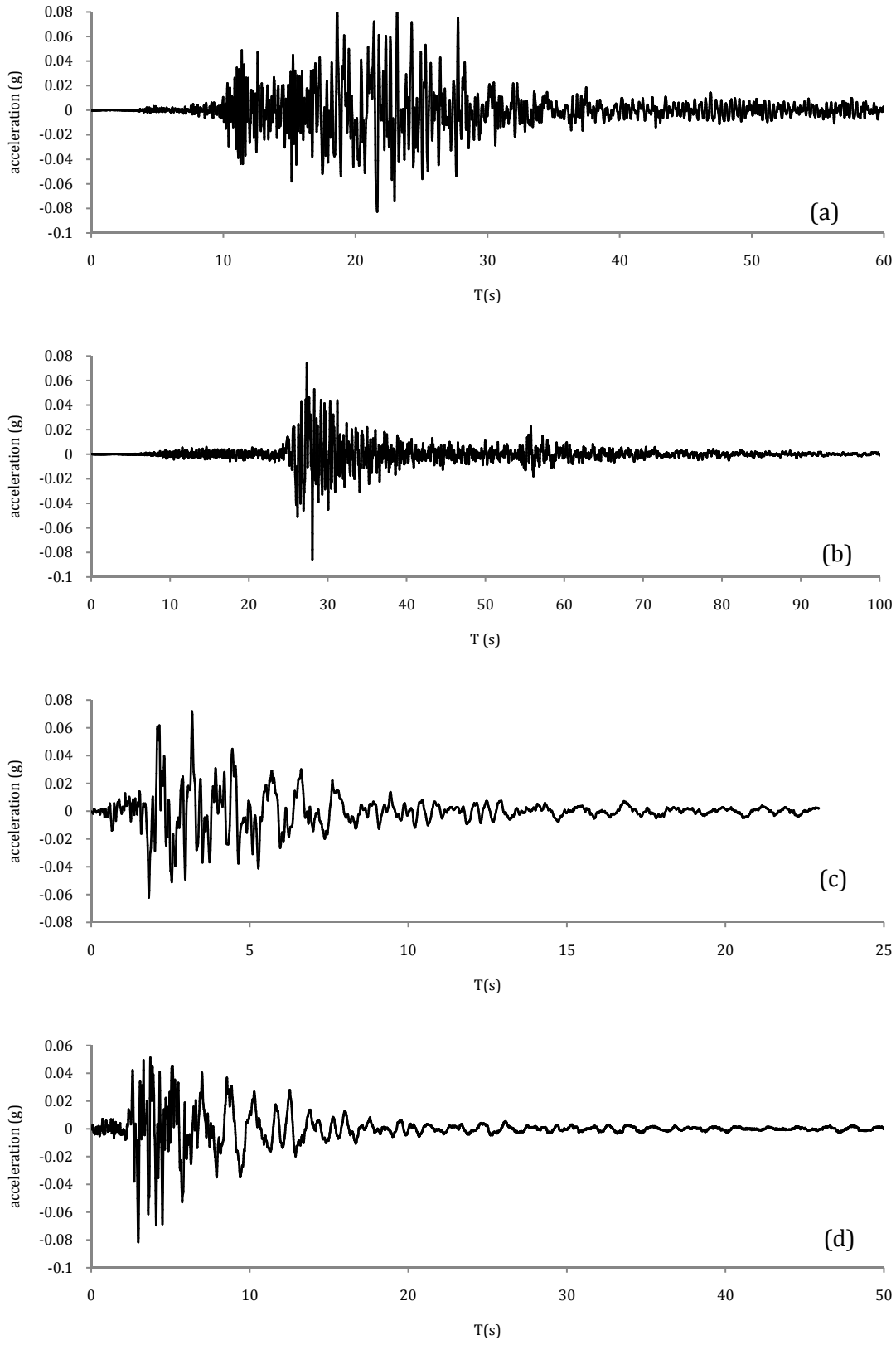


*Figure 7.33. Examples of the real records mentioned in table 1.12 :(a) Gulf of Akaba (y-ST2898); (b) Izmit (x-ST766); (c) Almiros aftershock (x- ST1300); and (d) Umbria Marche aftershock (y-ST265).*

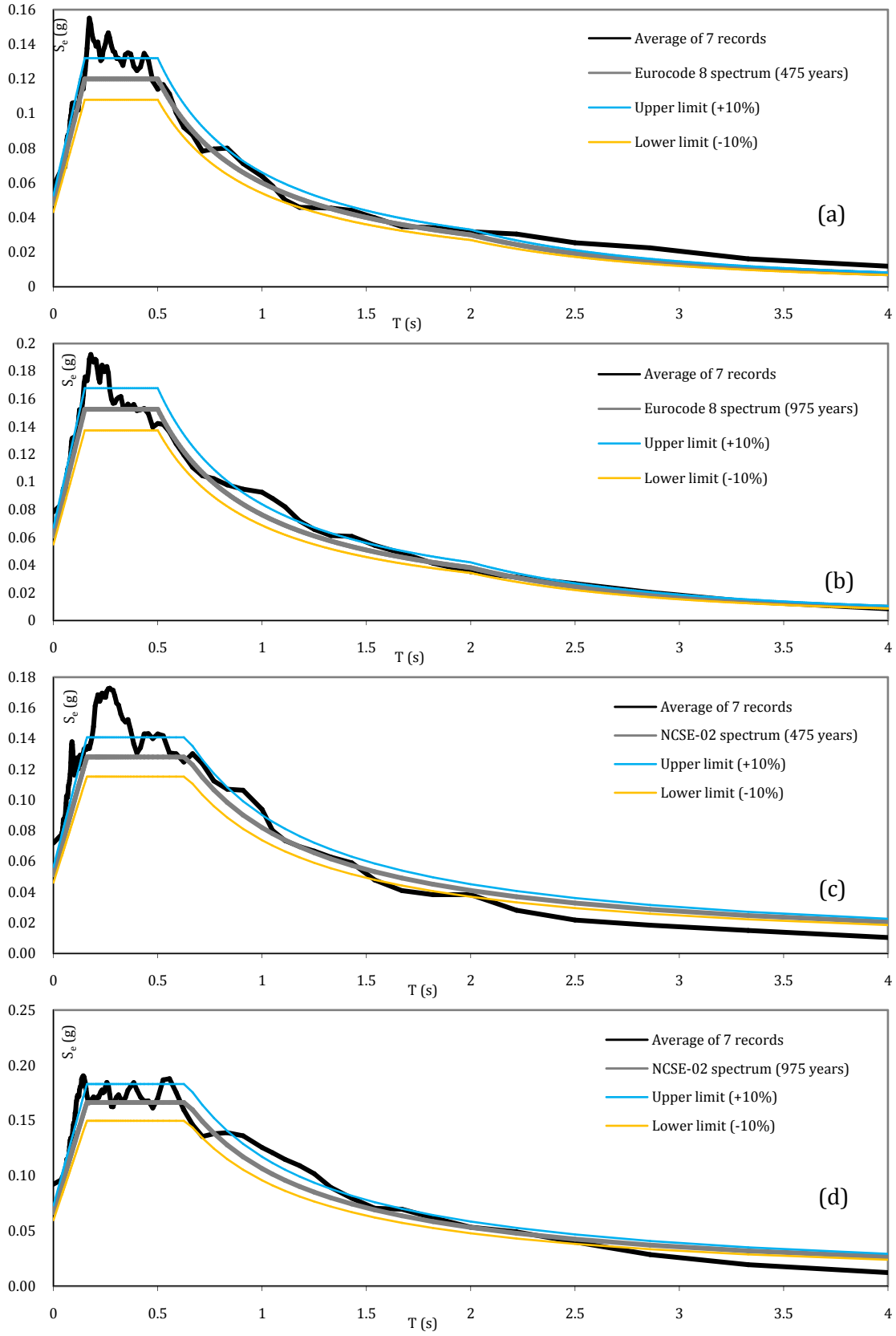


*Figure 7.34. Spectra of the four cases using REXEL: (a) Eurocode 8 (475 years); (b) Eurocode 8 (975 years); (c) NCSE-02 (475 years); and (d) NCSE-02 (975 years).*

### 7.6.1.3 Comparison between the artificial and the real records

A comparison between the average spectra of the artificial and the real records is shown in Figure 7.35. It can be seen that for the four cases considered, very near spectra were found. Also, when comparing the PGA (Figure 7.36) near values could be noticed.

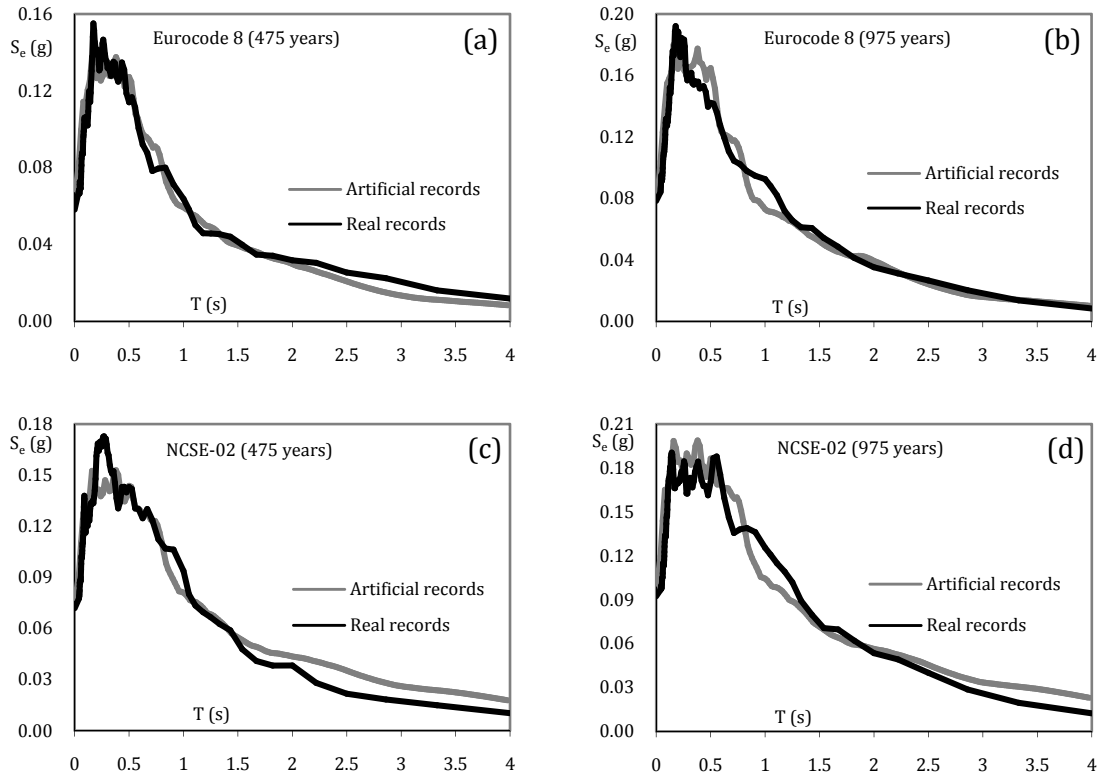


*Figure 7.35. Comparing spectra of the artificial and the real records: (a) Eurocode 8 (475 years); (b) Eurocode 8 (975 years); (c) NCSE-02 (475 years); and (d) NCSE-02 (975 years).*

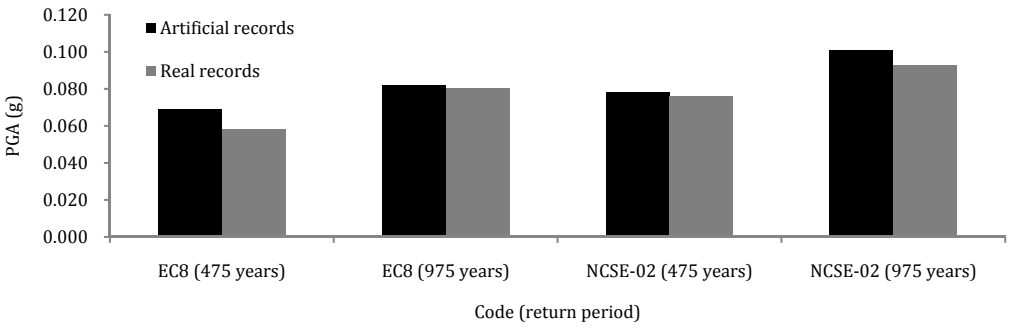


*Figure 7.36. Comparison between the average PGA (g) of the artificial and the real records.*

### 7.6.2 Time step and damping model

The analysis was carried out using one accelerogram only in one direction. The accelerogram in Figure 7.29-d was applied to the cathedral in the longitudinal direction (see results in section 7.6.3.1) and then in the transversal direction (see results in section 7.6.3.2). The time step Δt was adopted making reference to chapter 2, section 2.8.3.4. Table 7.6 presents the number of modes and the corresponding cumulative mass participation calculated from the updated FE model (refer to chapter 6). It was observed that considering 600 modes resulted in a cumulative mass participation of 89%, 100% in the longitudinal and the transversal directions, respectively, which satisfied the requirements of the Eurocode 8 (CEN, 2004). Thus, substituting $T_{600}$ (0,0407 s) in Equation 2.10 (see chapter 2) gave Δt = 0,002 s. The applied accelerogram had $t_d$ of 7,38 s, this resulted in a number of time steps =7,38/0,002= 3690 which was too much. Therefore, Δt of 0,01 s was considered and the number of the time steps was reduced to 738 (7,38/0,01). This meant that the highest considered $T_i$ equaled 20×0,01=0,2 s. This period was the same as the one of the mode number 44. Considering 44 modes gave a cumulative mass participation of about 73% and 63% in the longitudinal and the transversal directions, respectively. Although the used Δt did not satisfy the Eurocode 8 requirements, it was less computational time demanding. In addition, Δt was small enough compared with the earthquake duration so it satisfied Equation 2.9 (see chapter 2). The previously discussed reasoning was based on that followed in the nonlinear dynamic analysis of St. George of the Latins church (Trujillo, 2009; Lourenço et al., 2012).

*Table 7.6. The number of considered modes and the corresponding cumulative mass participation (%).*

| Direction | Number of considered modes | | | | | | |
|---|---|---|---|---|---|---|---|
| | 50 | 100 | 200 | 300 | 400 | 500 | 600 |
| Longitudinal | 70 | 73 | 78 | 82 | 87 | 88 | 89 |
| Transversal | 79 | 91 | 96 | 98 | 99 | 99 | 100 |

To introduce damping in the model, the Rayleigh damping model was used (see chapter 2, sections 2.8.3.3). The first mode was considered as the $i^{th}$ mode, since it has a significant mass participation in the longitudinal direction (see chapter 4). The $j^{th}$ mode was the mode number 44 as found from the previous calculations of Δt. Assuming a reasonable damping of 0,05 (Mendes, 2012; Cagnan, 2012; Peña et al., 2010), the Rayleigh coefficients were calculated as $a_0$=0,68858 and $a_1$=0,00253. Figure 7.37 shows the variation of Rayleigh damping along the natural frequencies of the cathedral. As seen, the

damping is 0,05 or less in the range from 1,41 Hz (mode 1) to 4,92 Hz (mode 44) then values more than 0,05 can be noticed for the modes higher than 44.

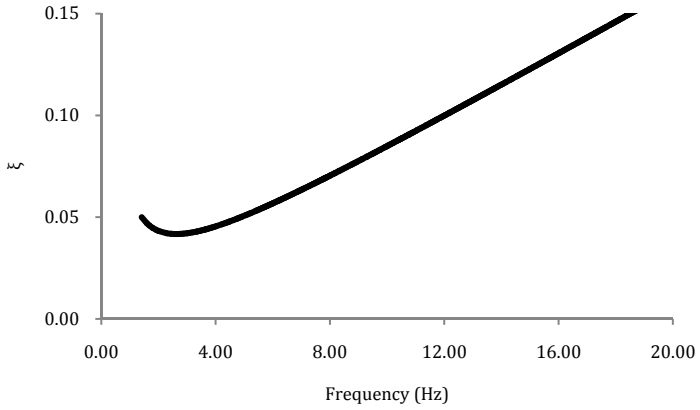


*Figure 7.37. Distribution of Rayleigh damping along the cathedral modes.*

### 7.6.3 Results

#### 7.6.3.1 Analysis for earthquake acting in the longitudinal direction

The cathedral was able to resist the complete time history without collapse. The analysis lasted for 8 days and about 12 hours using a standard PC provided with Intel ® Core ™ i5 of 2.67 GHz and RAM of 8 GB.

Regarding the displacement history in time, it was found that the points with the highest displacement were the same as found in the pushover analysis in ±X directions, refer to Figures 7.3 and 7.7. In Figure 7.38 the displacements' time histories of the control points previously considered in the pushover analysis are shown. The displacements obtained from this analysis were compared with those obtained from the pushover analysis in Table 7.7. It can be observed that the values of the two analyses were different for all control points.

The damage at the two time steps of the maximum displacements (points "a" and "b" in Figure 7.38) are depicted in Figure 7.39. These damage patterns had the same scale of those presented for the pushover analysis in Figures 7.4, 7.5, 7.6, 7.8 and 7.9. It is noticed that the damaged locations were the same as that found by the pushover analysis in ±X directions. However, lesser damage than the pushover cases could be noticed because the absolute maximum resisted load was 0,071g which was lesser than the capacities obtained by the pushover as can be noticed in Figure 7.40 that shows the relation between the displacements of the control points and the seismic load multiplier (the horizontal reaction/the self weight).

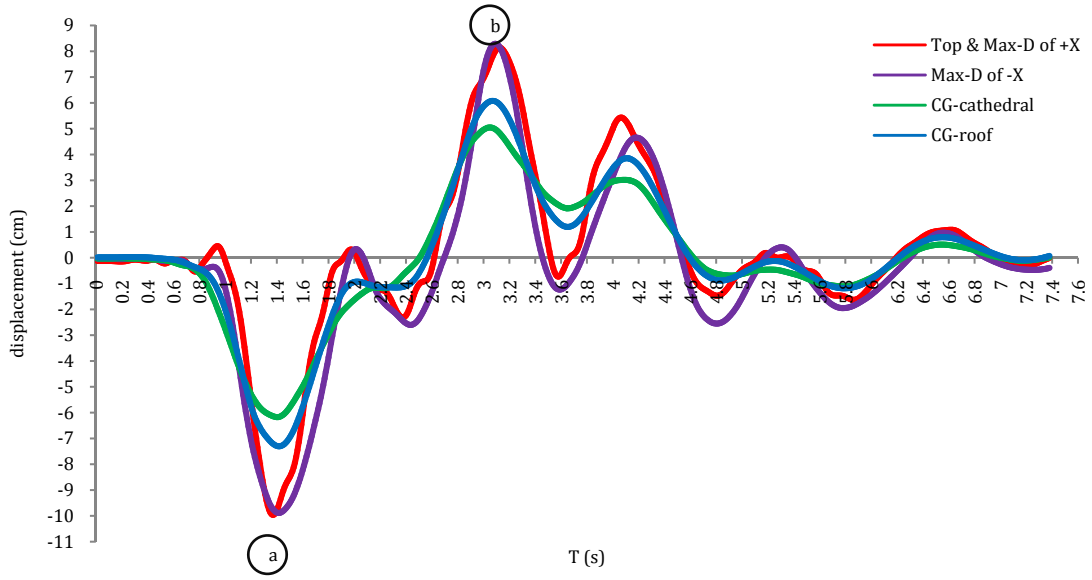


*Figure 7.38. Time histories of the displacements of the considered control points.*

*Table 7.7. Control points displacements from pushover (±X) and nonlinear dynamic analyses.*

| Case | Control point | | | |
|---|---|---|---|---|
| | CG-cathedral | CG-roof | Max-D | Top |
| Pushover +X | 4,0 | 7,3 | 13,8 | 13,8 |
| Pushover –X | 3,0 | 4,7 | 13,5 | 6,0 |
| Nonlinear dynamic | 6,2 | 7,3 | 10,0 | 10,0 |

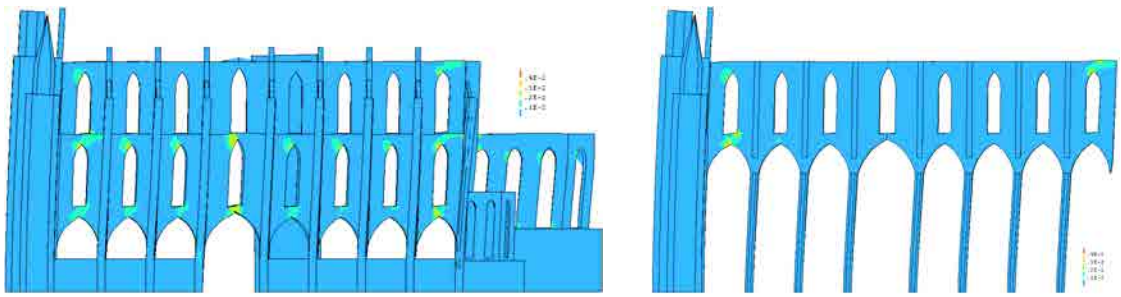

Damage pattern at the maximum negative displacement (point “a” in Figure 7.38)

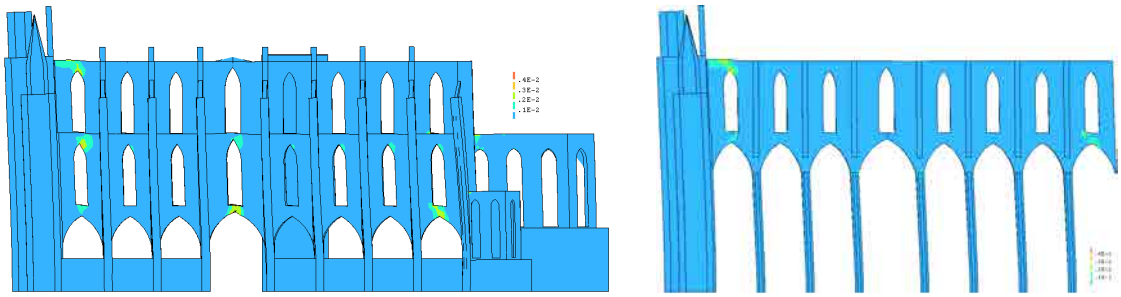

Damage pattern at the maximum positive displacement (point “b” in Figure 7.38)

*Figure 7.39. Damage pattern in the two typical resisting frames. Contour of maximum principal strain plotted on deformed mesh.*

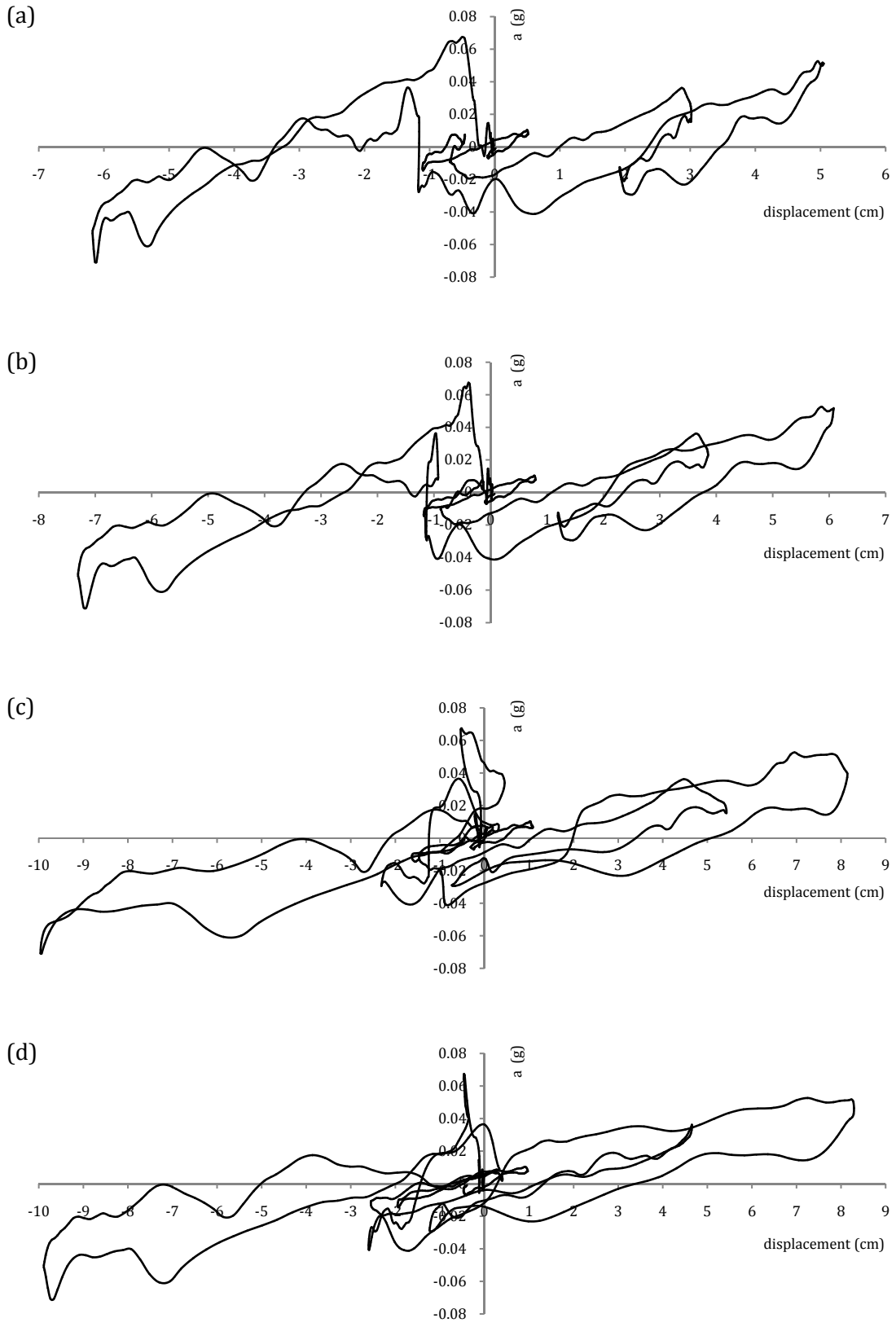


*Figure 7.40. Relation between seismic load multiplier and displacements of control points: (a) CG-cathedral; (b) CG-roof; (c) Top & Max-D of +X; and (d) Max-D of –X.*

### 7.6.3.2 Analysis for earthquake acting in the transversal direction

The cathedral resisted the full accelerogram without collapse. The analysis lasted for 5 days and about 12 hours. Figure 7.41 reports the time history of the different control points previously considered. Also in this analysis the displacements found were different from those obtained by the pushover analysis, Table 7.8.

The same locations of hinges previously found by the pushover analysis were obtained by the nonlinear dynamic analysis with clearly less damage than the pushover cases in ±Y directions, Figure 7.42. This was found (as the previous case of the longitudinal direction) because the absolute maximum resisted load was 0,09g which was 31% and 57% less than the those resisted in +Y and –Y, respectively, using the pushover analysis. Finally, Figure 7.43 shows for some points the relation between the displacements and the seismic load multiplier.

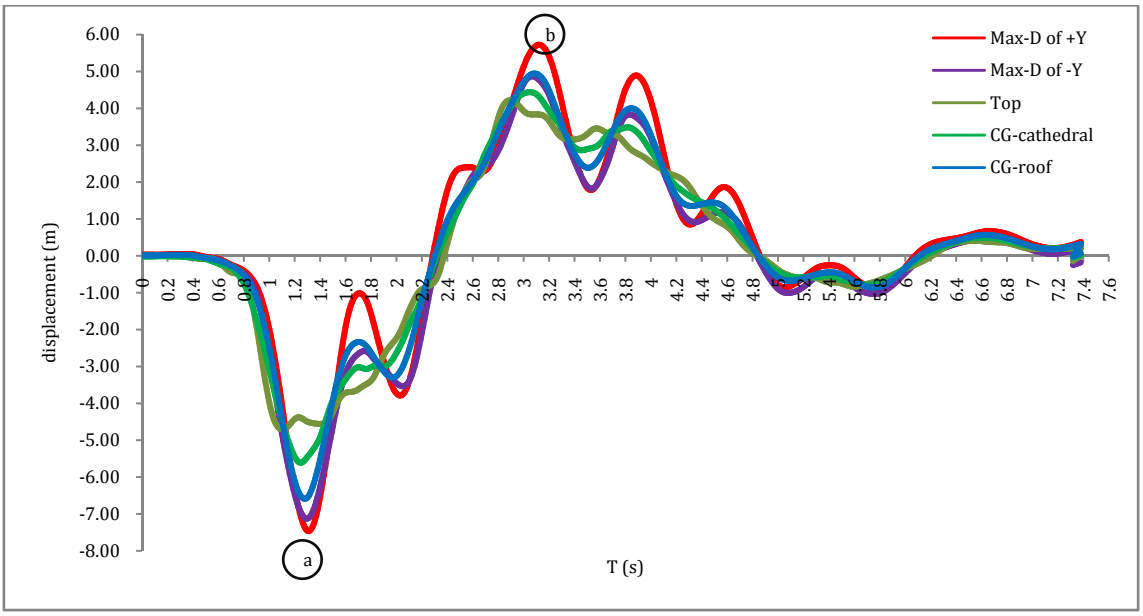


*Figure 7.41. Time history of the displacements of the considered control points.*

*Table 7.8. Control points displacements from pushover (±Y) and nonlinear dynamic analyses.*

| Case | Control point | | | |
|---|---|---|---|---|
| | CG-cathedral | CG-roof | Max-D | Top |
| Pushover +Y | 2,4 | 4,5 | 7,6 | 0,9 |
| Pushover –Y | 2,3 | 3,6 | 8,5 | 1,0 |
| Nonlinear dynamic | 5,6 | 6,6 | 7,5 | 4,7 |

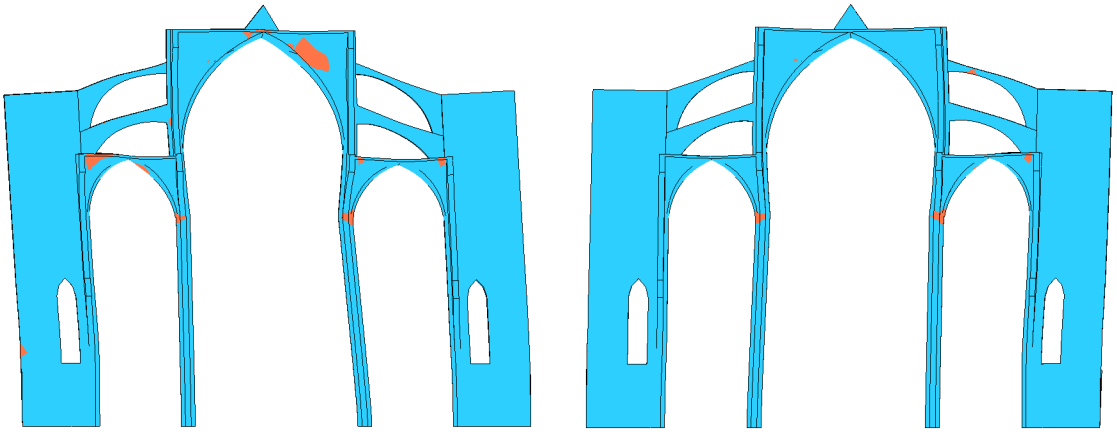

*Figure 7.42. Damage pattern in a typical frame (frame 2). Contour of maximum principal strain plotted on deformed mesh: (left) damage pattern at the maximum negative displacement, point "a" in Figure 7.41, (right) Damage pattern at the maximum positive displacement (point "b" in Figure 7.41).*

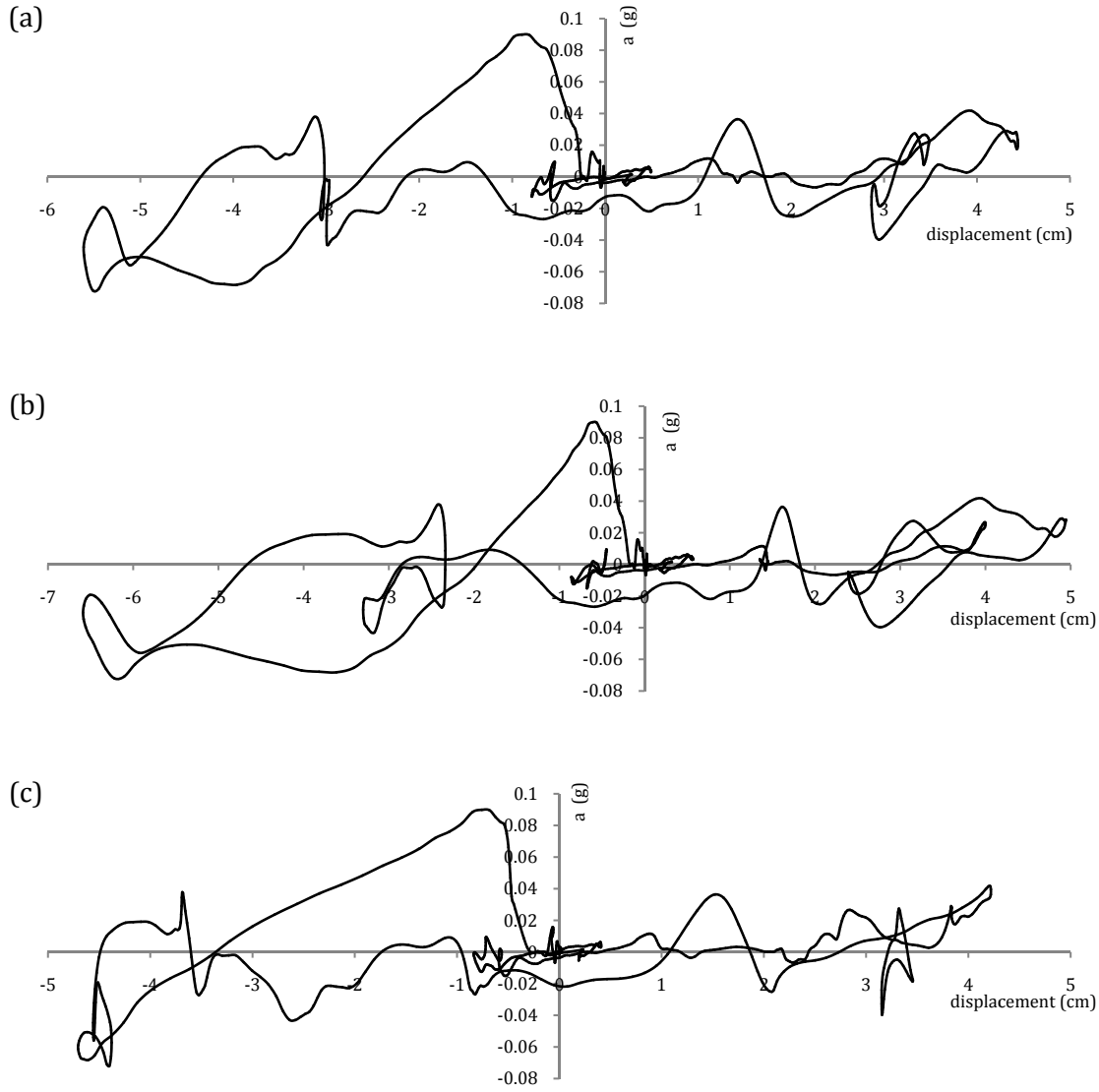

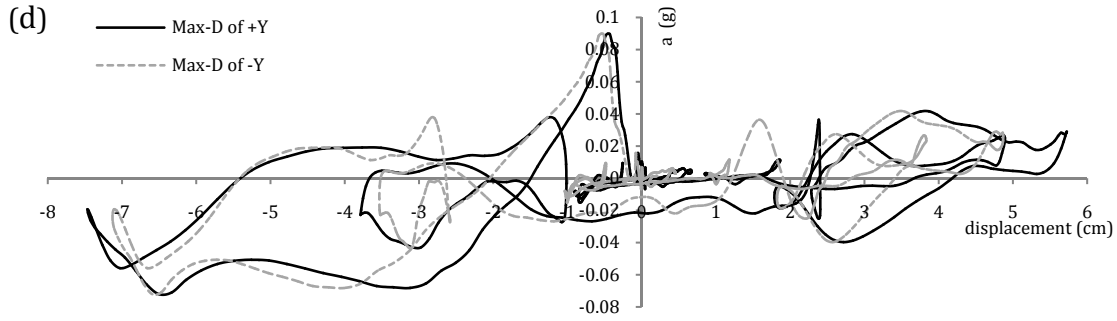


*Figure 7.43. Relation between seismic load multiplier and displacements of control points: (a) CG-cathedral; (b) CG-roof ; (c) Top; and (d)Max-D of +Y and Max-D of –Y.*

## 7.7 Evaluation of the seismic performance

The N2 method was used to evaluate the seismic performance of the cathedral. The theoretical background of the method was discussed in chapter 2. A total of 64 performance points were determined. Those were obtained from 4 directions of seismic analysis × 4 control points × 2 codes × 2 return periods.

Figure 7.44 shows, as an example, the application of the method to the evaluation of the seismic performance in +X direction considering the control point CG-cathedral and the Eurocode 8 with a return period of 975 years. The found values were 0,421 m/s$^2$ (0,043g) and 0,06m for the performance load multiplier ($LM_p$) and the performance displacement ($D_p$), respectively. In Table 7.9 the results for the rest of cases are reported. It was always observed that the lowest and the highest $D_p$ and $LM_p$ were attributed to the cases of EC-08 with return period of 475 years and NCSE-02 with return period of 975 years, respectively. Near values for $D_p$ and $LM_p$ were obtained for the other two cases of EC-08 (return period of 975) and NCSE-02 (return period of 475 years) because the descending branch of these two spectra were near to each other (see Figure 7.2).

The performance points were found on the elastic branch of the equivalent bilinear curves except for (1) the control point Top in the case of +Y direction regardless the demand spectra or the return period; (2) the control point Top in the case of –Y direction with the return period of 975 years and regardless the demand spectra. It can be noticed that the $LM_p$ for the first case was 0,09g and for the second case was 0,11g, see Table 7.9.

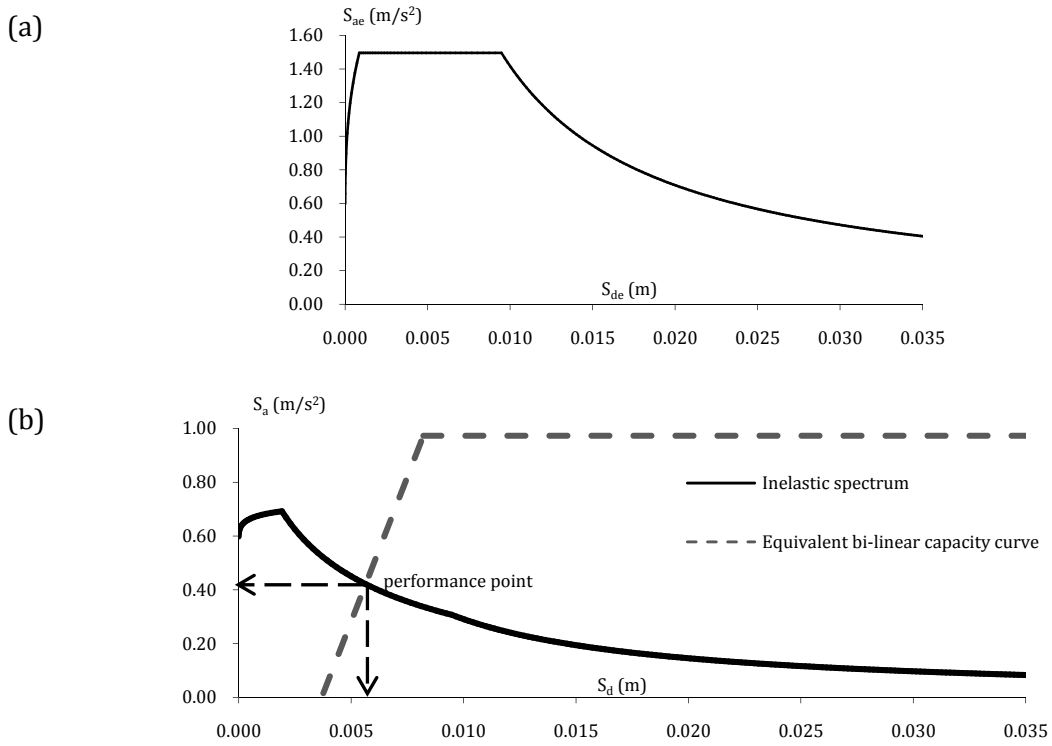


*Figure 7.44. Application of the N2 method to the control point of CG-cathedral (case of +X direction) and EC-08 (return period of 975 years): (a) The elastic response spectrum in AD (acceleration – displacement) format; and (b) the performance point.*

*Table 7.9. The performance displacements Dp (cm) and the performance load multiplier LMp (a (g)) for the different control points.*

| Analysis Direction | Code (return period, years) | CG-cathedral | | CG-roof | | Top | | Max-D | |
|---|---|---|---|---|---|---|---|---|---|
| | | $D_p$ | $LM_p$ | $D_p$ | $LM_p$ | $D_p$ | $LM_p$ | $D_p$ | $LM_p$ |
| +X | EC-08 (475) | 0,5 | 0,032 | 0,9 | 0,024 | 1,1 | 0,018 | 1,1 | 0,018 |
| | EC-08 (975) | 0,6 | 0,043 | 1,1 | 0,035 | 1,4 | 0,025 | 1,4 | 0,025 |
| | NCSE-02 (475) | 0,6 | 0,043 | 1,1 | 0,036 | 1,4 | 0,029 | 1,4 | 0,029 |
| | NCSE-02 (975) | 0,7 | 0,060 | 1,2 | 0,050 | 1,7 | 0,040 | 1,7 | 0,040 |
| -X | EC-08 (475) | 0,7 | 0,040 | 0,9 | 0,029 | 1,3 | 0,028 | 1,0 | 0,019 |
| | EC-08 (975) | 0,8 | 0,055 | 1,1 | 0,041 | 1,5 | 0,038 | 1,2 | 0,025 |
| | NCSE-02 (475) | 0,8 | 0,053 | 1,1 | 0,042 | 1,6 | 0,042 | 1,2 | 0,028 |
| | NCSE-02 (975) | 0,9 | 0,071 | 1,2 | 0,059 | 2,0 | 0,058 | 1,6 | 0,038 |
| +Y | EC-08 (475) | 0,5 | 0,043 | 0,9 | 0,030 | 0,9 | 0,090 | 0,8 | 0,022 |
| | EC-08 (975) | 0,6 | 0,057 | 1,0 | 0,043 | 1,4 | 0,090 | 0,9 | 0,032 |
| | NCSE-02 (475) | 0,6 | 0,056 | 0,9 | 0,043 | 1,6 | 0,090 | 0,9 | 0,032 |
| | NCSE-02 (975) | 0,7 | 0,076 | 1,1 | 0,060 | 2,6 | 0,090 | 1,0 | 0,045 |
| -Y | EC-08 (475) | 0,7 | 0,042 | 0,7 | 0,047 | 0,8 | 0,092 | 0,7 | 0,023 |
| | EC-08 (975) | 0,8 | 0,060 | 0,8 | 0,065 | 1,0 | 0,110 | 0,8 | 0,031 |
| | NCSE-02 (475) | 0,8 | 0,057 | 0,8 | 0,062 | 0,8 | 0,104 | 0,8 | 0,032 |
| | NCSE-02 (975) | 0,8 | 0,081 | 0,8 | 0,087 | 2,0 | 0,110 | 0,9 | 0,045 |

To highlight the effect of the control point choice on the evaluation of the cathedral seismic safety, the ratios between the maximum displacements and the $D_p$ are shown in Figure 7.45. In this figure, it is clear that the highest ratios were found (for any of the analysis directions) when using the point Max-D. The two control points CG-cathedral and CG-roof showed near ratios and lesser ones than those of Max-D point.

As expected, the point Top presented larger displacements (higher than CG-cathedral and CG-roof and lesser than Max-D) only for the case of +X direction. In the -X direction, the ratios were near to those of CG-cathedral and CG-roof. In the ±Y directions, the ratios were small. Recalling that the point Top was located on the top of the west façade gable, it seemed that using it for the case of +X direction (the west façade is pushed outside its plane) is appropriate and representative choice. However, using it for the other directions seemed to be inadequate to represent the displacement capacity of the cathedral.

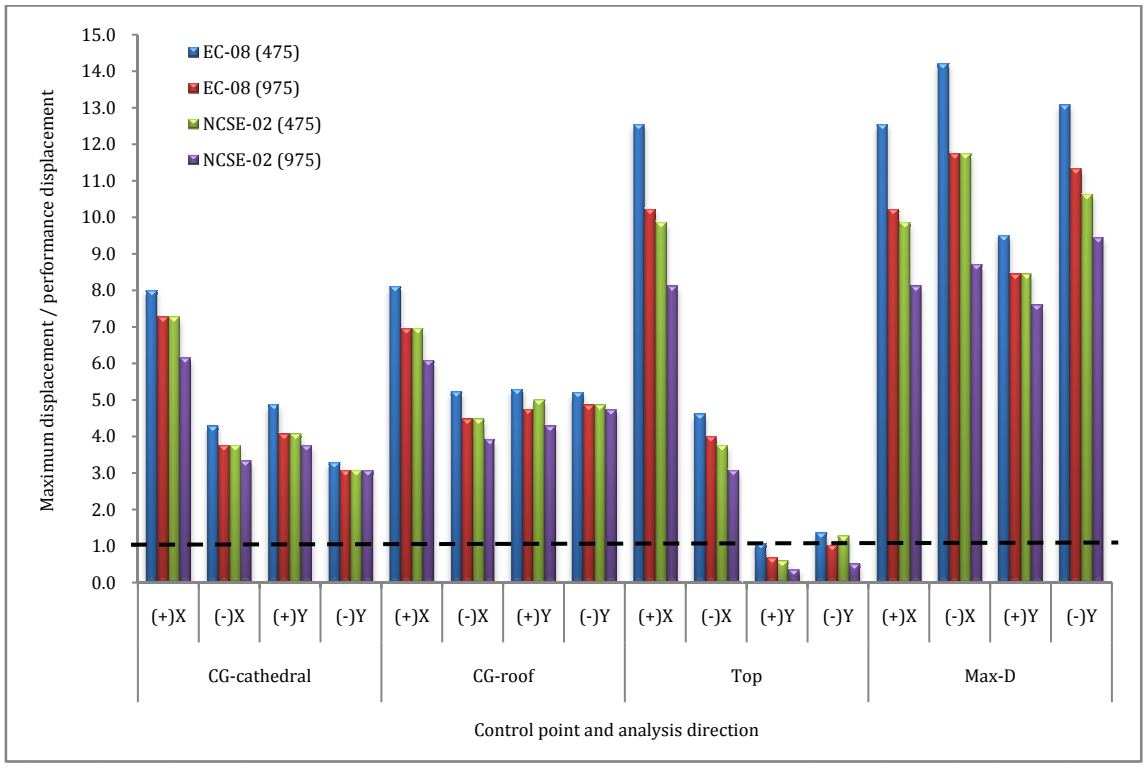


*Figure 7.45. Evaluation of seismic safety in terms of displacements: ratios between maximum displacements and performance displacements.*

Similarly, the ratios between the collapse load multiplier and the $LM_p$ are shown in Figure 7.46. The same comments mentioned on the displacements comparison, can be

mentioned again on the load multiplier comparison. It was found that the point Max-D gave the highest ratios and the point Top did not give reasonable values for all directions except the +X one. Slightly higher ratios were obtained for the point CG-roof than those obtained for CG-cathedral. For any combination of demand spectrum, return period, analysis direction and control point, no ratio less than one was found. This is an indicator of the sufficient seismic capacity of the cathedral.

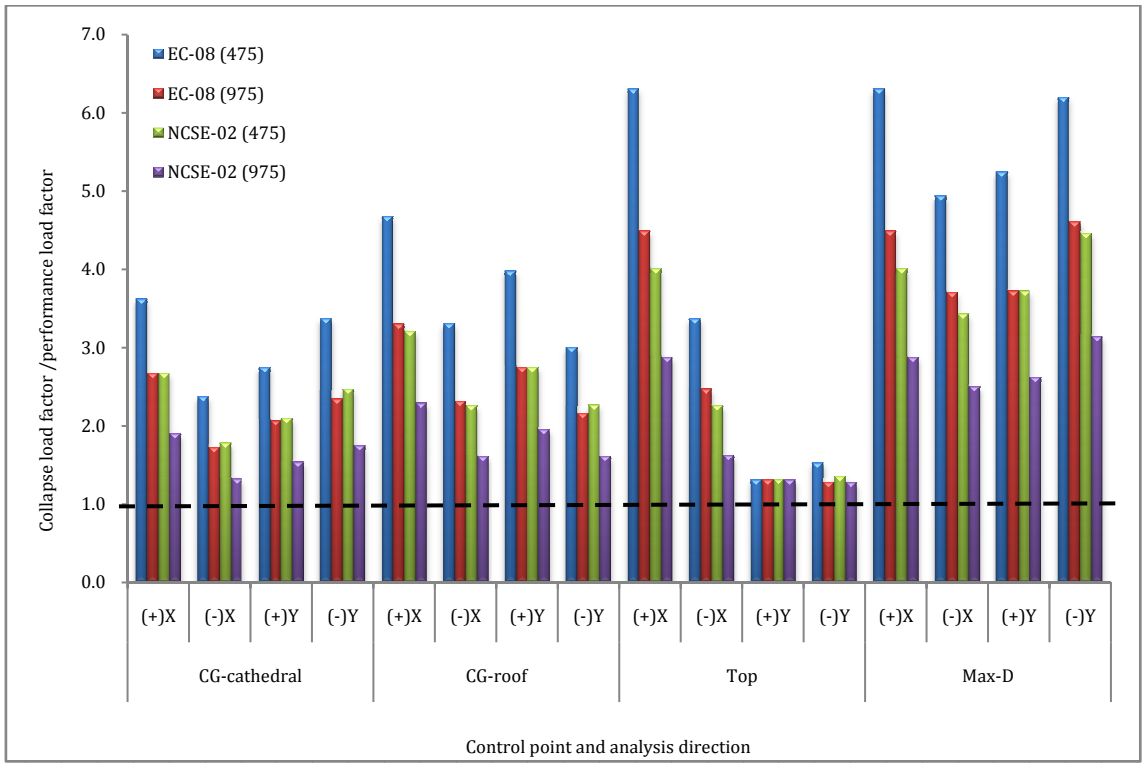


*Figure 7.46. Evaluation of seismic safety in terms of load multipliers: ratios between collapse load multipliers and performance load multipliers.*

## 7.8 Conclusions

In this chapter the seismic analysis of Mallorca cathedral was carried out using three different analysis techniques, these were the pushover analysis, the kinematic limit analysis and the nonlinear dynamic analysis. Afterwards, the seismic performance was evaluated using the N2 method. The main conclusions are discussed hereinafter.

The cathedral showed different capacities depending on the direction of the applied seismic loads. Higher capacity was noticed when the seismic loads were applied in the transversal direction than that found in the longitudinal one. In the transversal direction, the buttresses which represented the main seismic-resistant elements were loaded in their stiffer in-plane direction resulting in higher capacity. When the seismic loads were

applied in the longitudinal direction, lower capacity was found because the buttresses were loaded in their weaker out-of-plane direction.

The observed collapse mechanism for the seismic analysis in the longitudinal direction was the overturning of the facades. The damage was also noticed to be concentrated around the large windows openings in the clerestory walls and the apse walls, the top and the bases of the columns and the main nave vault's bay adjacent to the west façade. For the analysis in the transversal direction, a collapse mechanism composed of a number of hinges in the typical bays of the cathedral was noticed, these hinges were developed in the flying arches, the arches and vaults of the naves, the top and bases of the columns and the bases of the buttresses.

The sensitivity analysis carried out, only in the longitudinal direction, on some of the nonlinear masonry properties showed that (1) the tensile strength had a significant effect on the capacity because the observed collapse mechanism was controlled by cracking, (2) the modulus of elasticity had also a significant effect on both of the capacity and the maximum displacement, (3) increasing the compressive strength or the ultimate cracking strain did not increase the capacity but reducing these parameters reduced the capacity significantly. In all cases, the same collapse mechanism, previously mentioned, was observed.

Using the kinematic limit analysis, a good match was noticed between the found capacities by this technique and that found using the pushover analysis. The nonlinear dynamic analysis gave the same collapse mechanism like that found by the pushover analysis. However, this type of analysis was found to be very time demanding for such a large historical cathedral which prevented a detailed analysis using a sufficient number of seismic events.

Using the N2 method for evaluating the seismic performance of the cathedral, several performance points were checked using the capacity curves of the different analysis directions, two seismic codes and two return periods. The results showed that the cathedral does not need any strengthening for increasing its seismic capacity. However, other interventions including, for instance, repairing of cracks and regular maintenance should always be considered.

# CHAPTER 8

# METHODOLOGICAL CONSIDERATIONS ON SEISMIC ASSESSMENT OF LARGE HISTORICAL STRUCTURES

## 8.1 Introduction

Some considerations on the different investigation activities carried out within this research are provided in this chapter. The concept of a knowledge-based assessment is first discussed. Next, the global applied seismic assessment approach within this research is presented. A focus is then made to some considerations when carrying out the dynamic identification tests, the dynamic monitoring, the updating of the numerical model of the historical structure and the seismic assessment. These are the main involved investigation activities within the employed approach.

## 8.2 Meaning of knowledge-based assessment

When assessing the safety of a historical structure, knowledge limitations about the structure is one of the main problems to face. Relevant information about the historical structure may not be known. For instance, it may not be easy to gather sufficient information about the construction history, the used construction technique, the strength of materials, the internal morphology of the structural elements, the architectural alterations, the previous collapses and the subsequent repairs, etc. At the same time, if the safety assessment recommends any intervention in the structure, this intervention should comply with the concept of minimum intervention. This intervention is the one that causes the minimum alteration to the historical structure authenticity (conserving original materials, architectural concepts, structural configurations, etc.) while allowing to reach the targeted level of safety.

Gathering sufficient information may significantly contribute, through a better understanding of the features and problems of the building, to design a minimal intervention and avoid unnecessary strengthening operations. This knowledge can be obtained by using different investigation activities oriented to obtain enough and meaningful information on the local and the global levels of the historical structure. On the local level, it is possible to use non-destructive test (NDT) and/or minor-destructive tests (MDT) (flat jack test, GPR, tomography, etc.) that may offer valuable information. However, the obtained information is correct only for the limited locations of these tests and if no sufficient number of tests is carried out to reflect the variability in the used materials, the results may be statistically not relevant. In addition, some local tests, such as coring, might not be allowed to preserve the integrity of the structure. Therefore, it is essential to use global inspection techniques like dynamic identification tests and different types of monitoring that may be able to provide knowledge about the global behavior of

the structure. Monitoring, in specific, may contribute to a better understanding of the present structural behavior under different normal and exceptional actions

Summarizing, a knowledge-based assessment approach is the one that aims at gathering sufficient information about the historical structure by integrating different investigation activities, especially those oriented to characterize the global behavior of the historical structure, such as, in particular, monitoring.

## 8.3 Global approach for seismic assessment

Figure 8.1 presents schematically the global approach that has been derived from the study of Mallorca cathedral. As can be noticed, the approach includes three interconnected phases; these are the knowledge gain phase, the assessment phase and the intervention phase. The first phase is oriented to gain sufficient knowledge about the historical structure at both the local and global levels. This knowledge is obtained by employing inspection, dynamic identification and dynamic monitoring. The following phase is devoted to the structural assessment using basically a numerical model of the structure built based on the inspection results and satisfactory updated based on the dynamic investigation results. This second phase is expected to characterize the safety of the structure for different actions and the need for intervention. In the last phase, the intervention can be designed considering the numerical model and then assessed using again the dynamic investigations.

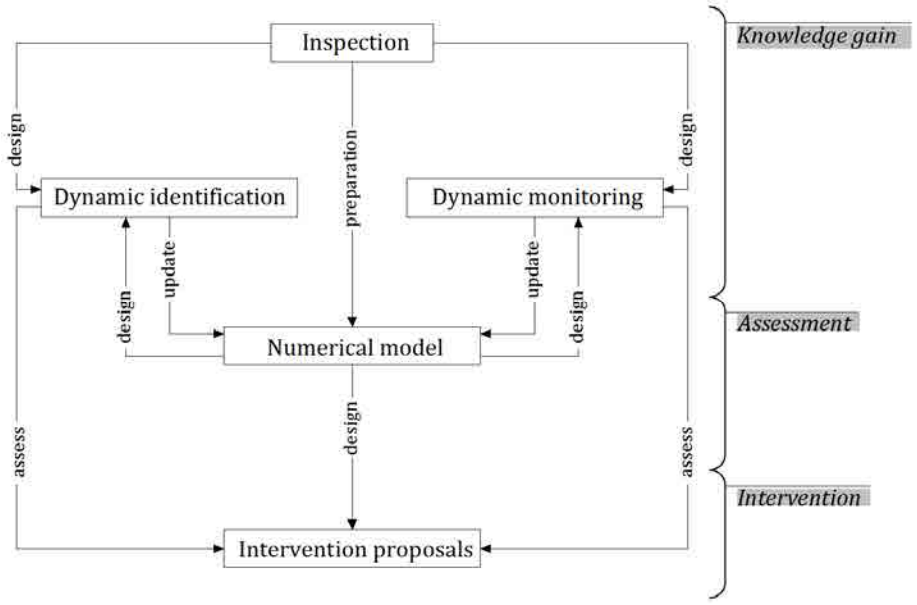


*Figure 8.1. Global approach for structural assessment of historical structures.*

Each of the above mentioned phases includes different activities or steps. These are discussed in the following paragraphs.

The first phase includes the following activities:

(I) performing a historical research to collect information about several issues such as the start and the end of the construction, any interruption periods within the construction process, the source of the construction materials, the prevailing architectural styles at the time of the construction, structures built following the same architectural style in other regions, the existence of any previous buildings at the construction site, the modifications in the structure design, and previous seismic events and the corresponding effects, among other relevant historical aspects;

(II) carrying out a visual inspection aiming at understanding the structural system, recognizing the type of used masonry; noticing any cracks, any perceptible deformations, any changes in openings by enlarging or closing; observing any previous interventions using for instance ties; and looking for any remaining evidences of the construction process like temporary ties or openings; among other important observations;

(III) producing the geometrical documentation, cracking surveys and deformations survey as well as the necessary plans, elevations and sections;

(IV) exploiting in-situ NDT's and MDT's to obtain qualitative and quantitative data on the local and the global levels of the structure. For instance, it is recommended to gain sufficient knowledge about the structural elements internal composition, the strengths of the used construction materials, and the characteristics of the foundation and foundation soil, among other related data. Here, the dynamic investigations are necessary to characterize the global dynamic behavior of the structure.

In the second phase, the collected information is used to create an initial numerical model. As seen in Figure 8.1, this model has an essential role. It is used in the design of the dynamic identification tests, as well as, the dynamic monitoring system. For instance, it can be used to provide guidance on the strategic locations of the sensors. The inspection results, such as the cracking survey, can be also considered in the design of the dynamic investigations. For instance, some dynamic tests configurations may be designed so as to characterize the possible effect of cracks on the global response.

The modal parameters emerged from the dynamic identification and monitoring are then used to update the numerical model. The experimental and numerical modal frequencies can be compared using the frequency discrepancy ($D_f$) and the experimental

and numerical modal shapes can be matched using the Modal Assurance Criteria (MAC). Obtaining a solution with minimum $D_f$ and maximum MAC will contribute to upgrade the model, allowing its later usage for seismic assessment. The obtained results are then used to evaluate the structure performance and safety. More details are given in the following sections about the adopted methodologies for these partial investigations.

If needed, interventions are proposed in the last step. It is recommended to propose more than a solution so as to allow a comparison among different solutions. For obvious reasons, only the ones allowing attaining the structural reliability target (the required safety level) should be considered. Among these, the solution that better complies with the concept of minimum intervention should be preferred. In choosing the final solution, aspects such as sufficient efficiency, ease of execution, possible future enhancing or removing (reversibility), and cost, among other relevant aspects should be also considered. The intervention proposals are examined, if possible, using the numerical model. The model works like a virtual laboratory in which the efficiency of each proposal can be characterized and measured. However, assessing the intervention using only the numerical model is not enough. Using other in-situ inspection techniques as a way to assess the intervention implementation is recommended. This is needed because it is expected that the intervention should result in positive sings like the increase in the overall stiffness of the historical structure and also the improvement of the connection between different parts of the structure. On the long term, the intervention effect and quality can be examined using dynamic monitoring. The dynamic monitoring system should work for at least one year such that the seasonal evolution of modal parameters can be observed. Longer periods of monitoring should be also considered to allow a better judgment of the intervention efficiency.

## 8.4 Considerations on the dynamic identification

In Figure 8.2, an approach for the dynamic identification of historical is shown. It includes four main phases (1) tests design, (2) tests execution and preliminary identification, (3) detailed identification and (4) evaluation. Each of these phases and the interconnection between them are discussed in the following paragraphs.

The identification process starts with the design of the dynamic identification tests. An initial inspections and an initial modal analysis are proposed as a first step. The inspection should include cracking survey and, when possible, an initial dynamic identification tests.

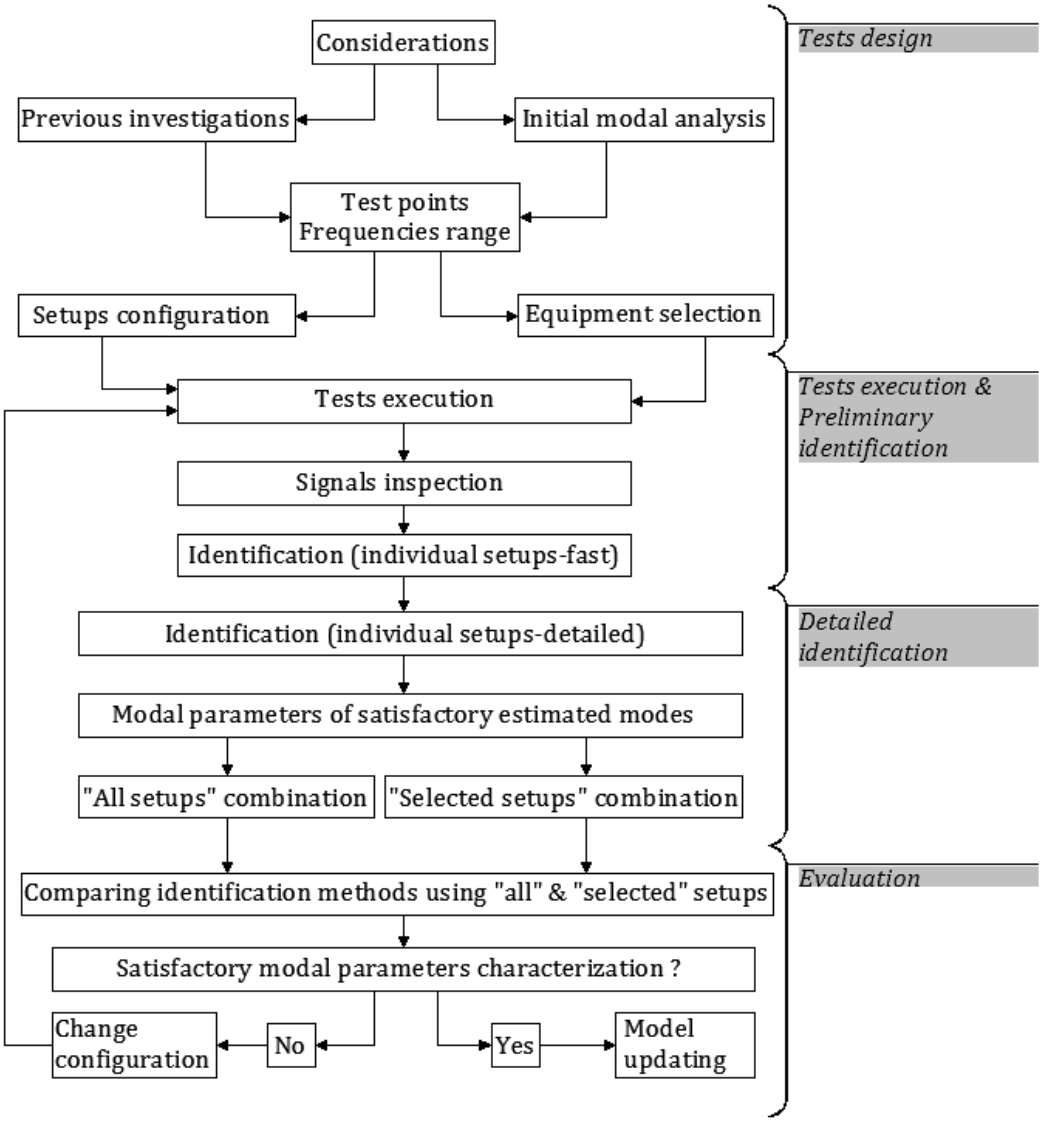


*Figure 8.2. Approach for dynamic identification of historical structures.*

If successful, the initial dynamic tests can provide information on the historical structure natural frequencies. The fundamental period of the historical structure and the range of natural frequencies are the most needed information. The first information is used to set the measurement time which, according to well established criteria, can be taken from 1000 to 2000 times the structure fundamental period. The second information is used to select the appropriate frequency range of sensors.

The cracking survey can highlight the places where the separation between different parts of the historical structure is evident. For large historical construction, it is possible in some cases, to identify a possible separation between macro-elements such as a separation between the façade of a church and its main nave or between the minaret of a mosque and the adjacent perimeter wall. These separations may be caused due to past

earthquakes, soil settlements or other effects. Specific setups can be defined to investigate the effect of such separations on the mode shapes of the historical structure.

A preliminary numerical modal analysis is essential in this phase. The structure fundamental period and its range of frequencies can be obtained by this analysis, even if approximate, and used as previously mentioned. It is also important to have an estimate for the modal shapes. In the design of tests, the focus should be in the characterization of global mode shapes because dynamic test will be normally carried out using a limited number of sensors. In addition, those mode shapes are the ones that are more relevant in the updating of the numerical model. If a sufficient number of sensors can be used, the local modes can be also considered. The strategic points to accommodate the sensors can be efficiently selected based on this initial modal analysis. It is possible to compare the normalized modal displacements of a number of candidate points and select the ones with the highest values. It is needless to say that other factors like the accessibility to some places in the historical structure and the lengths of the used cables are also of importance in designing the tests configuration.

The second phase of the approach is the execution of tests and the preliminary identification. The environmental circumstances of the tests should be investigated. In specific, the environmental actions that are known to have an effect on the dynamic behavior, such as the temperature, should be known. Any near meteorological station to the historical structure can provide this information— in case that no thermometers or hygrometers are used during tests. Also, if the structure is located in an open location and the wind may affect its dynamic behavior by exciting some of its mode, the wind parameters (the direction and the velocity) should be obtained.

The recorded signals (usually accelerations) should be visualized and checked for any anomalies. For instance, the effect of ringing of a tower bells during tests can be noticed in the signals in a form of higher peaks. The level of excitation during tests can be checked by calculating the Root Mean Square (RMS) of the measured signals. This quantity should be calculated for each channel, and then a comparison between the RMS's of all channels can be used to generate complete image on the level of excitation.

A fast and relatively accurate identification method like the FDD can be used at this stage. By processing each setup alone, it is possible to notice how many modes are contained in the signals. Moreover, it is expected that not all modes may be identified in all setups because higher modes are difficult to excite in case of using only ambient vibration.

Therefore, it is necessary to determine the number of modes that are identified in the different setups.

The third phase is the detailed dynamic identification. More advanced techniques than the FDD should be used at this stage, such as the Stochastic Subspace Identification (SSI) and the poly reference Least Squares Complex Frequency (pLSCF). The information obtained from the preliminary identification can be confirmed and refined. The possibility of applying both qualitative and quantitative criteria is an important advantage of these techniques over the FDD. The damping ratios can be also estimated with these advanced techniques.

In this detailed identification, the quality of the identified modes and the efficiency of the used setups configuration can be checked. Regarding the modes, it is possible to decide which modes are identified with good quality of estimation and in which setups. The modes that are not reliably identified (such as those that appear in a few setups and disappear in many other setups) should be determined. Regarding the setups, it may be possible to decide which ones are able to detect many modes and which ones only afford the detection of a few modes.

The post processing of each setup may allow concluding which modes are trustily estimated and which group of setups can be selected as optimal setups for their identification. To obtain the modal parameters of any mode, it is proposed to use two different setup combinations. The first combination is the conventional one in which all the setups are combined. The second one is to combine only the set of "selected optimal setups" for the mode.

When a modal parameter of a mode is identified from the different used identification methods with near values, its identification can be trusted. If, on the contrary, there is a scatter in the values, its identified value should be treated with caution. It is expected that using the set of "selected setups" should improve the quality of estimating a mode's modal parameters. Interested reader is referred to chapter 4 for an application of this approach.

## 8.5 Considerations on the dynamic monitoring

Installing a dynamic monitoring is recommended after carrying out dynamic identification tests. In principle, the dynamic monitoring system allows recording higher vibrations levels under captured seismic events and wind episodes which could allow a better characterization of the modal parameters. The dynamic monitoring system is interesting, specifically, in low seismic places where normally only low seismic motions

will be captured during the monitored period. In more seismic locations, using a threshold governed system, rather than a continuous one, may be more appropriate due to economic and technical reasons.

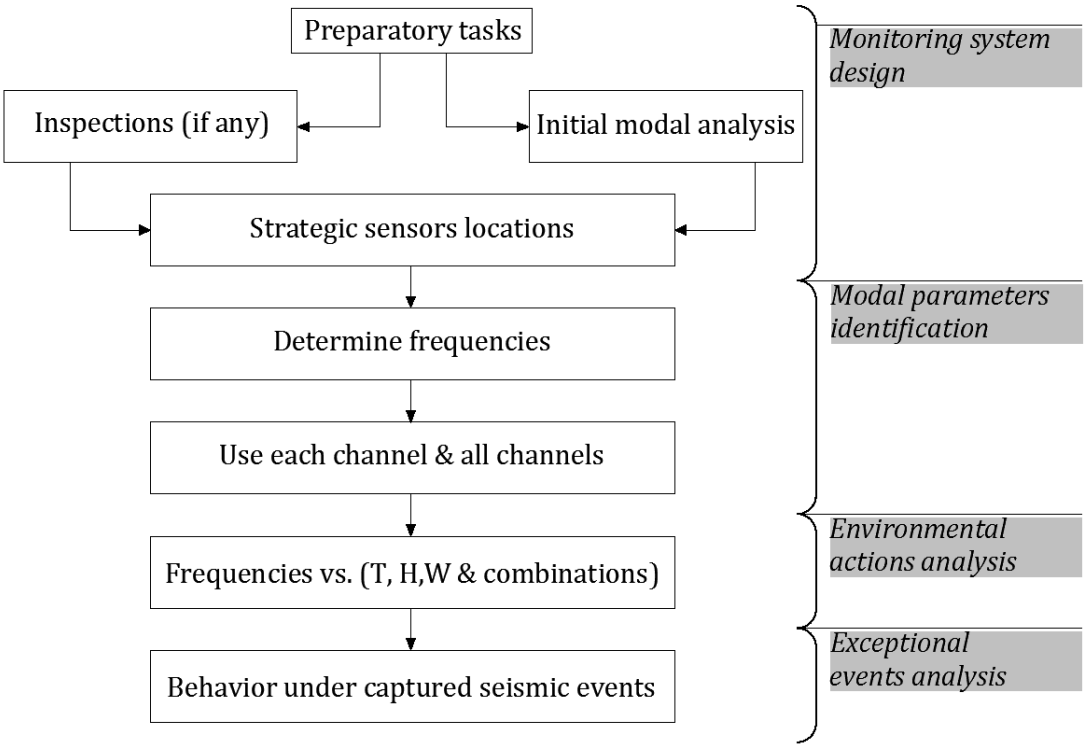


*Figure 8.3. Approach for dynamic monitoring of historical structures.*

A flowchart for an approach for dynamic monitoring is presented in Figure 8.3. As can be seen, the approach has four phases (1) monitoring system design, (2) modal parameters identification, (3) analysis of environmental actions and (4) analysis of exceptional events. The details of each phase and the flowchart are explained in the following paragraphs. The work done in chapter 5 is an application of this approach.

The first phase is devoted to the design of the dynamic monitoring system. It involves the selection of the strategic points that can accommodate the sensors and the type of the monitoring system. Certain previous investigation results (if available) and an initial modal analysis are proposed to be considered in the selection process. The previous investigations that are of interest are the cracking survey and the dynamic identification tests, among other possible ones.

The points that are located near cracks should be avoided for the location of sensors because of the expected disturbance in the recorded signals due to the local vibration. In particular, the vicinity of separation cracks between macro-elements, such as cracks between the façade and the rest of the structure should be avoided.

An initial modal analysis carried out using a numerical model of the historical structure can be of large assistance in the strategic points' selection. This selection can be based on comparing the normalized modal displacements of a number of candidate points. The candidate points can be selected based on the results of any previous dynamic investigations and based on practical reasons like the safeguard places that can safely accommodate the sensors for long periods. These points are usually located at the higher levels of the historical structure like the roof level. The points that showed their adequacy in any previous dynamic tests should be considered again as possible candidate points. After choosing a set of candidate points, the points with the highest normalized modal displacements should be prioritized in the selection, thus, ensuring satisfactory characterization of the dynamic behavior of the structure. On the contrary, points with small modal displacements should be avoided.

Furthermore, if a sufficient number of sensors is used allowing the identification of the mode shapes, the points' choice should be oriented to characterize the global modes rather than the local ones. This can be done by choosing the points that always move in the global modes and avoid the points that only move in the local modes. For instance, a point on an arch of a church main nave is preferred to a point on the church spire. The former would be found to have considerable modal displacements in the church global modes, whereas the latter might move only in the local mode associated to the spire. Also, local modes of arches or vaults appear normally with frequencies very different from those of the entire structure modes so that they can be distinguished.

When possible, one or more sensors should be placed at the ground level. The comparison between the signals registered at the ground level and a higher level (for instance at the roof) in the vicinity of any captured seismic events may indicate how the structure reacts to the event and how much is the amplifications at the higher levels. It may also contribute to identify soil-interactions effects.

An appropriate type of dynamic monitoring system should be selected. In case of a historical structure situated in a low to moderate seismic area, a continuous system that records the vibration measurements (preferably acceleration) continuously without setting any threshold is recommended to allow for the detection of the expected seismic events of low energy. A dynamic monitoring system with a previously described threshold may be used in locations with higher seismic intensity. In this case, periodic measurements during day and night, in addition to the events higher than the prescribed threshold, should be recorded. This allows following the changes in the dynamic behavior

under the varying environmental actions (temperature, humidity, wind, etc.) between day and night.

The second phase is the identification of the modal parameters, in specific the natural frequencies of the monitored historical construction. Natural frequencies can be normally obtained by the system, even if only one sensor is used. Identifying the mode shapes needs a large number of sensors and identifying damping ratios requires advanced identification methods.

It is proposed to investigate the identification of the natural frequency of any mode by using the results of each monitoring channel in each direction, i.e., the longitudinal direction, the transversal direction, and the vertical direction, in case of using a tri-axial sensor.

The target is to reveal the predominant direction/s in which the mode can be identified. A comparison with what was found by the dynamic identification tests, if carried out before installing the monitoring system, should be made. The identification of the mode by each channel is investigated in terms of the percentage of the mode detection. This percentage is calculated as

$$= 100 \text{ X } \frac{N_m}{N_t} \qquad \textit{Equation 8.1}$$

where, $N_m$ is the total number of appearances of the mode in all identification charts of the channel and $N_t$ is the total number of all identification charts of the channel.

The type of the identification chart of the channel depends on the used identification method. If the peak picking is used, the chart is the power spectral density. If more advanced methods like the stochastic subspace identification ones are used this chart is a stabilization diagram. For each mode, a comparison between the calculated percentages in the different directions should be made. From the comparison, it is expected to find the relative importance of the movement experienced by global modes in different directions.

After this calculation, the identified frequencies for each mode from all channels are averaged. The evolution of the frequency in time is analyzed in order to investigate possible trends, the steady state (unchanged trends over time) and any abnormalities over time. A statistical study on the frequency should be made to reveal the significance of its variation and also to compare the identified values with those found by the dynamic identification tests—if carried out.

The third phase is oriented to study the effects of the environmental actions on the modal parameters and again, the natural frequencies in specific. The environmental actions of concern are temperature, humidity and wind. These parameters can be obtained from a static monitoring system installed in the historical structure; otherwise, the values obtained from a near meteorological station can be used.

The correlation between the natural frequencies and each action should be studied first. Regarding temperature effects, and due to the cracks that may exist in historical masonry structures, it is expected to observe a positive correlation between the natural frequencies and temperature. This would be attributed to the cracks' closing (increase in the stiffness) and opening (decrease in the stiffness) with temperature increasing and decreasing, respectively. Regarding humidity effects, a negative relation would be expected and could be explained by considering that humidity increase results in water content increase for mortar and blocks which in turn increases the masonry mass and decreases the structure's natural frequencies. Regarding wind effects, each of the wind parameters (velocity and direction) should be investigated alone, and then the influence of both parameters should be investigated. Some modes may be only excited for certain combinations of such wind parameters. The correlation between the natural frequencies and the different combinations of the environmental actions should be studied. Adopting a linear regression model may provide good results. However, the adoption of nonlinear regression models (quadratic and cubic) should not be disregarded.

In this phase also, a more detailed study of the effect of temperature on natural frequencies can be carried out using thermography monitoring. An infrared (IR) camera can be placed in the historical structure and can cover a large portion of it. The recorded IR photos can be processed and the masonry temperature of different structural elements can be calculated. For the times of installing the thermography monitoring system, it is recommended to perform it so that the seasonal temperature changes can be revealed. Two periods in the extreme environmental conditions can be monitored, for instance, one period in summer and another in winter. The correlation between the masonry temperature and the external as well the internal temperatures should be checked. The correlation between these temperatures and the structure's natural frequencies should be also investigated.

In the last phase, the analysis of the dynamic behavior of the historical structure under any captured seismic events and significant wind episodes should be carried out. The occurrence of a seismic event of interest can be checked by following the daily seismic

events recorded by a seismological station in the area of the structure. The captured seismic events are evaluated and if considered significant for the structure further calculations are carried out. The evaluation can be carried out using the spectrograms (time-frequency distribution) of the different monitoring channels. The spectrogram can clearly show the arrival time, the frequency content and the duration of the captured seismic event. More calculations (power spectral densities, coherence and transfer functions) can be performed on the recorded signals that contain the captured event before, during, and after the arrival of the seismic event. The target is to reveal any effect on the structure response. This effect can be detected, for instance, in the form of a decrease in the natural frequencies due to the stiffness degradation during the earthquake. Another possible effect may be found in the increase in the damping ratios as damping highly depends on the excitation levels.

## 8.6 Considerations on numerical model updating

A flowchart for an approach to numerical model updating of historical structures is shown in Figure 8.4. As can be noticed, it has three phases (1) correlation, (2) updating and (3) evaluation. The details of each phase and the flowchart are explained in the following paragraphs.

The first phase is oriented to a correlation process. In this phase, experimental modes estimated from dynamic identification tests are correlated with numerical modes obtained from an initial model. For this purpose, a sufficiently accurate initial model is needed. To do so, qualitative and quantitative comparisons should be carried out. The experimentally identified mode shapes can be in some cases easily correlated with their numerical counterpart if they have near frequencies and clearly similar mode shapes. If this is not the case, they can be qualitatively compared with a number of candidate numerical modes and initially correlated. To justify this initial qualitative correlation, a quantitative correlation is carried out by calculating the $D_f$ and MAC values. The numerical modes giving the lowest $D_f$ and the highest MAC can be considered for the definitive correlation.

The second phase is oriented to the updating of the initial model and it includes the modifications of some aspects of the model until reaching a minimum difference between the experimental and the numerical frequencies and the highest coincidence between the experimental and the numerical mode shapes. For this purpose, four aspects can be checked and modified in the model, among other possible ones. These aspects are the

model geometry (and more specifically, the influence of parts not modeled into detail), the boundary conditions (more specifically, the influence of the foundation and the foundation soil), the mechanical properties of materials and finally the damage experienced by the historical construction. Other possibilities should be also considered, such as modifying the density, changing the dimensions of cross sections, the simulation of the internal morphology of sections, in case that there is no sufficient information available.

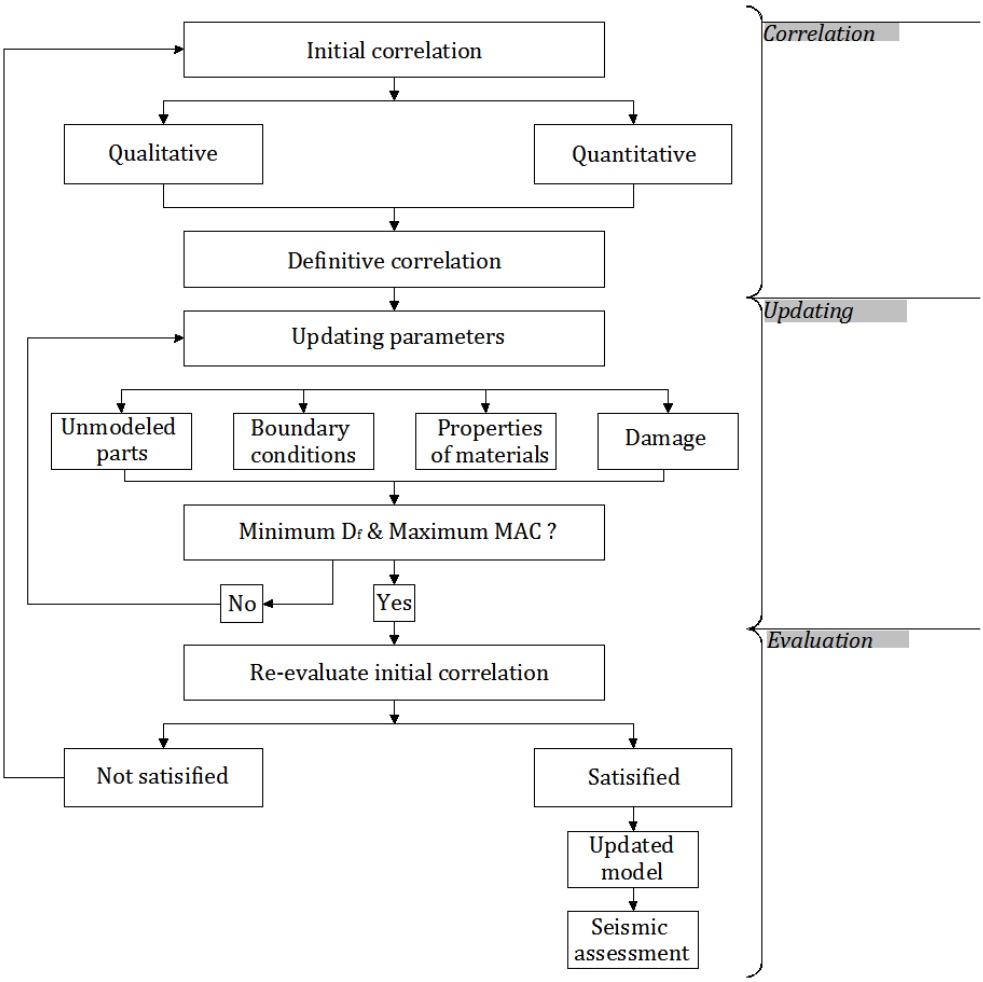


*Figure 8.4. Approach for historical construction model updating.*

Clearly, each of the aforementioned aspects has a potential influence on the dynamic behavior of the historical structure. Appropriate modifications of any of them may approximate the numerical frequencies and mode shapes to the experimental ones. Regarding the geometry, attention should be paid to the possible influence of secondary structural members not initially included in the model (because they first judged as not relevant) which, however, may show to have influence on the global stiffness of the

structure. This might be the case of any elements (walls, vaults) that connect the vertical supporting elements (columns, buttresses).

The mechanical properties of the materials, like the modulus of elasticity, can be modified as a way to update the model. This will be normally necessary as the information on such properties and particularly of the masonry's Young's modulus, is in many cases insufficient and inaccurate. It may not be necessary to modify the properties of all the materials of the structure, but only of those structural members (such as buttresses) having a large influence on the structure's stiffness amount and distribution.

Regarding the boundary conditions, the connections with other parts of the structure (like towers and minarets) or with adjacent buildings (like cloisters or houses) should be revised and tried in the updating process. Also the soil-structure interaction is to be investigated. A detailed description of the soil structure interaction may require the modeling of a significant portion of the foundation soil. In turn, a detailed modeling of the interaction with adjacent buildings may require a detailed description of the structure of these buildings in the model. These detailed descriptions may require a too large and refined model requiring, in turn, very large computer effort. As an alternative, simplified descriptions of both the soil-structure interaction and the influence of adjacent buildings can be done by means of adequately calibrated springs or elastic members.

Finally, the influence of major existing damage must be considered and eventually simulated in the model in order to obtain an improved matching between the experimental and numerical dynamic parameters. In particular, large and profound cracks that can affect the integrity of the structure should be modeled in the model. A simple approach to include these cracks is to double the nodes along the crack length. Other more sophisticated approaches may include the usage of interface elements. After trying the aforementioned aspects, the updating process should stop when reaching a satisfactory result in terms of $D_f$ and MAC values for most of the modes. The model to select as the best one will be the model judged to produce an optimal compromise regarding the $D_f$ and MAC values for most vibration modes. It must be taken into account that normally, the model cannot be updated so that all the modes can reach a minimum difference with the experimental frequencies (minimum $D_f$) and a maximum matching with the experimental mode shapes (maximum MAC). Therefore, the analyst should stop the updating process when the minimum $D_f$ value and the maximum MAC value are judged, respectively, sufficiently small and sufficiently large for most of the modes.

The last step is to evaluate the initial correlation using the final model. This can be done by recalculating again the $D_f$ and the MAC values. In case that no significant changes are found, the model can be considered accurate enough and can be used in the following step of assessment of the seismic analysis. Otherwise, a different correlation can be considered again and the updating process can be performed another time. The reader is referred to chapter 6 for an application of this approach.

## 8.7 Considerations on seismic assessment

Figure 8.5 shows an approach for the seismic assessment of historical construction. The seismic assessment is carried out using the pushover analysis, the kinematic limit analysis and the nonlinear dynamic analysis. The three analysis techniques are used in a combined way. The N2 method is used to evaluate the performance in combination with pushover analysis and kinematic limit analysis. Using the N2 method, the safety is judged by comparing the seismic capacity and the maximum displacement with the performance ones. Based on the safety evaluation, the necessary interventions are proposed. The details of the approach considered are given below.

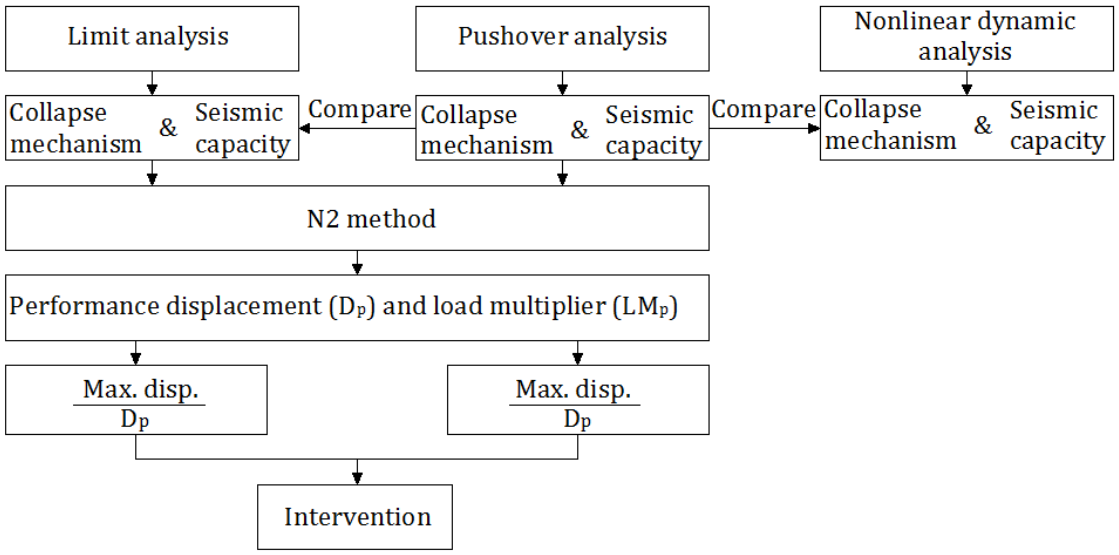


*Figure 8.5. Approach for the seismic assessment of historical structures.*

For seismic analysis, different techniques are proposed to be used including kinematic limit analysis and more complex techniques such as the nonlinear static and dynamic analyses. Before performing the seismic analysis, it is important, whenever possible, to investigate, through historical research, how the historical structure has responded to and the damage and possible partial collapses caused by previous earthquakes (investigation of the seismic performance). This preliminary understanding is

relevant especially in case of large historical construction, whose seismic resistance usually involves the contribution of many interacted structural elements.

It is proposed to assess the seismic behavior using first the pushover analysis. In this analysis, the numerical model of the historical structure is fed with the nonlinear material properties. To reveal the dependency of the results on the used materials properties, a sensitivity analysis is essential. For this parametric analysis, the reference model should be the one resulting from the model updating described in the previous section.

The main results of concern of the pushover analysis are the collapse mechanisms and the seismic capacity. The seismic capacity is visualized in the form of a capacity curve. To draw this curve, it is noticed that using only one control point may lead to either overestimating or underestimating of the seismic safety of the historical construction. Therefore, four control points are proposed. Those are the full structure center of gravity, the roof center of gravity, the point with the highest elevation and the point with the maximum displacement in the considered direction of analysis. The analyst may even add more points if necessary.

To cross check the seismic capacity of the building, the kinematic limit analysis technique should be also used. To define the macro-blocks, three aspects should be considered: (1) the collapse mechanisms deduced from the pushover analysis; (2) the existence of separations between different parts of the structure; and (3) the observed collapse mechanisms of similar historical structures that have already experienced earthquakes. The obtained seismic capacity should be compared with that found by the pushover analysis. In any case, applying kinematic analysis requires a previous detailed inspection and understanding of the structure of the building and its damage.

In case of having different results from the pushover analysis and the kinematic limit analysis, the reason for having different results should be first checked. For pushover analysis, the results depend on the input materials parameters and those may not be known with certainty. The definition of the models corresponding to both pushover analysis and kinematic analysis must be rechecked and improved until both approaches yield the same or sufficiently similar damage and collapse mechanisms. Also, the geometrical properties, like the thicknesses of the structural elements, should be known with certainty to correctly carry out the calculations of the weights and the corresponding lever arms.

It should be noticed that the kinematic limit analysis may, in some cases, be used before the pushover analysis. This may be the case if the macro-blocks are well

characterized based on visual inspection of the historical structure due to, for instance, the existence of critical wide cracks between certain parts of the structure. It is recommended to use the kinematic limit analysis before the pushover analysis only if the macro-blocks can be defined easily.

A more advanced technique that best describe the seismic behavior of the historical structure is nonlinear dynamic analysis. However, it is computationally very demanding and its applicability to large historical structures is still limited by the capacity of current computers. Artificial or recorded seismic events can be used. Many seismic codes, for instance, the Eurocode 8 (CEN, 2003), require the usage of at least seven records. This means that a near to comprehensive nonlinear dynamic analysis should include seven records multiplied by two orthogonal directions which results in 14 analyses. The number of analyses becomes larger when considering both types of possible earthquakes, far-field and near-field, and when the vertical component of the event is considered. The collapse mechanism and the seismic capacity of this analysis should be compared with the results of aforementioned techniques.

The evaluation of the seismic performance is carried out in the next step. First, it is needed to determine the seismic demand in the form of the elastic response spectrum of the construction's site according to the applied seismic code and considering different return periods. Second, the usage of N2 method is proposed to obtain the performance points using different combinations of the considered response spectra and the control points' capacity curves. It should be noticed that the N2 method is used in combination with the capacity curves of the pushover analysis and the kinematic limit analysis, whereas, the nonlinear dynamic analysis provides directly a verification of the seismic performance

In the last step, it is proposed to judge the seismic safety based on comparing the maximum displacements and capacities with the performance displacements and capacities using different control points. Using this comparison, the structural engineer is guided when deciding about the need for any seismic upgrading interventions. An application for this approach has been shown in chapter 7.

# CHAPTER 9

# CONCLUSIONS AND FUTURE WORK

## 9.1 Introduction

This research aimed at contributing to the topic of the seismic assessment of large historical masonry structures through the employment of a general methodology that was based on the integrated application of experimental and numerical approaches. The cathedral of Mallorca, an impressive medieval construction, was studied as a real case. In this chapter, the conclusions concerning the state-of-the-art review, the case study and the investigated methodology are discussed. At the end, some future investigations are proposed.

## 9.2 Conclusions

### 9.2.1 On the state-of-the-art

- The dynamic identification tests are carried out on a historical structure, among other reasons to obtain the experimental modal parameters that can be used to calibrate and update numerical models. Ambient Vibration Testing (AVT) is more used than Forced Vibration Testing (FVT) because it is quicker, cheaper, needs less equipment, and does not interrupt the operation of the historical structure. Nevertheless, it has limitations such as the low signal to noise ratio and the fact that some modes may not be excited during tests. It is difficult to extract reliable damping ratios because of its dependency on the excitation level which is commonly very low in AVT and some modes may not be identified for the same reason. As a rule of thumb, the testing time can be taken as 1000 to 2000 times structure's fundamental period.
- Dynamic monitoring is an effective tool to study the evolution of modal parameters in time, to reveal the effect of environmental actions on modal parameters, to capture the dynamic response of the structure under exceptional events like earthquakes and to assess the effectiveness of interventions. Based on the few available case studies in the literature, it was noticed that the natural frequencies increase with the temperature probably due to the closing of cracks and its effect on the stiffness of the structure. Under the effect of a seismic event with a considerable magnitude, it has been noticed that 1) the natural frequencies decrease but they may recover their initial value after the event if no residual damage had occurred, 2) the damping ratios increase significantly during a seismic event of a considerable magnitude and 3) the mode shapes do not change in a significant way in spite of the changes experienced by the natural frequencies and the damping ratios.

- The Infrared thermography offers interesting applications for the inspection of historical structures. For instance, it can be utilized to 1) reveal the masonry texture covered by plaster layers, 2) observe the activeness of cracks, 3) show the homogeneity of the used construction materials, 4) investigate the moisture problems due to rainwater seepage and 5) estimate the efficiency of FRP strengthening to masonry structures.
- The numerical modeling of heritage structures faces significant challenges derived from the complexity of the materials, the morphology and the actions. Accordingly, it is necessary to validate and update their numerical models against possible modeling inaccuracies and uncertainties. There are several methods for model updating and it has been noticed that for historical structures, the manual method is the most widely used. In the case of bridges and towers (and similar structures), very good correlation in terms of frequency discrepancy ($D_f$) and the Modal Assurance Criteria (MAC) can be found between the experimental and numerical modal parameters. This is not the case for other types of historical structures such as houses and churches, for which it may be difficult to find a good correlation between numerical and experimental modal parameters (particularly the mode shapes) due to, for instance, the complexity of these structures, the limited number of measured points, and the difficulty in correct reproducing of the existing damage.
- Historical masonry structures show very early cracking under applied loads because of their almost null tensile strength. Consequently, the non-linear analysis is the recommended method for their structural assessment. It allows for tracing the complete response of the structure from the elastic range up to complete failure. However, it should be kept in mind that the results of such analysis depend significantly on the input nonlinear materials properties.
- Currently, the pushover analysis is widely used for seismic assessment of historical structures. However, pushover analysis has significant limitations. For instance, when the higher modes of vibration become important, the nonlinear dynamic response may differ from the predictions of the pushover analysis. Also, the seismic capacity depends on the applied load pattern. For some case studies, it has been found that the load pattern proportional to the first mode shape produces a lower capacity than that proportional to the mass. Generally, the nonlinear dynamic analysis is preferred to the pushover analysis. It has been observed in some case studies on tall historical structures that the nonlinear dynamic analysis provides better predictions of real damage than pushover. However, the nonlinear dynamic analysis faces several challenges. Among them are the dependency of the results on the input earthquakes records, the complexity of time-integration

algorithms, the difficulties in damping representation and the large needed computational and storage resources. It should be noticed that, generally, the accurate assessment of the seismic capacity of historic structures via numerical models is a relatively demanding task. The usage of other simplified methods, for instance kinematic limit analysis, is recommended to cross check the results.

### 9.2.2 On the previous studies carried out on Mallorca cathedral

The studies that have been carried out on Mallorca cathedral have been reviewed. These studies covered some aspects of the cathedral, such as its construction history, static and dynamic monitoring campaigns, and the seismic assessment, among others. The conclusions of the review on these studies are presented in the following paragraphs.

- The construction lasted for about three centuries and this long process resulted in the perceptible deformations seen nowadays, especially in the columns. Some parts of the cathedral collapsed and were rebuilt, as in specific, the main nave vaults of the fourth bay (from the choir), possibly because of their large dimensions and the corresponding technical problems in keeping their stability for long periods using temporary devices. In turn, a large part of the vaults were reconstructed in the 18$^{th}$ c. This reconstruction might be due to the deterioration and losing of the mortar because of the presence of salt in the stone. The west façade was demolished and rebuilt in 19$^{th}$ c. because of the concern caused by a very large out-of-plumb. Cracks still exist in many structural elements of the cathedral including the columns, the vaults and the clerestory walls.
- The chemical analysis showed that most of the cathedral was built using limestone. The geo-physical inspection using GPR and seismic tomography showed that the columns have internal solid composition and the buttresses and the clerestory walls have two outer leaves and an internal one of a lower strength. The static monitoring revealed that the crack between the sixth vault and the supporting arch is the one with the highest cumulative rate of around 10mm/century. The dynamic monitoring system showed the clear influence of temperature on the natural frequencies of the cathedral.
- Evaluating the seismic safety using the capacity spectrum method on many possible collapse mechanisms employing many different seismic demands showed that the cathedral is able to resist possible earthquakes although experiencing some damage. The seismic analysis carried out using a FE model of a typical bay predicted the collapse to occur due to the appearance of a sufficient number of hinges as to determine a collapse mechanism. Hinges appear in the flying arches, the main nave vault and the lateral vaults.

### 9.2.3 On the new studies carried out on Mallorca cathedral

***On the dynamic identification***

The dynamic identification of the cathedral was performed using AVT. Four different modal parameters identification methods were used and their results were compared. The main conclusions are:

- The points near to the mid span of the arches of the main and the lateral naves were the strategic points to accommodate the sensors. These points had considerable modal displacements and proved their suitability because they allowed a satisfactory characterization of the global dynamic behavior of the cathedral.
- The configuration of the sensors had an influence on the possibility of identifying the modes. It was noticed that more modes appeared in the setups in which the sensors were transversally arranged than those appeared when the sensors were longitudinally arranged. This can be related to the fact that most of the identified modes are characterized by predominant transverse movement. Also, it is important to note that the wind was blowing mainly in the transversal direction during tests. In fact, the identification of the first transversal mode of the cathedral was particularly eased by its excitation by wind blowing in this direction.
- It was possible to identify eight modes. The natural frequencies of all of them were satisfactory identified. However, only the mode shapes and the damping ratios of three modes were satisfactory identified. These modes were global ones with high mass participation, which made their identification more attainable than in the case of more local ones.
- The identified damping ratios showed scattered values. This can be attributed to the dependency of the damping ratios with the excitation level which was low during the AVT and did not allow for a better characterization of this parameter. The damping ratios measured for the satisfactory identified modes varied between 1% and 1,5%. This value is judged too low for a historical masonry structure with distributed cracks. This law value can be attributed again to the difficulty of characterizing the damping ratios under low levels of excitations.

***On the dynamic monitoring***

A continuous dynamic monitoring campaign was installed for a period of more than 15 months during the years 2010, 2011 and 2012. The obtained results allowed for a

detailed observation of the dynamic properties with time under environmental actions and some captured seismic events. The main conclusions are:

- The obtained frequencies for the eight modes under low level of excitation during the AVT were confirmed by the dynamic monitoring campaign under higher levels of excitation in the vicinity of higher wind speeds and some captured seismic events.
- The global modes of the cathedral were more detectable than the local ones because of their higher mass participation. Also, the sensors locations were chosen so that the detection of global modes could be achieved.
- For the modes from 2 to 8, temperature was a more influential environmental parameter than humidity and wind. The changes in the frequencies of these modes, in terms of CV, were between 2,3 to 3,7% and their percentual variation was between 10,4 to 18,5 %.
- One mode correlated well with wind and was detectable only when wind was acting according to a certain direction and velocity.
- The usage of a higher cost continuous dynamic monitoring system was useful in capturing very low intensity seismic events. These events would not be detected with the usage of a lower cost triggered system. Therefore, this type of monitoring seems interesting for the dynamic identification of large buildings in low seismic zones.
- For the recorded earthquakes, it was observed a doubling of some frequency peaks. This was probably due to the breathing crack effect, i.e. the opening of the cracks that resulted in decreasing the stiffness, and therefore in; lower value of the natural frequency.

***On the thermography monitoring***

A seasonal thermography monitoring (as a complementary study for the dynamic monitoring) was used. An Infrared (IR) camera was installed in the winter and the summer of 2011 for two weeks in each to monitor the internal stone surface temperature of a large portion of the cathedral. The correlation between the cathedral natural frequencies and the internal stone surface temperature of some selected structural elements was investigated and compared with the correlation with the external and the internal temperatures. The main conclusions are:

- The internal stone surface temperature of the columns, vaults, arches and walls wasin phase and very near to each other.

- In summer, it was observed that the internal stone surface temperature did not always vary according to the external temperature because the stone was not able to radiate the stored heat as fast as the rapidly increasing external temperature. This also resulted in a low correlation between the cathedral frequencies and the stone internal surface temperature. Therefore, the natural frequencies of the cathedral were better correlated with the external temperature than that with the internal stone surface temperature.
- In winter, the stone surface temperature was in phase with the external temperature. A better correlation than in summer between the cathedral frequencies and the stone surface temperature was found.

***On the model updating***

A manual updating approach was used. The updating of the cathedral initial model was uncoupled, i.e. the stiffness of the longitudinal stiffness was adjusted using the first mode shape and then the transversal direction stiffness was adjusted using the second mode shape. The updating process involved many trials such as modifying the defined geometry, trying connecting the tower to the cathedral, using elastic foundations, simulating the damage, and changing the modulus of elasticity of the buttresses. The main conclusions are:

- The model modification that allowed a higher matching between the experimental and numerical results was the improvement of the model by including secondary structural members not implemented in a first version of the model. These members were the longitudinal walls between buttresses and the vaults of the lateral chapels. For the transversal direction, decreasing the modulus of elasticity of the buttresses improved the modal matching by slightly decreasing the cathedral stiffness in this direction.
- The numerical model was updated to a satisfactory extend. It reached $D_f$ values around 2% or less for two global modes and two local modes affecting mostly single parts of the structure. Moreover, the two global modes of the cathedral had an average MAC of 0,82which indicated a good match between experimental and numerical mode shapes.

***On the seismic assessment***

The seismic assessment was carried using the nonlinear static and dynamic analyses and the kinematic limit analysis. A parametric analysis was performed on the material properties that mostly affected the seismic capacity. The N2 method was used to evaluate the seismic performance. The main conclusions are:

- The seismic resistance of the cathedral in the longitudinal direction is lower than that in the transversal direction. This is due to the fact that in the former case the buttresses (the main earthquake-resisting elements) are loaded by lateral loads acting in their out-of-plan direction, whereas, in the latter case, the buttresses are loaded in their stronger in-plane direction. Something similar occurs regarding the contribution of the main façade to the overall stiffness and strength.
- In the longitudinal direction, the collapse can occur due to the overturning of the facades. The zones that can be severely damaged are those around the large windows of the clerestory walls and the apse walls, the first bay of the central nave vault after the west faced, and the top and bases of the columns.
- In the transversal direction, the collapse can occur due to the cracks (hinges) appearing in the flying arches, the arches and vaults of the naves, the top and bases of the columns and the bases of the buttresses.
- Changing the tensile strength was found to be very influential on the capacity. Both the capacity and the maximum displacement were observed to change significantly with the variation of the modulus of elasticity. The capacity and the maximum displacement varied only slightly when increasing the compressive strength or the ultimate crack strain, but they were reduced significantly when reducing these two material parameters.
- The capacities found by the kinematic limit analysis in the longitudinal direction were comparable to those found with the pushover analysis.
- The cathedral resisted the applied earthquakes in the nonlinear dynamic analysis without collapsing and the observed damage was lesser than that observed in the pushover analysis. This type of advanced analysis is still challenging due to its computational requirements. It was found that the required computational time was in order of several days. This fact made it difficult the application of a sufficient number of seismic events as required by seismic codes and also to carry out a sensitivity analysis.
- Good match in the collapse mechanisms was found between the pushover analysis and the nonlinear dynamic analysis.
- The cathedral showed satisfactory safety levels — evaluated in terms of the ratios between the maximum displacements and capacities and their performance counterparts. Therefore, no any deep seismic strengthening intervention is required. However, injecting the cracks and repointing the joints with mortar loss is recommended. This may allow for any future earthquakes dissipation by cracking in

previously damaged (and later repaired) parts without resulting in new cracks in other more structurally compromised locations of the cathedral's structural elements.

### 9.2.4 On the applied general methodology

- The interconnection between inspection, numerical modeling, dynamic investigation activities and intervention proposals is essential to achieve a successful structural assessment of a historical structure.
- The numerical model of the structure has a critical role in the applied methodology. An initial model built using the inspection results can provide guidance for the design of the dynamic investigation activities. For instance, it can be used in selecting the strategic locations of the sensors. The obtained results from these investigations can be used then to validate the initial model until having a sufficiently updated model which can be used then in the seismic assessment followed by performance and safety evaluation.
- The efficiency of the proposed seismic upgrading interventions can be checked using the updated numerical model that can be used as a virtual laboratory in which the efficiency of each proposal can be characterized. The efficiency of the intervention should be assured on the short term using in-situ inspection and on the long term using different monitoring techniques that should work for a sufficient period of time.

## 9.3 Future work

### 9.3.1 On Mallorca cathedral

- It is recommended to continue the dynamic monitoring of the building in order to further improve the information obtained and the numerical model. The monitoring should consist of installing again at the same points the dynamic monitoring system accompanied with sensors for measuring temperature, humidity and wind. The target is to further investigate the cathedral behavior under environmental actions and future captured seismic events. Furthermore, increasing the number of sensors is recommended to allow for a better identification of the mode shapes and their dependency with the environmental actions.
- It is proposed to refine the post-processing of the monitoring data using advanced identification methods such as Stochastic Subspace Identification (SSI)because they are more accurate than the previously used PP technique. In addition, the application of

these methods may allow for the estimation of the damping ratios. As mentioned, the damping ratios were not satisfactory identified in the present research.

- It is proposed to apply an automatic modal parameters identification procedure to the obtained data by the dynamic monitoring system. The objective is to intensify the number of times of the calculations of the modal parameters. Hence, this could allow for a better monitoring of their evolution in time and with the environmental actions.
- It is also proposed to apply damage identification algorithms on the experimental dynamic information registered during the already captured seismic events or during possible future events. By applying such algorithms further investigations could be carried out on the observed nonlinear behavior of the cathedral (the peak doubling). This research might provide more insight on the extent and significance of the existing damage in the cathedral.
- It is proposed to carry out a complete nonlinear dynamic analysis using a sufficient number of records representing a set of representative earthquakes for the location of the cathedral. Also, a sensitivity analysis might be done by means of nonlinear dynamic analysis by varying the properties of the materials properties and the damping ratios.
- The effect of the adopted constitutive model on the seismic assessment can be analyzed by employing alternative constitutive equations. In particular, the total strain crack model (see for instance, Feenstra et al., 1991) could be used as an improvement to the approach adopted in the present research.

### 9.3.2 On the studies of historical structures

- The employment of the dynamic monitoring in the assessment of the dynamic behavior of historical structures is in need for further investigation. Such technique, as in particular, the continuous one, seems attractive for structures in low to moderate seismic intensity zones allowing capturing wind episodes and seismic events with low energy. Also, it allows for a detailed tracking of the dynamic behavior under the effect of the environmental actions.
- The application of the dynamic monitoring as an early warning system could be investigated. An automatic procedure could be created in which a range of the natural frequencies of the structure could be set up, and when surpassed, an alarming message could be sent to the system operator. Consequently, pre-determined fast intervention plans could be carried out. These procedures seem attractive, particularly, for historical structures in high seismic zones.

- In the post-processing of dynamic identification tests, the proposed combination of "optimal selected setups" can be applied to other case studies to further investigate its adequacy.
- When carrying out model updating of a numerical model of a historical structure, dynamic monitoring results may be used to perform "a real time" updating. For instance, instead of assuming one value for the masonry modulus of elasticity that could result in a good match between the experimental modal parameters obtained from dynamic identification tests and the numerical modal parameters, a range of values could be assumed. This range reflects the changes in the stiffness of the structure with closing and opening of the cracks due to, mainly, temperature changes.

This page is intentionally left blank.

# REFERENCES

**A**

[1] Abacilar, P. (2010). Damage survey and collapse mechanisms due to seismicty in Gothic churches around Catalonia region and Mallorca. *MSc Thesis, Technical University of Catalonia, Spain.*

[2] Adler, D. (1969). *Metric Handbook: Planning and Design Data*. Second edition. Architectural press, Oxford, UK.

[3] Ademovic, N. (2011). Structural and seismic behavior of typical masonry buildings from Bosnia & Herzegovina. *MSc Thesis, University of Minho, Portugal*.

[4] Ademovic, N., Hrasnica, M., & Oliveira, D. V. (2013). Pushover analysis and failure pattern of a typical masonry residential building in Bosnia and Herzegovina. *Engineering Structures, 50,* 13-29.

[5] Aguilar, R. (2010). Dynamic structural identification using wireless sensor networks. *PhD Thesis, University of Minho, Portugal.*

[6] Akansel, V., Ameri, G., Askan, A., Caner, A., Erdil, B., Kale, Ö., & Okuyucu, D. (2013). The 23 October 2011 Mw 7.0 Van (Eastern Turkey) earthquake: Interpretations of recorded strong ground motions and post earthquake conditions of nearby structures. *Earthquake Spectra.*

[7] Alaboz. M. (2009). Dynamic identification and modal updating of St. Torcato church. *MSc Thesis, University of Minho, Portugal.*

[8] Allemang, J. R. (2003). The modal assurance criterion – twenty years of use & abuse. *Sound and Vibration 37:8*, 14–21.

[9] Alonso, F. J., Ordaz, J. & Esbert, R. M. (1996). Deterioro selective de la piedra de construcción de la catedral de Palma de Mallorca. *Geogaceta, 20 (5):* 1228-1231.

[10] Alves, C., Vasconcelos, G., Fernandes, F. M., & Silva, S. M. (2014). Deterioration of the granitic stone at Misericórdia chapel in Murça (northern Portugal). In Amoeda, R., Lira, S. & Pinheiro, C. (c) *Proc. of the International Conferenece on Preservation, Maintenance and Rehabilitation of Hisotircal Buildings and Structrues (REHAB 2014)*.

[11] Andersen, P., Brincker, R., Peeters, B., De Roeck, G., Hermans, L., & Krämer, C. (1999). Comparison of system identification methods using ambient bridge test data. *In Proc. of the 17th International Modal Analysis Conference (IMAC),* 8-11 February, Orlando, Florida, USA.

[12] Andreini, M., De Falco, A., Giresini, L., & Sassu, M. (2014). Mechanical Characterization of Masonry Walls with Chaotic Texture: Procedures and Results of In-Situ Tests. *International Journal of Architectural Heritage, 8(3)*, 376-407.

[13] Angotti, F., Vignoli, A., Giuseppetti, G., Panzeri, P. (1992). Experimental evaluation of the dynamic behaviour of a stone masonry building causing progressive damage. *In Proc. of the 10th World Conference on Earthquake Engineering,* Madrid, Spain.

[14] Antonelli. K., Astakhov, V. P., Bandyopadhyay, A., Bhatia, V., Claus, R. O., Dayton, D., Eren, H., Hyatt, R.M., Janas, V.F., Karlsson, N, Khokine, A, Ko, J., Kong, W.,L, Ku, S., Mayer, J.R.R, Nyce, D.S., & Pedersen, T. O. (1999). Displacement measurement, linear and angular. In Webster, J. G. (Ed-in-Chief), *The Measurement, Instrumentation, and Sensors Handbook*. Boca Raton, Florida: CRC Press LLC.

[15] António, A., Costa, A., Moreira, D. & Neves, N. (2012). Seismic analysis and strengthening of Pico Island Churches. *Bulletin of Earthquake Engineering, 10(1)*, pp.181--209.

[16] Antoniou, S. (2002). Pushover analysis for seismic design and assessment of RC structures. *PhD Thesis, University of London, UK.*

[17] Antoniou, S., & Pinho, R. (2004). Advantages and limitations of adaptive and non-adaptive force-based pushover procedures. *Journal of Earthquake Engineering, 8(4)*, 497-522.

[18] Aoki, T. & Sabia, D. (2005). Structural identification and seismic performance of brick chimneys, Tokoname, Japan. *Structural Engineering and Mechanics, 21 (5),* 553–570.

[19] Aoki, T., & Sabia, D. (2006). Structural characterization of a brick chimney by experimental tests and numerical model updating. *Masonry International, (2)*, 41-52.

[20] Aoki, T., Sabia, D., Rivella, D., & Komiyama, T. (2007). Structural characterization of a stone arch bridge by experimental tests and numerical model updating. *International Journal of Architectural Heritage, 1(3)*, 227-250.

[21] Aoki, T., Sabia, D., & Rivella, D. (2008). Influence of experimental data and FE model on updating results of a brick chimney. *Advances in Engineering Software, 39(4)*, 327-335.

[22] Aprile, A., Pelà, L., & Benedetti, A. (2006) Vulnerabilità sismica di ponti ad arco in muratura di pietrame. *XVI Convegno Italiano di Meccanica Computazionale, 28 giugno, Bologna.*

[23] Araiza, J. C. (2003). Dynamic assessment of structural building components. *PhD Thesis, Technical University of Catalonia, Spain.*

[24] Armstrong, D., Sibbald, A., Fairfield, C. & Forde, M. (1995). Modal analysis for masonry arch bridge spandrel wall separation identification. *NDT and E International: 28 (6)*, pp. 377--386.

[25] ASCE (2007). *Seismic Rehabilitation of Existing Buildings*, American Society of Civil Engineers, Reston, VA.

[26] ASTM (2002). *ASTM E 519–02, Standard Test Method for Diagonal Tension (Shear) in Masonry Assemblages*. In Annual Book of ASTM Standards. West Conshohock, PA: ASTM International.

[27] ASTM (2004a). *Standard Test Method for In-Situ Compressive Stress Within Solid Unit Masonry Estimated Using Flat-Jack Measurements*, ASTM Standard C 1196-04.

[28] ASTM (2004b). *Standard Test Method for In-Situ Measurement of Masonry Deformability Properties Using the Flat-Jack Method*, ASTM Standard C 1197-04.

[29] ASTM (2011). *Standard Practice for Thermographic Inspection of Insulation Installations in Envelope Cavities of Frame Buildings*, ASTM Standard C1060.

[30] Atamturktur, S., Pavic, A., Reynolds, P., & Boothby, T. (2009). Full-scale modal testing of vaulted gothic churches: lessons learned. *Experimental Techniques, 33(4)*: 65-74.

[31] Atamturktur, S. (2009a) Calibration under uncertainty for finite element models of masonry monuments. *PhD Thesis, Pennsylvania State University, USA.*

[32] Atamturktur, S. (2009b). Validation and verification under uncertainty applied to fi nite element models of historic masonry monuments. *27th Society of Experimental Mechanics (SEM) International Modal Analysis Conference (IMACXXVII)*, Orlando, Florida, USA.

[33] Atamturktur S, Hemez F, & Unal, C. (2010) *Calibration Under Uncertainty for Finite Element Models of Masonry Monuments*. Los Alamos National Laboratory, Los Alamos (1st Edition).

[34] Atamturktur, S., & Laman, J. A. (2012). Finite element model correlation and calibration of historic masonry monuments: review. *The Structural Design of Tall and Special Buildings, 21(2)*, 96-113.

[35] Atamturktur, S., Hemez, F. M., & Laman, J. A. (2012). Uncertainty quantification in model verification and validation as applied to large scale historic masonry monuments. *Engineering Structures, 43*, 221-234.

[36] ATC (1996). *Seismic Evaluation and Retrofit of Concrete Buildings, Vol. 1, ATC 40,* Applied Technology Council, Redwood City.

[37] ATC (2002). *Evaluation and Improvement of Inelastic Seismic Analysis Procedures*, *ATC 55*, Applied Technology Council, Redwood City.

[38] Augusti, G., Ciampoli, M., & Giovenale, P. (2001). Seismic vulnerability of monumental buildings. *Structural Safety, 23(3)*, 253-274.

[39] Avdelidis, N. P., and Moropoulou, A. (2003). Emissivity considerations in building thermography. *Energy and Buildings, 35(7)*, 663-667.

[40] Avdelidis, N. P., & Moropoulou, A. (2004). Applications of infrared thermography for the investigation of historic structures. *Journal of Cultural Heritage, 5(1)*, 119-127.

[41] Azuaje, M. M. (2012). Estudio del subsuelo de la catedral de Santa María de Palma de Mallorca mediante El método de refracción de microtremores. *MSc Thesis, Technical University of Catalonia, Spain.*

**B**

[42] Bagavathiappan, S., Lahiri, B. B., Saravanan, T., Philip, J., & Jayakumar, T. (2013). Infrared thermography for condition monitoring–a review. *Infrared Physics & Technology, 60*, 35-55.

[43] Barreira, E., de Freitas, S. S., de Freitas, V. P., & Delgado, J. M. P. Q. (2013). Infrared Thermography Application in Buildings Diagnosis: A Proposal for Test Procedures. In *Industrial and Technological Applications of Transport in Porous Materials* (pp. 91-117). Springer Berlin Heidelberg.

[44] Baruch, M., & Bar Itzhack, I. Y. (1978). Optimal weighted orthogonalisation of measured modes. *AIAA journal, 16(4)*, 346-351.

[45] Bazzurro, P., & Luco N. (2003). *Report for Pacific Earthquake Engineering Research (PEER)*. Center Lifelines Program Project 1G00.

[46] Beck, J. L., & Katafygiotis, L. S. (1998). Updating models and their uncertainties. I: Bayesian statistical framework. *Journal of Engineering Mechanics, 124(4)*, 455-461.

[47] Beconcini, M. L., Croce, P. & Mengozzi, M. (2006). Dynamic Monitoring and Model Updating of a Masonry Bell Tower in Pisa. In Lourenço, P. B., Roca, P., Modena, C. & Agrawal, S. (Eds.) *Structural Analysis of Historical Constructions*, pp. 659-666.

[48] Bendat, J.S. & Piersol, A.G. (1993). *Engineering Applications of Correlation and Spectral Analysis*, New York: Wiley.

[49] Bensalem, A., Fairfield, C. & Sibbald, A. (1995). Non-destructive testing for arch bridge assessment. In *proc. of the 1st international conference on arch bridges*, UK, pp. 459-468.

[50] Bensalem, A., Ali-Ahmed, H., Fairfield, C. A. & Sibbald, A. (1998). Non-destructive testing as a tool for detection of gradual safety factor deterioration of loaded arches. *Arch Bridges*, Anna Sinopoli (Eds.), A.A. Balkema, Rotterdam, 271–279.

[51] Bernal, D. & Gunes, B. (2002). Damage localization in output-only systems: a flexibility based approach. In *Proc. of the 20th International Modal Analysis Conference (IMAC)*, February 4-7, Los Angeles, California, pp. 1185-1191.

[52] Betti, M. & Galano, L. (2012). Seismic Analysis of Historic Masonry Buildings: The Vicarious Palace in Pescia (Italy). *Buildings, 2(2)*, pp.63-82.

[53] Binda, L., Modena, C., Casarin, F., Lorenzoni, F., Cantini, L., & Munda, S. (2011a). Emergency actions and investigations on cultural heritage after the L'Aquila earthquake: the case of the Spanish Fortress. *Bulletin of Earthquake Engineering, 9(1)*, 105-138.

[54] Binda, L., Cantini, L., Cucchi, M. (2011b). Thermovision: Applications in conservation field to detect hidden characteristics of building structures. *11th North American Masonry Conference*, 5-8 June, Minneapolis, USA.

[55] Block, P., DeJong, M., & Ochsendorf, J. (2006a). As hangs the flexible line: Equilibrium of masonry arches. *Nexus Network Journal, 8(2)*, 13-24.

[56] Board of the Alhambra and Generalife. (2012). *Presupuesto de la comunidad autónoma de Andalucia. Patronto de la Alhambra y Generalife*. Retrieved from http://www.juntadeandalucia.es/haciendayadministracionpublica/planif_presup/presupuesto2012/estado/programas/programas-e-36.pdf

[57] Bocca, P., Carpinteri, A. & Valente, S. (1989). Fracture mechanics of brick masonry: size effects and snap-back analysis. *Materials and Structures, 22(5)*, 364-373.

[58] Bommer, J. J., & Ruggeri, C. (2002). The specification of acceleration time-histories in seismic design codes. *European Earthquake Engineering 16(1)*, 3–17.

[59] Bommer, J. J. & Acevedo, A. B. (2004). The use of real earthquake accelerograms as input to dynamic analysis. *Journal of Earthquake Engineering, 8(S1)*, 43-91.

[60] Bosiljkov, V., Maierhofer, C., Koepp, C., & Wöstmann, J. (2010). Assessment of structure through Non-Destructive Tests (NDT) and Minor Destructive Tests (MDT) investigation: case study of the church at Carthusian monastery at Žiče

(Slovenia). *International Journal of Architectural Heritage: Conservation, Analysis, and Restoration, 4(1)*, 1-15.

[61] Boromeo, L. (2010). Dynamic monitoring analysis of Mallorca Cathedral. *MSc thesis, Technical University of Catalonia, Spain.*

[62] Borri, A., Castori, G., & Corradi, M. (2014). Determination of shear strength of masonry panels through different tests. *International Journal of Architectural Heritage,* In press.

[63] Bourgeois, J. (2013). Simulation of the effect of auxiliary ties used in the construction of Mallorca Cathedral. *MSc Thesis, Technical University of Catalonia, Spain.*

[64] Bournas, D. A., Negro, P., & Taucer, F. F. (2013). Performance of industrial buildings during the Emilia earthquakes in Northern Italy and recommendations for their strengthening. *Bulletin of Earthquake Engineering*, 1-22.

[65] Bracci, J. M., Kunnath, S. K., & Reinhorn, A. M. (1997). Seismic performance and retrofit evaluation of reinforced concrete structures. *Journal of Structural Engineering, 123(1)*, 3-10.

[66] Brandonisio, G., Lucibello, G., Mele, E., & Luca, A. D. (2013). Damage and performance evaluation of masonry churches in the 2009 L'Aquila earthquake. *Engineering Failure Analysis, 34*, 693-714.

[67] Brincker, R., Zhang, L., & Andersen, P. (2000a). Output-Only Modal Analysis by Frequency Domain Decomposition. In P. Sas & D. Moens (Eds.), *Proc. of ISMA25: International Conference on Noise and Vibration Engineering*, Katholieke Universiteit, Leuven, pp. 717-723.

[68] Brincker, R., Zhang, L., & Andersen, P. (2000b). Modal identification from ambient responses using frequency domain decomposition. In *Proc. of the 18th International Modal Analysis Conference (IMAC)*, 7-10 February, San Antonio, Texas, USA.

[69] Brincker, R., Zhang, L., & Andersen, P. (2001a). Modal identification of output-only systems using frequency domain decomposition. *Smart Materials and Structures, 10(3)*, 441-445.

[70] Brincker, R.; Ventura, C. & Andersen, P. (2001b). Damping estimation by Frequency Domain Decomposition. In *Proc. of 19th International Modal Analysis Conference (IMAC)*, 5-8 February, Orlando, Florida, USA.

[71] Brincker, R., Ventura, C. & Andersen, P. (2003a). Why output-only modal testing is a desirable tool for a wide range of practical applications. In *Proc. of the 21st*

*International Modal Analysis Conference (IMAC)*, February 3-6, Kissimmee, Florida, USA.

[72] Brincker, R., & Andersen, P. (2003b). A way of getting scaled mode shapes in output only modal testing. In *Proc. of 21st International Modal Analysis Conference (IMAC)*, February 3-6, Kissimmee, Florida, USA.

[73] Brincker, R. & Andersen, P. (2006). Understanding Stochastic Subspace Identification. In *Proc. of 24th International Modal Analysis Conference (IMAC)*, January 29 – February 2, St. Louis, Missouri, USA.

[74] Brignola, A., Frumento, S., Lagomarsino, S., & Podesta, S. (2008). Identification of shear parameters of masonry panels through the in-situ diagonal compression test. *International Journal of Architectural Heritage, 3(1)*, 52-73.

**C**

[75] Cabboi, A. (2014). Automatic operational modal analysis: challenges and applications to historic structures and infrastructures. *PhD Thesis, University of Cagliari, Italy*.

[76] Cabboi, A., Gentile, C. & Saisi, A. (2014). Automated modal and structural identification of a stone-masonry bell-tower for SHM. In *Proc. of the 9th International Conference on Structural Dynamics*, 30 June-2 July, Porto, Portugal.

[77] Cabboi, A., Gentile, C. & Saisi, A. (2013a).Frequency tracking and F.E. model identification of a masonry tower. *Proc. of the Int. Conf. IOMAC 2013*, 14 - 15 May, Guimaraes, Portugal.

[78] Cabboi, A., Magalhaes, F., Gentile, C. & Cunha, A. (2013b). Automatic operational modal analysis: Challenges and practical application to a historic bridge. In *Proc. 6th ECCOMAS conference on Smart Structures and Materials*, 24-26 June, Torino, Italy.

[79] Caetano, E. (2000). Dynamic of cable-stayed bridges: experimental assessment of cable-structure interaction. *PhD Thesis, University of Porto, Portugal.*

[80] Cagnan, Z. (2012). Numerical models for the seismic assessment of St. Nicholas Cathedral, Cyprus. *Soil Dynamics and Earthquake Engineering, 39*, 50-60.

[81] Cakti, E., Oliveira, C. S., Lemos, J. V., Saygılı, Ö., Görk, S., & Zengin, E. Earthquake Behavior of Historical Minarets in Istanbul. *4th ECCOMAS Thematic Conference on Computational Methods in Structural Dynamics and Earthquake Engineering*, Kos Islands, Greece, 12-14 June.

[82] Cantieni R. (2005). Experimental methods used in system identification of civil engineering structures. *1st International Operational Modal Analysis Conference (IOMAC)*, 26-27 April, Copenhagen, Denmark. pp. 249–260.

[83] Capecchi, D. Vestroni, F. Antonacci, E. (1990). Experimental study of dynamic behaviour of an old masonry building. *9th European Conf. on Earth. Eng.*, Moscow.

[84] Capurso, F. E. (2011). Seismic analysis and strengthening of Mallorca cathedral. *MSc Thesis, Technical University of Catalonia, Spain.*

[85] Carder, D.S. (1936a). *Vibration observations*. Chapter 5 in Earthquake Investigations in California 1934-1935. U.S. Dept. of Commerce, Coast and Geologic Survey, Special Publication No. 201, Washington, D.C., U.S.A.

[86] Carder, D. S. (1936b). Observed vibrations of buildings. *Bulletin of the Seismological Society of America, 26(3)*, 245-277.

[87] Carder, D. S. (1937). Observed vibration of bridges. *Bulletin of the Seismological Society of America, 27(4)*, 267–89.

[88] Carne, T. G. & Stasiunas, E. C. (2006). Lessons learned in modal testing—part 3: Transient excitation for modal testing, more than just hammer impacts. *Experimental Techniques, 30(3)*, 69-79.

[89] Carpentieri, G. (2011) Design–oriented analysis methods for masonry structures in seismic areas: theoretical formulation and validation on experimental results. *MSc Thesis, università degli studi di Salerno, Italy.*

[90] Casarin, F. (2006). Structural assessment and seismic vulnerability analysis of a complex historical building. *PhD Thesis, University of Trento/ University of Padova, Italy.*

[91] Casarin, F. and Modena, C. (2006). Structural assessment and seismic vulnerability analysis of the Reggio Emilia cathedral, Italy. In Lourenço, P., Roca, P., Modena, C. and Argawal, S. (Eds.), *Structural analysis of historical constructions*, pp. 1263-1270.

[92] Casarin, F. and Modena, C. (2008). Seismic assessment of complex historical buildings: Application to Reggio Emilia Cathedral, Italy. *International Journal of Architectural Heritage, 2 (3)*, pp. 304--327.

[93] Casarin, F., Lorenzoni, F., Islami, K. & Modena, C. (2011). Dynamic identification and monitoring of the churches of St. Biagio and St. Giuseppe in L'Aquila. *4th International Conference on experimental Vibration Analysis for Civil Engineering Structures*, 3-5 October, Varenna, Italy.

[94] Casati, M. J. & Gálvez, J. C. (2009). The influence of the masonry mechanical properties in the structural behaviour of the Leon's cathedral. *Materiales de Construcción, 59(294)*, 75-96.

[95] Caselles, O., Clapés, J., Osorio, R., Canas, J. A. Pujades, Ll. G. & Pérez-Gracia, V. (2004). Tomografia sísmica de las columnas de la catedral de Mallorca. *4ª Asamblea Hispano-Portuguesa de Geodesia y Geofisica*, 3-7 Febraury, Figueira de Foz, Portugal.

[96] Caselles, J. O. , Clapés, J. , Osorio, R. , Canas , J. A. , Pujades , L. G. & Pérez-Garcia, V. (2005). Integrated geophysical survey applied to the Mallorca cathedral. *67th EAGE Conference& Exhibition*, Madrid, Spain, 13-16 June.

[97] Caselles, O., Martínez, G., Clapés, J, Roca, P. & Canas, J. A. (2006). Non-destructive geophysical surveys for dynamic characterization of Mallorca cathedral. *1st European Conference on Earthquake Engineering and Seismology*, 3-8 September, Geneva, Switzerland.

[98] Caselles, J. O., Clapes, J., Osorio, R., Martínez, G., Canas, J. A., Pujades, L. G. & Pérez-Gracia, V. (2007). Integrated geophysical survey for prospecting Mallorca cathedral soil. *Gepphysical Research Abstracts, Vol. 9*, 03513, 2007.

[99] Caselles, O., Clapés, J., Martínez, G., Roca, P. & Pérez-Gracia, V. (2009). Caracterización dinámica del terreno de cimentación de la catedral de Mallorca, España. *17th National Congress of seismic engineering*, La Ciudad de Puebla, Mexico, 11-14 November.

[100] Caselles, O., Martínez, G., Clapes, J., Roca, P. & Pérez, M. (2013). Application of Particle Motion Technique to Structural Modal Identification of Heritage Buildings. *International Journal of Architectural Heritage*, in press.

[101] Casolo, S. (2000). Modelling the out-of-plane seismic behaviour of masonry walls by rigid elements. *Earthquake engineering & structural dynamics, 29(12)*, 1797-1813.

[102] Castellazzi, G., Gentilini, C. and Nobile, L. (2013). Seismic vulnerability assessment of a historical church: limit analysis and nonlinear finite element analysis. *Advances in Civil Engineering, Volume 2013*, Article ID 517454.

[103] Cattari, S., Degli Abbati, S., Ferretti, D., Lagomarsino, S., Ottonelli, D., & Tralli, A. (2013). Damage assessment of fortresses after the 2012 Emilia earthquake (Italy). *Bulletin of Earthquake Engineering*, 1-33.

[104] Ceci, A. M., Contento, A., Fanale, L., Galeota, D., Gattulli, V., Lepidi, M., & Potenza, F. (2010). Structural performance of the historic and modern buildings of the University of L'Aquila during the seismic events of April 2009. *Engineering Structures, 32(7)*, 1899-1924.

[105] CEN (2004) *Eurocode 8 - Design Provisions for Earthquake Resistance of Structures, Part 1.1: General rules, seismic actions and rules for buildings*, European prestandards ENV 1998, European Committee for Standardization, Brussels.

[106] CEN (2005) *Eurocode 6 - EN 1996-1-1:2005: Design of Masonry Structures. General Rules for Reinforced and Unreinforced Masonry Structures*. European Committee for Standardization, Brussels.

[107] Ceroni, F., Pecce, M. & Manfredi, G. (2009). Seismic assessment of the bell tower of Santa Maria del Carmine: problems and solutions. *Journal of Earthquake Engineering, Vol. 14,* p. 30-56.

[108] Chen, C. T. C. (2010). *Signals and Systems: A Fresh Look*. Retrieved from http://www.ee.sunysb.edu/~ctchen/

[109] CHIME (2000-2003). *Conservation of historical Mediterranean sites by innovative seismic protection techniques*. Funded by EC under the 5th Framework program.

[110] Chiostrini, S., Foraboshci, P., Vignoli, A., Galimberti, M., Meneghella, M. and Penzeri, P. (1991). Prove di vibrazioni forzate su un edificio in muratura: danneggiamento e nonlinearita. In *5th Congress of seismic engineering in Italy*, Palermo (pp. 601-610).

[111] Chiostrini, S., Foraboschi, P. & Vignoli, A. (1992). Structural analysis and damage evaluation of existing masonry buildings by dynamic experimentation and numerical modelling. In *Proc. of the 10th World Conference on Earthquake Engineering*, pp. 3481-3486.

[112] Chopra, A. K. (2000). *Dynamic of structures – Theory and Applications to Earthquake Engineering*. Prentice Hall.

[113] Chopra, A.K. and Goel, R. A. (2001). *Modal Pushover Analysis Procedure to Estimate Seismic Demands for Buildings: Theory and Preliminary Evaluation*. Report No. PEER 2001/03, Pacific Earthquake Engineering Research Center, University of California, Berkeley, CA.

[114] Chrysostomou, C., Kyriakides, N., Kappos, A., Kouris, L., Georgiou, E. and Millis, M. (2013). Seismic retrofitting and health monitoring of school buildings of Cyprus. *Open Construction and Building Technology Journal, 7*, pp.208-220.

[115] Chu, A. (1987) .Zeroshift of piezoelectric accelerometers in pyroshock measurements. Shock Vibration Information Center, *Shock Vibration Bulletin, 1*, 71-80.

[116] Circ. NTC08 (2009). Circolare, n.617, 2 febbraio 2009, del Ministero delle Infrastrutture e dei trasporti approvata dal Consiglio Superiore dei Lavori Pubblici, *Istruzioni per l'applicazione delle nuove norme tecniche per le costruzioni di cui al D.M. 14 gennaio 2008*.

[117] Clapés, J., Caselles, O., Osorio, R., Canas, J. A. Pujades, Ll. G. & Pérez-Gracia, V. (2004). Estudio mediante georradar de la catedral de Mallorca. *4ª Asamblea Hispano-Portuguesa de Geodesia y Geofisica*, 3-7 Febraury, Figueira de Foz, Portugal.

[118] Clark, M. R., McCann, D. M. & Forde, M. C. (2003). Application of infrared thermography to the non-destructive testing of concrete and masonry bridges. *NDT and E International, 36(4)*, 265-275.

[119] Clemente, R. (2006). Análisis estructural de edificios históricos mediante modelos localizados de fisuración. *PhD Thesis, Technical University of Catalonia, Spain*, (in Spanish).

[120] Clemente, R., Roca, P. & Cervera, M. (2006). Damage model with crack localization – application to historical buildings. In Lourenço, P. B., Roca, P., Modena, C. & Agrawal, S. (Eds.) *Structural analysis of historical constructions*, pp. 1125 – 1133.

[121] CNR-DT 200. (2004). *Guide for The Design And Construction of Externally Bonded FRP Systems for Strengthening Existing Structures*, Italy.

[122] Collins, J. D., Han, G. C., Hasselman, T. K. and Kenedy, B. (1974). Statistical Identification of Structures. *AIAA Journal, Vol. 12*.

[123] Corbi, O., Zaghw, A. H., Elattar, A. & Saleh, A. (2013). Preservation provisions for the environmental protection of Egyptian monuments subject to structural vibrations. *International Journal of Mechanics, 7(3)*: 172-179.

[124] Cornell, C. A. (2005). On earthquake record selection for nonlinear dynamic analysis. In *Proc. of the Luis Esteva symposium*, Mexico City, Mexcio.

[125] Correa, M.R. and Costa, A.C. (1992). Dynamic tests of the bridge over the Arade River. In: Fernandes, J.A. and Santos, L.O. (Eds.), *Cable-stayed Bridges of Guadiana and Arade, LNEC*.

[126] Cotič, P., Jagličić, Z., & Bosiljkov, V. (2013). Validation of non-destructive characterization of the structure and seismic damage propagation of plaster and

texture in multi-leaf stone masonry walls of cultural-artistic value. *Journal of Cultural Heritage.*

[127] Coutinho, D. (2010) Seismic analysis and strengthening of Mallorca cathedral. *MSc thesis, Technical University of Catalonia, Barcelona, Spain.*

[128] CPA (2003a). *Restauración de la portada principal de la catedral de Palma de Mallorca. Memoria final*. Report, available at: http://catedraldemallorca.info/principal/images/catedral/media/folletos/Memoria_Portada_Principal_Palma.pdf.

[129] CPA (2003b). *Restauración de la portada del Mirador de la catedral de Palma de Mallorca*. Report available at: http://catedraldemallorca.info/principal/images/catedral/media/folletos/Informe_visita_12_13_07_2012.pdf.

[130] Crandall, S. H. (1970). The role of damping in vibration theory. *Journal of Sound and Vibration, 11*, 3.

[131] Crawford, R. and Ward, H.S. (1964). Determination of the Natural Periods of Building. M*. Seism. Soc. Amer., Vol. 54*, pp. 1743-1756.

[132] CSA (2004). *Design of Masonry Structures*, Canadian Standards Association., S304.1, Ontario, Canada.

[133] Cuello, S. I. (2007). Dynamic analysis of Mallorca cathedral. *Graduation Thesis, Technical University of Catalonia, Spain*, (in Spanish).

[134] Cunha, Á. & Caetano, E. (2006). Experimental modal analysis of civil engineering structures. *Sound and Vibration, 40(6)*, 12-20.

[135] Cunha, Á., Caetano, E., Magalhaes, F. & Mountinho, C. (2006). From input-output to output-only modal identification of civil engineering structures. *1st International Operational Modal Analysis Conference (IOMAC)*, 26-27 April, Copenhagen, Denmark.

[136] Cunha, Á., Caetano, E., Magalhães, F., & Moutinho, C. (2013). Recent perspectives in dynamic testing and monitoring of bridges. *Structural Control and Health Monitoring, 20(6)*, 853-877.

[137] Cuzzilla, R. (2008). Application of capacity spectrum method to medieval constructions. *MSc Thesis, Technical University of Catalonia, Spain*.

[138] Cuzzilla, R. (2009). Seismic Assessment and Retrofit of Historical Masonry Structures. *PhD Thesis, University of Napoli Federico II, Italy.*

**D**

[139] D9.1-NIKER. (2012). *Individuation of Proper Buildings Where Applying the New Technologies*, Report, work package 9, NIKER project (2010-2012): New Integrated Knowledge-based approaches to the protection of cultural heritage from Earthquake-induced Risk. Funded by EC under the 7th Framework program, contract n. ENV2009-1-GA244123.

[140] D9.4-NIKER. (2012). *Report on the Use Of Monitoring as Knowledge Based Assessment and Early Warning Tool*. Report, work package 9, NIKER project (2010-2012): New Integrated Knowledge-based approaches to the protection of cultural heritage from Earthquake-induced Risk. Funded by EC under the 7th Framework program, contract n. ENV2009-1-GA244123.

[141] D10.4-NIKER. (2012). *Guidelines for Reliable Seismic Analysis and Knowledge Based Assessment of Buildings*. Report, work package 10, NIKER project (2010-2012): New Integrated Knowledge-based approaches to the protection of cultural heritage from Earthquake-induced Risk. Funded by EC under the 7th Framework program, contract n. ENV2009-1-GA244123.

[142] Dai, K., Opinel, P.A. and Huang, Y. (2013). Field dynamic testing of civil infrastructure-literature review and a case study. In *5th international conference on advances in experimental structural engineering.* November 8-9, Taipei, Taiwan.

[143] D'Ayala, D. and Speranza, E. (2003). Definition of collapse mechanisms and seismic vulnerability of historic masonry buildings. *Earthquake Spectra, 19*, 479–509.

[144] De Luca, F., Iervolino, I. & Cosenza, E. (2009). Un-scaled, scaled, adjusted and artificial spectral matching accelerograms: displacement-and energy-based assessment. *Proc. of 13th ANIDIS, L'ingegneria Sismica in Italia*, Bologna, Italy.

[145] De Matteis, G., Langone, I., Colanzi, F. & Mazzolani, F. M. (2007a). Experimental and numerical modal identification of the Fossanova Gothic cathedral. *Key Engineering Materials, 347*, 351-358.

[146] De Matteis, G., Colanzi, F., Eboli, A. & Mazzolani, F. M. (2008). Seismic vulnerability evaluation of the Fossanova Gothic church. In D'Ayala D. and Fodde E. (Eds.) *Structural Analysis of Historical Construction*. CRC Press Balkema, pp. 1225-1235.

[147] De Matteis, G. & Mazzolani, F. M. (2010). The Fossanova Church: seismic vulnerability assessment by numeric and physical testing. *International Journal of Architectural Heritage, 4(3)*, 222-245.

[148] De Silva, C. W. (2007). *Vibration—Fundamentals and Practice*, 2nd Edition, Taylor and Francis/CRC Press, Boca Raton, FL.

[149] De Sortis, A., Antonacci, E. & Vestroni, F. (2005). Dynamic identification of a masonry building using forced vibration tests. *Engineering Structures, 27(2)*: 155-165.

[150] De Stefano, A., & Clemente, P. (2005). SHM on historical heritage. Robust methods to face large uncertainties. In *Proc. 1st International Conference on Structural Condition Assessment, Monitoring and Improvement*, 12-14 December, Perth, W. Australia.

[151] De Stefano, A. (2007). Structural identification and health monitoring on the historical architectural heritage. *Key Engineering Materials 347*: 37–54.

[152] De Stefano, A., & Ceravolo, R. (2007). Assessing the health state of ancient structures: the role of vibrational tests. *Journal of Intelligent Material Systems and Structures, 18(8)*, 793-807.

[153] Derakhshan, H., Dizhur, D., Lumantarna, R., Cuthbert, J., Griffith, M. C. & Ingham, J. M. (2010). In-field simulated seismic testing of as-built and retrofitted unreinforced masonry partition walls of the William Weir House in Wellington. *Structural Engineering Society New Zealand (SESOC), 23(1)*, 51-61.

[154] Deierlein, G. G., Reinhorn, A. M. & Willford, M. R. (2010). Nonlinear structural analysis for seismic design. *NEHRP Seismic Design Technical Brief No, 4.*

[155] DIANA (2009) *Diana 9.4, user's manual*. The Netherlands: TNO Building and Construction Research. Available from www.diana.tno.nl.

[156] DIAS (2002-2005). *Integrated tool for in situ characterization of effectiveness and durability of conservation techniques in historical structures*. Funded by EC under the 5th Framework program, contract n. EVK4-CT-2002-00080 DIAS.

[157] Dizhur, D., Ingham, J., Moon, L., Griffith, M., Schultz, A., Senaldi, I., Magenes, G., Dickie, J., Lissel, S., Centeno, J. Ventura, C. Leite, J & Lourenco, P. B. (2011). Performance of masonry buildings and churches in the 22 February 2011 Christchurch earthquake. *Bulletin of The New Zealand Society For Earthquake Engineering, 44(4)*.

[158] Dogangun, A., Sezen, H., Tuluk, Ö. İ., Livaoğlu, R., & Acar, R. (2007). Traditional Turkish masonry monumental structures and their earthquake response. *International Journal of Architectural Heritage, 1(3)*, 251-271.

[159] Dogangun, A., Acar, R., Sezen, H., & Livaoglu, R. (2008). Investigation of dynamic response of masonry minaret structures. *Bulletin of Earthquake Engineering, 6(3),* 505-517.

[160] Dogangun, A. and Sezen, H. (2012). Seismic vulnerability and preservation of historical masonry monumental structures, *Earthquake and Structures, 3(1)*: 83–95.

[161] Dolce, M. (2009). The Abruzzo earthquake: effects and mitigation measures. *Disaster prevention workshop*, Stockholm, Hasselbacken, 27-29 July.

[162] Domenge, J. (1995a). *Traces D'una Fortuna Historiográfica*.

[163] Domenge, J. (1995b). *Tres Segles D'obras A La Seu*.

[164] Domenge, J. (1997). *L'obra De La Seu. El Procés De Construcció De La Catedral De Mallorca En El Tres-Cents*. Palma: Institut d'Estudis Baleàrics.

[165] Douglas, B. M., & Reid, W. H. (1982). Dynamic tests and system identification of bridges*. Journal of the Structural Division*, 108(ST10).

[166] Durukal, E. (1992). Structural identification and seismic vulnerability assessment of Aya Sofya. *MSc Thesis, Bogazici University, Turkey.*

**E**

[167] Eberhard, M. O. & Sozen, M. A. (1993). Behavior-based method to determine design shear in earthquake-resistant walls. *Journal of Structural Engineering, 119(2)*, 619-640.

[168] El-Attar, A. G., Saleh, A. M. & Zaghw, A. H. (2005). Conservation of a slender historical Mamluk-style minaret by passive control techniques. *Structural Control and Health Monitoring, 12(2)*: 157-177.

[169] El-Borgi, S., Smaoui, H., Casciati, F., Jerbi, K. and Kanoun, F. (2005). Seismic evaluation and innovative retrofit of a historical building in Tunisia. *Journal of Structural Control and Health Monitoring, 12(2)*: 179-196.

[170] El-Kafafy, M., Guillaume, P., & Peeters, B. (2013). Modal parameter estimation by combining stochastic and deterministic frequency-domain approaches. *Mechanical Systems and Signal Processing, 35(1)*, 52-68.

[171] Ellis, B. R. (1998). Non-destructive dynamic testing of stone pinnacles on the Palace of Westminster. Proc. of the institution of civil engineers. *Structures and buildings, 128(3)*, 300-307.

[172] Elices, M., Guinea, G. V. & Planas, J. (1992). Measurement of the fracture energy using three-point bend tests: Part 3—influence of cutting theP-δ tail. *Materials and Structures, 25(6)*, 327-334.

[173] Elmenshawi, A., Sorour, M., Mufti, A., Jaeger, L. G. & Shrive, N. (2010c). Damping mechanisms and damping ratios in vibrating unreinforced stone masonry. *Engineering Structures, 32(10)*, 3269-3278.

[174] Elnashai, A. S. (2002). Do we really need inelastic dynamic analysis? *Journal of Earthquake Engineering, 6(S1)*, 123-130.

[175] Elyamani, A. (2009). Wind and earthquake analysis of spire of cimborio of Barcelona cathedral. *MSc Thesis, Technical university of Catalonia, Spain.*

[176] Entwistle, K. (2001). *Basic Principles of the Finite Element Method*. 1st Edition. London: Maney, for the Institute of Materials.

[177] Erdik, M., Durukal, E., Yuzugullu, B., Beyen, K. & Kadakal, U. (1993). Strong-motion instrumentation of Aya Sofya and the analysis of response to an earthquake of 4.8 magnitude. *Proc. of the 3rd Conference: Structural Repair and Maintenance of Historical Buildings III*, Bath, UK, pp. 99-114.

[178] Erdik, M., Durukal, E. (1996). Use of strong motion data for the assessment of the earthquake response of historical monuments. *Proc. 11th World Conference on Earthquake Engineering*, 23-28 June, Acapulco, Mexico.

[179] Eren, H. (1999). Acceleration, vibration, and shock measurement. In Webster, J. G. (Ed-in-Chief), *The Measurement, Instrumentation, and Sensors Handbook*. Boca Raton, Florida: CRC Press LLC.

[180] EU-India (2004-2006). *Improving the seismic resistance of cultural heritage buildings*. Funded by EU-INDIA Economic Cross Cultural Programme, contract n. ALA/95/23/2003/077-122.

[181] Ewins, D.J. (2000a). *Modal testing, theory, practice and application*. Second Edition, Research Studies Press LTD, Hertfordshire, England.

[182] Ewins, D. J. (2000c). Adjustment or updating of models. *Sadhana, 25(3)*, 235-245.

**F**

[183] Fajfar, P. and Fischinger, M. (1988) N2–a method for nonlinear seismic analysis of regular buildings. *Proc. of the 9th World Conference on Earthquake Engineering*, Tokyo-Kyoto, Japan, pp. 111–116.

[184] Fajfar, P. and Gaspersič, P. (1996) The N2 method for seismic damage analysis of RC buildings. *Earthquake Engineering and Structural Dynamics Vol. 25*, pp 31– 46.

[185] Fajfar, P. A. (2000) A nonlinear analysis method for performance-based seismic design. *Earthquake Spectra 16(3):*573-592.

[186] Fajfar, P. A. (2002) Structural analysis in earthquake engineering- a breakthrough of simplified nonlinear methods. In *12th European conference on earthquake engineering*, 9-13 September, London, UK.

[187] Faella, G., Frunzio, G., Guadagnuolo, M., Donadio, A., & Ferri, L. (2012). The church of the nativity in Bethlehem: Non-destructive tests for the structural knowledge. *Journal of Cultural Heritage, 13(4)*, 27-41.

[188] Feenstra, P. H., De Borst, R., Rots, J. G. (1991). A comparison of different crack models applied to plain and reinforced concrete. In Van Mier, J. G. M., Rots, J. G., Bakker, A. (Eds.) *Fracture Process in Concrete, Rock and Ceramics*, EandFN Spon, The Netherlands, pp. 629–638.

[189] Felber, A. J. (1993). Development of a hybrid bridge evaluation system. *PhD Thesis, University of British Columbia, Vancouver, Canada.*

[190] FEMA (1997). *NEHRP guidelines for the seismic rehabilitation of buildings, FEMA Report 273*, Washington, D.C.

[191] FEMA (1999). *Evaluation of Earthquake Damaged Concrete and Masonry Wall Buildings, Basic Procedures Manual, ATC-43, FEMA 306*, Applied Technology Council, California.

[192] FEMA (2000). *Prestandard And Commentary for the Seismic Rehabilitation Of Buildings*, prepared for the SAC Joint Venture, published by the Federal Emergency Management Agency, FEMA-356, Washington, D.C.

[193] FEMA (2005). *Improvement of Nonlinear Static Seismic Analysis Procedures, FEMA Report 440*, Washington, D.C.

[194] FEMA (2009). *Effects of Strength and Stiffness Degradation on the Seismic Response of Structural Systems, FEMA Report 440a*, Washington, D.C.

[195] Feriche, M., Vidal, F., Alguacill, G., Arandal, C., Pérez-Muelas, J., Navarro, M. & Lemme, A. (2012). Performance of culutral heritage of Lorca (Spain) during the two small earthquakes of May 11th, 2011. In *Proc. of the 15th World Conference on Earthquake Engineering*, 24-28 September, Lisbon. Portugal.

[196] Freeman, S. A., Nicoletti, J. P. and Tyrell, J. V. (1975). Evaluation of existing buildings for seismic risk- A case study of Puget Sound Naval Shipyard, Bremerton,

Washington. *Proc. of the United States National Conference on Earthquake Engineering*, Berkeley, pp. 113-22.

[197] Freeman, S. A. (1998). Development and use of capacity spectrum method, Proc. of the 6th U.S. *National Conference on Earthquake Engineering*, May 31st -June 4th, Seattle, Washington.

[198] Freeman, S. A. (2004). Review of the development of the capacity spectrum method. *ISET Journal of Earthquake Technology, 41(1)*, 1-13.

[199] Friswell, M.I. & Mottershed, J.E. (1995). *Finite Element Model Updating in Structural Dynamics*, Kluwer Academic Publishers, London, UK.

**G**

[200] Gaudini, G., Modena, C., Casarin, F., Bettio, C. and Lucchin, F. (2008). Monitoring and strengthening interventions on the stone tomb of Cansignorio della Scala, Verona, Italy. In *Proc. of the 6th Internation Conference on Structural Analysis of Historical Constructions*, 2-4 July, Bath, UK, pp. 403-411.

[201] Gayo, E., & De Frutos, J. (1997). Interference filters as an enhancement tool for infrared thermography in humidity studies of building elements. *Infrared Phys. Technol., 38(4)*, 251-258.

[202] Genovese F, Vestroni F. (1998). Identification of dynamic characteristics of a masonry building. In *Proc. of the 11th European Conference on Earthquake Engineering*, Paris, France.

[203] Gentile, C. & Saisi, A. (2004). Dynamic based F.E. model updating to evaluate damage in masonry towers. *Proc. of 4th Int. Seminar on Structural Analysis of Historical Constructions*, 10-13 November, Padova, Italy, pp 439–449.

[204] Gentile, C. & Saisi, A. (2007). Ambient vibration testing of historic masonry towers for structural identification and damage assessment. *Construction and Building Materials, 21(6)*, 1311-1321.

[205] Gentile, C., Saisi, A. & Gallino, N. (2009). Operational modal analysis and FE modelling of a masonry tower. In *3rd International Operational Modal Analysis Conference (IOMAC)*, Portonovo, Italy, pp. 499-506.

[206] Gentile, C., Saisi, A. & Cabboi, A. (2012). Dynamic monitoring of a masonry bell tower. *8th International Conference on Structural Analysis of Historical Constructions*, 15-17 October, Wroclaw, Poland, pp. 2390-2397.

[207] Gentile, C., & Saisi, A. (2013). Operational modal testing of historic structures at different levels of excitation. *Construction and Building Materials, 48*, 1273-1285.

[208] Gibert, S. L. (2010). Joan Rubió I Bellver en Mallorca. Arquitectura y teoría. *PhD Thesis, University of Barcelona, Spain.*

[209] Godde, E. (2009). Static monitoring analysis of Mallorca cathedral. *MSc thesis, Technical University of Catalonia, Barcelona, Spain.*

[210] González, J. L. and Roca, P. (2003-2008). *Study of Structural-Constructive Behavior of Saint Mary Cathedral in the City Of Palma, Mallorca Island (Baleares)*. First Phase: Part I. (2003), Part II (2003), Part III (2004), Part IV (2004). Second Phase: Part V. (2008), Part VI (2008), Technical University of Catalonia, Spain, (In Spanish)

[211] González, R., Caballé, F., Domenge, J., Vendrell, M., Giráldez, P., Roca, P., & González J. L. (2008). Construction process, damage and structural analysis. Two case studies. In D'Ayala, D. and Fodde, E. (Eds.) *Structural Analysis of Historical Construction*. CRC Press Balkema, pp. 643–651.

[212] Government of Andalusia. (2013). *Turismo Cultural en Andalucía. Informe Annual.* www.andalucia.org/media/tinyimages/file/Turismo_Cultural_2013.pdf.

[213] Greening, P. D. (1999). Dynamic finite element modelling and updating of loaded structures. *PhD Thesis, University of Bristol, UK.*

[214] Grinzato, E., Bison, P. G. & Marinetti, S. (2002a). Monitoring of ancient buildings by the thermal method. *Journal of Cultural Heritage, 3(1)*, 21-29.

[215] Grinzato, E., Bressan, C., Marinetti, S., Bison, P. G. & Bonacina, C. (2002b). Monitoring of the Scrovegni Chapel by IR thermography: Giotto at infrared. *Infrared Phys.Technol. 43(3-5)*, 165-169.

[216] Gosse, J. (1986). *Technical guide to thermal processes*. Cambridge university press, UK.

[217] Guillaume, P., Verboven, P. & Vanlanduit, S. (1998). Frequency-domain maximum likelihood identification of modal parameters with confidence intervals. In *Conference Proc. of the 23rd International Seminar on Modal Analysis*, Leuven, Belgium.

[218] Guillaume, P., Verboven, P., Vanlanduit, S., Van Der Auweraer, H. & Peeters, B. (2003). A poly-reference implementation of the least-squares complex frequency-domain estimator. In *Proc. of IMAC* (Vol. 21, pp. 183-192).

[219] Guinea, G. V., Planas, J. & Elices, M. (1992). Measurement of the fracture energy using three-point bend tests: Part 1—Influence of experimental procedures. *Materials and Structures, 25(4),* 212-218.

[220] Gutermann, M. and Knaack, H. U. (2008). Strain assessment of historic masonry by cutting. In *Proc. of the 12th International Conference on Structural Faults and Repair*, 10-12 June, Edinburgh, Scotland.

**H**

[221] Haselton, C. B., Whittaker, A. S., Hortacsu, A., Baker, J. W., Bray, J. & Grant, D. N. (2012). Selecting and scaling earthquake ground motions for performing response-history analyses. In *Proc. of the 15th World Conference on Earthquake Engineering*, 24-28 September, Lisbon. Portugal.

[222] Hellier, C. (2003). *Handbook of Nondestructive Evaluation*. New York: Mcgraw-Hill.

[223] Herráez, J., A. (2012). *Inspección técnica portadas de la catedral de Palma de Mallorca*. Report, available at: http://www.catedraldemallorca.info/principal/images/catedral/media/folletos/CP1218.pdf.

[224] Heylen, W. & Sas, P. (2006). *Modal Analysis Theory and Testing*. Katholieke Universteit Leuven, Departement Werktuigkunde.

[225] Heyman, J. (1966). The stone skeleton. *International Journal of Solids and Structures, 2*:270–279.

[226] Heyman, J. (1995). *The Stone Skeleton: Structural Engineering of Masonry Architecture*. Cambridge University Press.

[227] Hillerborg, A., Modéer, M. and Petersson, P. E. (1976). Analysis of crack formation and crack growth in concrete by means of fracture mechanics and finite elements. *Cement and concrete research, 6(6)*, 773-781.

[228] Hillerborg, A. (1983). *Concrete Fracture Energy Tests Performed By 9 Laboratories According to a Draft RILEM Recommendation: Report to RILEM TC50-FMC*. Report TVBM.

[229] Hu, W. H., Cunha, Á., Caetano, E., Magalhães, F., & Moutinho, C. (2010). LabVIEW toolkits for output-only modal identification and long-term dynamic structural monitoring. *Structure and Infrastructure Engineering, 6(5)*, 557-574.

[230] Hu, W. H. (2012). Operational modal analysis and continuous dynamic monitoring of footbridges. *PhD Thesis, University of Porto, Portugal.*

[231] Huebner, K. H. (Eds.). (2001). *The Finite Element Method for Engineers*. John Wiley and Sons.

[232] Huerta, S. (2001). Mechanics of masonry vaults: the equilibrium approach. In: Lourenço, P.B. and Roca, P. (Eds.) *Historical Constructions*, University of Minho, Guimarães, pp. 47–69.

**I**

[233] Ibarra-Castanedo, C., Genest, M., Piau, J. M., Guibert, S., Bendada, A. & Maldague, X. P. (2007). Active infrared thermography techniques for the non-destructive testing of materials. In Chen, C. H. (Eds.), *Ultrasonic and Advanced Methods for Nondestructive Testing and Material Characterization.*

[234] IBC (2000). *International Building Code*. Falls Church (VA): International Code Council (ICC).

[235] IBC (2003). *International Building Code*: International Code Council (ICC).

[236] Ibrahim, S. R., Stravinidis, C., Fisette, E. and Brunner; O. (1989). Direct Two Response Response Approach for Updating Analytical Dynamic Models of Structums with Emphasis on Uniqueness. *Proc. IMAC 7*. pp. 340-346.

[237] Iervolino, I. & Cornell, C. A. (2005). Record selection for nonlinear seismic analysis of structures. *Earthquake Spectra, 21(3)*, 685-713.

[238] Iervolino, I., Maddaloni, G. & Cosenza, E. (2008). Eurocode 8 compliant real record sets for seismic analysis of structures. *Journal of Earthquake Engineering, 12(1)*, 54-90.

[239] Iervolino, I., Maddaloni, G. & Cosenza, E. (2009). A note on selection of time-histories for seismic analysis of bridges in Eurocode 8. *Journal of Earthquake Engineering, 13(8)*, 1125-1152.

[240] Iervolino, I., Galasso, C., and Cosenza, E. (2010). REXEL: computer aided record selection for code-based seismic structural analysis. *Bulletin of Earthquake Engineering. 8*:339-362.

[241] IILLESBA9.http://www.wunderground.com/weatherstation/WXDailyHistory.asp?ID=IILLESBA9

[242] Ivanovic, S. S., Trifunac, M. D. & Todorovska, M. I. (2000). Ambient vibration tests of structures—a review. *ISET Journal of Earthquake Technology, 37(4)*: 165-197.

[243] Ivorra, S., Pallares, F. J. & Adam, J. M. (2011). Masonry bell towers: dynamic considerations. *Structures and Buildings, Vol. 164*, Issue SB1, February 2011.

## J

[244] Jaiswal, K., Wald, D. & D'Ayala, D. (2011). Developing empirical collapse fragility functions for global building types. *Earthquake Spectra, 27(3)*, 775-795.

[245] Jamal, R. and Steer, R. (1999). Filters. In Webster, J. G. (Ed-in-Chief), *The Measurement, Instrumentation, and Sensors Handbook*. Boca Raton, Florida: CRC Press LLC.

[246] James, G. H., Carne, T. G., Lauffer, J. P. & Nard, A. R. (1992). Modal testing using natural excitation. *10th International Modal Analysis Conference (IMAC)*, 3-7 February, San Diego, USA.

[247] Jiménez-Alonso, J.F., Sáez, A. (2011). Application of operational modal analysis and model updating technique for the validation and characterization of structural models. *1st International Congress on Mechanical models in structural engineering,* University of Granada, pp. 61-68.

[248] Jingjiang, S., Ono, T., Yangang, Z. & Wei, W. (2003). Lateral load pattern in pushover analysis. *Earthquake Engineering and Engineering Vibration, 2(1)*, 99-107.

[249] Jo, Y. H., & Lee, C. H. (2014). Quantitative modeling of blistering zones by active thermography for deterioration evaluation of stone monuments. *Journal of Cultural Heritage*. In press.

## K

[250] Kadakal, U. and Yuzugullu, O (1996). A comparative study of the identifica1ion methods, for the autoregressive modeling from the ambient vibration records. *Soil Dynamics and Earthquake Eng., Vol. 15*, No. 1, pp. 45-49.

[251] Kammer, D. C. (1991). Sensor placement for on-orbit modal identification and correlation of large space structures. *Journal of Guidance, Control, and Dynamics, 14(2),* 251-259.

[252] Kandemir-Yucel, A., Tavukcuoglu, A., & Caner-Saltik, E. N. (2007). In situ assessment of structural timber elements of a historic building by infrared thermography and ultrasonic velocity. *Infrared physics & technology, 49(3)*, 243-248.

[253] Kim, S. & D'Amore, E. (1999). Push-over analysis procedure in earthquake engineering. *Earthquake Spectra, 15(3)*, 417-434.

[254] Kordatos, E. Z., Exarchos, D. A., Stavrakos, C., Moropoulou, A., & Matikas, T. E. (2013). Infrared thermographic inspection of murals and characterization of

degradation in historic monuments. *Construction and Building Materials, 48*, 1261-1265.

[255] Korkmaz, S. Z., & Korkmaz, H. H. (2013). The structural damages and collapse types in Turkey, observed after the recent earthquake. *Advanced Materials Research, 747*, 437-440.

[256] Korkmaz, S. Z. (2013). Observations on the Van Earthquake and Structural Failures*. Journal of Performance of Constructed Facilities*, 2013.

[257] Krawinkler, H. & Seneviratna, G. D. P. K. (1998). Pros and cons of a pushover analysis of seismic performance evaluation. *Engineering structures, 20(4)*, 452-464.

[258] Kulkarni, S.R. (2014). *Information signals*. Course notes. Retrieved from http://www.princeton.edu/~cuff/ele201/kulkarni_text/signals.pdf

[259] Kunnath, S. K., Reinhorn, A. M. & Lobo, R. F. (1992). IDARC Version 3.0: A program for the inelastic damage analysis of reinforced concrete structures. In *Technical Report NCEER (Vol. 92)*. US National Center for Earthquake Engineering Research.

**L**

[260] Lagomarsino S, Galasco A, Penna A. (2002) Pushover and dynamic analysis of U.R.M. buildings by means of a non-linear macro-element model. In: *Proceeding of the international conference on earthquake loss estimation and risk reduction.* Bucharest, Romania, October 24-26.

[261] Lagomarsino, S., Giovinazzi, S., Podestà, S., Resemini, S. (2003). *Vulnerability assessment of historical and monumental buildings handbook,* Report in WP5, RISK-EU project: An advanced approach to earthquake risk scenarios with application to different European towns, contract no. EVK4-CT-2000-00014.

[262] Lagomarsino, S. (2012). Damage assessment of churches after L'Aquila earthquake (2009). *Bulletin of Earthquake Engineering, 10(1)*, 73-92.

[263] Lança, P. (2005). Structural analysis of multi-ribbed vaults: high choir of the jeronimos Monastery as a case-study. *MSc Thesis, University of Minho, Portugal*.

[264] Lawson, R. S., Vance. V. & Krawinkler, H. (1994). Nonlinear static pushover analysis. Why, when and how? In *Proc. of the 5th US National Conference on Earthquake Engineering*, vol.1. Chicago, IL: Earthquake Engineering Research Institute. 283–292.

[265] Léger, P. & Dussault, S. (1992). Seismic-energy dissipation in MDOF structures. *Journal of Structural Engineering, 118(5)*, 1251-1269.

[266] Leite, J., Lourenco, P. B., & Ingham, J. M. (2013). Statistical assessment of damage to churches affected by the 2010–2011 Canterbury (New Zealand) earthquake sequence. *Journal of Earthquake Engineering, 17(1)*, 73-97.

[267] Lent, B. (2009). Simple steps to selecting the right accelerometer. *Sensors Magazine 26(3),* March issue.

[268] Lin, R. M. (1991). Identification of dynamic characteristics of nonlinear structwes. *PhD Thesis, Imperial College of Science, Technology and Medicine, London, UK.*

[269] Llompart, G. (1995). El Coro, La catedral de Mallorca. Pascual, A. (coord.), Palma.

[270] Llorens, M., Mata, P., Araiza, J. C. & Roca, P. (2001). Damage characterization in stone columns by dynamic test. Application to the Cloister of Girona Cathedral, Spain. In: Lourenço, P.B. and Roca, P. (Eds.) *Historical Constructions*, University of Minho, Guimarães, 469-478.

[271] Loewenstein, E.B. (1999). Analog-to-digital converters. In Webster, J. G. (Ed-in-Chief), *The Measurement, Instrumentation, and Sensors Handbook*. Boca Raton, Florida: CRC Press LLC.

[272] Lorenzoni, F., Casarin, F., Modena, C., Caldon, M., Islami, K. and Da Porto, F. (2013). Structural health monitoring of the Roman Arena of Verona, Italy. *Journal of Civil Structural Health Monitoring, 3 (4)*, pp. 227—246.

[273] Lorenzoni, F. (2013). Integrated methodologies based on structural health monitoring for the protection of cutural heritage buildings. *PhD Thesis, University of Trento, Italy.*

[274] Lourenço, P. B. (1996). Computational strategies for masonry structures. *PhD Thesis, Delft University of Technology*, the Netherlands.

[275] Lourenço, P.B., Oliveira, D.V. & Mourão, S. (2001). Numerical analysis as a tool to understand historical structures. The example of the Church of Outeiro. In: G. Arun, N. Seçkin (Eds.) *Studies in ancient structures*, p. 355-364. Istanbul : Yildiz Technical University.

[276] Lourenço, P.B. & Krakowiak, K. J. (2004). The Stability of the vaults of the Monastery of Jerónimos church. *Métodos computacionais em engenharia*. 31 May-2 June, Lisbon.

[277] Lourenço P.B. (2005b). Assessment, diagnosis and strengthening of Outeiro Church, Portugal. *Construction and Building Materials, 19*, 634–645.

[278] Lourenço, P. B., Almeida, J. C. & Barros, J. A. (2005a). Experimental investigation of bricks under uniaxial tensile testing. *Masonry International, 18(1)*, 11–20.

[279] Lourenço, P. B., Oliveira, D. V., Roca, P. & Orduña, A. (2005b). Dry joint stone masonry walls subjected to in-plane combined loading. *Journal of Structural Engineering, 131(11)*, 1665-1673.

[280] Lourenço, P. B., Krakowiak, K. J., Fernandes, F. M. & Ramos, L. F. (2007a). Failure analysis of Monastery of Jerónimos, Lisbon: How to learn from sophisticated numerical models. *Engineering Failure Analysis, 14(2)*, 280-300.

[281] Lourenço, P. B. & Lança, P. (2010). Safety assessment of high choir of the church of Santa Maria of Belém, at the Jerónimos monastery, subject to action of a pipe organ (in Portuguese). *8th congress of seismology and seismic engineering*, SÍSMICA 2010, 20-23 October, University of Aveiro, Portugal.

[282] Lourenço, P. B., Trujillo, A., Mendes, N. & Ramos, L. F. (2012a). Seismic performance of the St. George of the Latins church: Lessons learned from studying masonry ruins. *Engineering structures, 40*, 501-518.

[283] Luco, N. & Bazzurro, P. (2007). Does amplitude scaling of ground motion records result in biased nonlinear structural drift responses? *Earthquake Engineering and Structural Dynamics, 36(13)*, 1813-1835.

**M**

[284] MACEC 3.2, (2011) a MATLAB Toolbox for Experimental and Operational Modal Analysis, developed by Edwin Reynders and Guido De Roeck. Copyright © KU Leuven, Belgium.

[285] Magalhaes, F., Cunha, A., & Caetano, E. (2009). Online automatic identification of the modal parameters of a long span arch bridge. *Mechanical Systems and Signal Processing, 23(2)*, 316-329.

[286] Magalhães, F. (2010). Operational modal analysis for testing and monitoring of bridges and special structures. *PhD Thesis. University of Porto, Portugal.*

[287] Magalhães, F., Cunha, Á., Caetano, E., & Brincker, R. (2010). Damping estimation using free decays and ambient vibration tests. *Mechanical Systems and Signal Processing, 24(5)*, 1274-1290.

[288] Magalhães, F. & Cunha, Á. (2011). Explaining operational modal analysis with data from an arch bridge. *Mechanical systems and signal processing, 25(5)*, 1431-1450.

[289] Maia, N. & Silva, J. (1997). *Theoretical and experimental modal analysis*, Research Studies Press Ltd.

[290] Maia, N. & Silva, J. (2001). Modal analysis identification techniques. Philosophical Transactions of the Royal Society of London. *Series A: Mathematical, Physical and Engineering Sciences, 359(1778)*, 29-40.

[291] Maldague, X. and Moore, P. O. (2001). *Infrared and thermal testing*. Columbus, OH: American Society for Nondestructive Testing.

[292] Mark, R. (1982). *Experiments in Gothic structure*. 1st ed. Cambridge, Mass.: MIT Press.

[293] Martínez, E., Castillo, A., Martínez, I., & Castellote, M. (2013). Methodology for intervention in historical elements: the case of the belfry of the convent of Nuestra Señora de la Consolación, (Alcalá de Henares-Madrid-Spain). *Informes de la Construcción, 65(531)*, 359-366.

[294] Martínez, G., Roca P., Caselles O. and Clapés J. (2006). Characterization of the Dynamic Response for the Structure of Mallorca Cathedral. *Structural Analysis of Historical Constructions*. Vol I: 601-608.

[295] Martínez, G. (2007). Seismic vulnerability for middle and long span masonry historical buildings (in Spanish). *PhD thesis, Technical University of Catalonia, Barcelona, Spain.*

[296] Martínez, G., Roca, P., Caselles, O., Clapés, J. and Barbat, A.H. (2007) Determinación experimental y analítica de las propiedades dinámicas para la Catedral de Mallorca. *Structural Engineering (Intersections/Intersecţii), 4(2)*, Article No.4.

[297] Martínez, G., Roca, P., Caselles, O., Clapés, J. and Barbat, A.H. (2008). Analytical damage survey for the Mallorca Cathedral. 3rd *International Conference on Engineering Failure Analysis*. Spain, 13-16 July 2008.

[298] Masjedian, M. H., & Keshmiri, M. (2009). A review on Operational Modal Analysis researches: classification of methods and applications. *3rd International Operational Modal Analysis Conference*, May 4 - 6, Portonovo, Italy, pp. 707-718.

[299] Mares, C., Mottershead, J. E. & Friswell, M. I. (2006). Stochastic model updating: part 1—theory and simulated example. *Mechanical Systems and Signal Processing, 20(7)*, 1674-1695.

[300] Maynou, J. (2001). Estudi estructural del pòrtic tipus de la catedral de Mallorca mitjançan l'estàtica gràfica. *Graduation Thesis, Technical University of Catalonia, Spain* (in Catalan).

[301] Mazzotti, C., Sassoni, E. & Pagliai, G. (2014). Determination of shear strength of historic masonries by moderately destructive testing of masonry cores. *Construction and Building Materials, 54*, 421-431.

[302] McConnell, K. G. & Varoto, P. S. (1995). *Vibration testing: theory and practice*. New York: Wiley.

[303] MC (2005). *Measurement Computing, USA, Data acquisition handbook*, 3rd Edition, Retrieved from: www.mccdaq.com/support/data-acquistion-handbook.aspx.

[304] Medeiros, P., Vasconcelos, G., Lourenço, P. B. & Gouveia, J. (2013). Numerical modelling of non-confined and confined masonry walls. *Construction and Building Materials, 41*, 968-976.

[305] Meli, R., Rivera, D. & Miranda, E. (2001). Measured seismic response of the Mexico City Cathedral. In: Lourenço, P.B. and Roca, P. (Eds.) *Historical Constructions*, University of Minho, Guimarães, pp. 877-886.

[306] Mendes, N. (2012). Seismic assessment of ancient masonry buildings: shaking table tests and numerical analysis. *PhD Thesis, University of Minho, Portugal.*

[307] Mendes, N. & Lourenco, P. B. (2013). Seismic performance of ancient masonry buildings: a sensitivity analysis. *4th ECCOMAS Thematic Conference on Computational Methods in Structural Dynamics and Earthquake Engineering*, Kos Islands, Greece, 12-14 June.

[308] Mendoza, L., Reyes, A. and Luco, J.E. (1991). Ambient vibration tests of Mexicali general hospital. *Earthquake Spectra, 7(2),* pp. 281-300.

[309] Meneses, M. F. N. (2013). Sensitivity analysis of the seismic behavior of ancient masonry buildings. *MSc Thesis, Uninversity of Minho, Portugal.*

[310] Michel, C., Guéguen, P. & Bard, P. Y. (2008). Dynamic parameters of structures extracted from ambient vibration measurements: An aid for the seismic vulnerability assessment of existing buildings in moderate seismic hazard regions. *Soil Dynamics and Earthquake Engineering, 28(8)*, 593-604.

[311] Milosevic, J., Gago, A. S., Lopes, M. & Bento, R. (2013). Experimental assessment of shear strength parameters on rubble stone masonry specimens. *Construction and Building Materials, 47*, 1372-1380.

[312] Minghini, F., Milani, G. & Tralli, A. (2014). Seismic risk assessment of a 50 m high masonry chimney using advanced analysis techniques. *Engineering Structures, 69,* 255-270.

[313] Ministry of industry, energy and tourism. (2012). *Movimientos Turísticos en Fronteras (Frontur) y Encuesta de Gasto Turístico (Egatur)*. Retrieved from http://www.iet.tourspain.es/es-es/estadisticas/frontur/Paginas/default.aspx.

[314] Mohamad, G., Lourenço, P. B. & Roman, H. R. (2007). Mechanics of hollow concrete block masonry prisms under compression: Review and prospects. *Cement and Concrete Composites, 29(3)*, 181-192.

[315] Moslem, K. and Trifunac, M.D. (1986). *Effects of soil structure interaction on the response of buildings during strong earthquake ground motions*. Report No. 86-04, Dept. of Civil Eng., Univ. of Southern California, Los Angeles, California, U.S.A.

[316] Modena, C., Rossi, P. P., Zonta, D. (1997). Static and dynamic investigation on the roman amphitheatre (Arena) in Verona. *Proc., IABSE Int. Colloquium, Inspection and Monitoring of the Architectural Heritage*, Seriate, 1997, Ferrari Ed., Clusone (BG), pp. 73-80.

[317] Molins, C. (1996). Un modelo para el análisis del comportamiento resistente de construcciones de obra de fábrica. *PhD Thesis, Technical University of Catalonia, Spain.*

[318] Molins, C. & Roca, P. (1998). Capacity of masonry arches and spatial frames. ASCE *Journal of Structural Engineering, 124(6)*: 653-663.

[319] Moon, L. M., Dizhur, D., Ingham, J. M., & Griffith, M. C. (2012). Seismic performance of masonry buildings in the Christchurch earthquakes 2010-2011: A progress report. In *Australian Earthquake Engineering Society 2012 Conference*.

[320] Mosoarca, M. & Gioncu, V. (2013). Failure mechanisms for historical religious buildings in Romanian seismic areas. *Journal of Cultural Heritage, 14(3)*, 65-72.

[321] Mottershead, J. E. & Friswell, M. I. (1993). Model updating in structural dynamics: a survey*. Journal of Sound and Vibration, 167(2)*, 347-375.

[322] Moropoulou, A., Labropoulos, K. C., Delegou, E. T., Karoglou, M., & Bakolas, A. (2013). Non-destructive techniques as a tool for the protection of built cultural heritage. *Construction and Building Materials, 48*, 1222-1239.

[323] MSJC (Masonry Standards Joint Committee) (2002). *Building code requirements for masonry structures, ACI 530-02/ASCE 5-02/TMS 402-02,* American Concrete Institute, Structural Engineering Institute of the American Society of Civil Engineers, The Masonry Society, Detroit.

[324] Mulhern, M.R and Maley, R.P. (1973). *Building Period Measurements before, during and after the San Fernando, California, Earthquake of February 9, 1971*. U.S. Depart.

of Commence, National Oceanic and Atmospheric Administration, Washington, D.C., U.S.A., Vol. 1, Part B, pp. 725-733.

[325] Murcia, J. (2008). Seismic Analysis of Santa Maria del Mar Church in Barcelona. *MSc Thesis, Technical university of Catalonia, Spain.*

[326] Murcia, J., Das, A. K., Roca, P., & Cervera, M. (2009). Seismic safety analysis of historical masonry structures using a damage constitutive model. 2nd International Conference on Computational Methods in Structural Dynamics and Earthquake Engineering, COMPDYN09, 22-24 June, Rhodes, Greece.

[327] Mwafy, A. M. & Elnashai, A. S. (2001). Static pushover versus dynamic collapse analysis of RC buildings. *Engineering structures, 23(5)*, 407-424.

**N**

[328] Nasser, M. A. (2001). Dynamic analysis of arched style masonry structures. In *IMAC-XIX: A Conference on Structural Dynamics*, (Vol. 2, pp. 1363-1369).

[329] NCSE-02 (2002). *Norma de construcción sismo resistente – Parte general y edificación*. (In Spanish).

[330] Newmark, N. M. (1959). A method of computation for structural dynamics. In *Proc. ASCE* (Vol. 85, No. 3, pp. 67-94).

[331] NIKER (2010-2012). *New Integrated Knowledge-based approaches to the protection of cultural heritage from Earthquake-induced Risk*. Funded by EC under the 7th Framework program, contract n. ENV2009-1-GA244123. www.niker.eu.

[332] NTC (2008). *Norme Tecniche per le Costruzioni*, D.M. 14 gennaio 2008, Suppl. ord. n° 30 alla G.U. n.29 del 4/02/2008.

**O**

[333] Ochsendorf, J. A., Hernando, J. I. & Huerta, S. (2004). Collapse of masonry buttresses. *Journal of Architectural Engineering*, 10(3), 88-97.

[334] O'Donnell, A. P., Beltsar, O. A., Kurama, Y. C., Kalkan, E. & Taflanidis, A. A. (2011). Evaluation of ground motion scaling methods for analysis of structural systems. *In ASCE Structures Congress*.

[335] Oliveira, C. S., Çaktı, E., Stengel, D., & Branco, M. (2012). Minaret behavior under earthquake loading: The case of historical Istanbul. *Earthquake Engineering & Structural Dynamics, 41(1)*, 19-39.

[336] Oliveto, G. & Greco, A. (2002). Some observations on the characterization of structural damping. *Journal of Sound and Vibration, 256(3)*, 391-415.

[337] Olivito, R. S. & Zuccarello, F. A. (2009). Quality control and monitoring of FRP applications to masonry structures. *Strain, 45(4)*, 340-348.

[338] ONSITEFORMASONRY (2001-2004). *On-site investigation techniques for the structural evaluation of historic masonry buildings*, Funded by EC under the 5th Framework program, contract n contract no: EVK4-CT-2001-00060.

[339] O.P.C.M. 3274 (2003). *Primi elementi in materia di criteri generali per la classificazione sismica del territorio nazionale e di normative tecniche per le costruzioni in zona sismica*, G.U. n. 105, 8 Maggio 2003 (in Italian).

[340] O.P.C.M 3274 (2004) *Primi elementi in materia di criteri generali per la classificazione sismica del territorio nazionale e di normative tecniche per le costruzioni in zona sísmica* (in Italian).

[341] O.P.C.M 3431 (2005). Ulteriori modifiche ed integrazioni alla Ordinanza PCM 3274 *Primi Elementi in Materia di Criteri Generali per la Classificazione Sismica del Territorio Nazionale e di Normative Tecniche per le Costruzioni in Zona Sismica* (in Italian).

[342] Orfanidis, S. J. (1996). *Introduction to signal processing*. Englewood Cliffs, N.J.: Prentice Hall.

[343] Otani, S. (1980). Nonlinear dynamic analysis of reinforced concrete building structures. *Canadian Journal of Civil Engineering, 7(2)*, 333-344.

[344] Ozturk, M. (2013). Field Reconnaissance of the October 23, 2011 Van, Turkey Earthquake (Mw= 7.2): Lessons Learned from Structural Damages. *Journal of Performance of Constructed Facilities.*

**P**

[345] Pallas-Areny, R. (1999). Amplifiers and signal conditioners. In Webster, J. G. (Ed-in-Chief), *The Measurement, Instrumentation, and Sensors Handbook*. Boca Raton, Florida: CRC Press LLC.

[346] Paoletti, D., Ambrosini, D., Sfarra, S., & Bisegna, F. (2013). Preventive thermographic diagnosis of historical buildings for consolidation. *Journal of Cultural Heritage, 14(2)*, 116-121.

[347] Parloo, E., Guillaume, P. & Van Overmeire, M. (2002). Sensitivity-based operational mode shape normalisation. *Mechanical Systems and Signal Processing, 16(5)*, 757-767.

[348] Pau, A. & Vestroni, F. (2008). Vibration analysis and dynamic characterization of the Colosseum. *Structural Control and Health Monitoring: 15 (8)*, pp. 1105-1121.

[349] Pau, A., & Vestroni, F. (2011). Dynamic characterization of ancient masonry structures. *Advances in Vibration Analysis Research*, Intech, 213-230.

[350] Pau, A. & Vestroni, F. (2013). Vibration assessment and structural monitoring of the Basilica of Maxentius in Rome. *Mechanical Systems and Signal Processing, 41(1)*, 454-466.

[351] Paupério, E., Romao, X.& Costa, A. (2012). Seismic damage to churches: observations from the 2011 Lorca (Spain) earthquake. In *Proc. of 15th World Conference on Earthquake Engineering,* 24-28 September, Lisbon. Portugal.

[352] Peeters, B. & De Roeck, G. (1999). Reference-based stochastic subspace identification for output-only modal analysis. *Mechanical Systems and Signal Processing, 13(6)*: 855-878.

[353] Peeters, B. (2000). System identification and damage detection in civil engineering. *PhD Thesis, Katholieke Universiteit Leuven, Belgium.*

[354] Peeters, B. and De Roeck, G. (2001). Stochastic system identification for operational modal analysis: a review. *Journal of Dynamic Systems, Measurement, and Control, 123(4)*, pp.659--667.

[355] Peeters, B., Van der Auweraer, H., Guillaume, P. & Leuridan, J. (2004). The PolyMAX Frequency-Domain Method: a new standard for modal parameters estimation? *Shock and Vibration (11)*, 395-409.

[356] Peeters, B. & Van der Auweraer, H. (2005). PolyMAX: a revolution in operational modal analysis. In: Brinker R, Møller N (Eds.) *1st International Operational Modal Analysis Conference (IOMAC)*, 26-27 April, Copenhagen, Denmark. , pp 41–52.

[357] Peeters, B., El-kafafy, M. & Guillaume, P., (2012). The new PolyMAX Plus method: confident modal parameter estimation even in very noisy cases. *International Conference on Noise and Vibration Engineering*, 17-19 September, Leuven, Beligum.

[358] Pelà, L., Aprile, A., Benedetti, A. (2009). Seismic assessment of masonry arch bridges, *Engineering Structures, 31*, pp. 1777-1788.

[359] Pelá, L., Cervera, M. & Roca, P. (2011). Continuum model for inealstic behaviour of masonry. *Congresso dell'Associazione Italiana di Meccanica Teorica e Applicata,* 12-15 September, Bologna, Italy.

[360] Peña, F. (2004). Correlation between tensile strength and the collapse mechanism of brick masonry constructions. *Proc. of 4th Int. Seminar on Structural Analysis of Historical Constructions*, 10-13 November, Padova, Italy, pp 1165-1174.

[361] Peña, F., Lourenço, P. B., Mendes, N. & Oliveira, D. V. (2010). Numerical models for the seismic assessment of an old masonry tower. *Engineering Structures, 32(5),* 1466-1478.

[362] Pereira, A. S. (2009). The opportunity of a disaster: the economic impact of the 1755 Lisbon earthquake. *The Journal of Economic History, 69(02)*, 466-499.

[363] Pérez-Gracia ,V.; Caselles ,J.O.; Clapes , J.; Osorio ,R.; Martínez ,G.; Canas ,J.A. (2009). Integrated near-surface geophysical survey of the Cathedral of Mallorca. *Journal of Archaeological Science, 36(7),* Pages 1289-1299.

[364] Pérez-Gracia, V., Caselles, J., Clapés, J., Martínez, G. & Osorio, R. (2013). Non-destructive analysis in cultural heritage buildings: Evaluating the Mallorca cathedral supporting structures. *NDT and E International, 59*, pp.40-47.

[365] PERPETUATE (2010-2012). *Performance-based approach to the earthquake protection of cultural heritage in European and Mediterranean countries*. Funded by EC under the 7th Framework program, grant agreement n° 244229.

[366] Petersson, P. E. (1982). *Comments on the method of determining the fracture energy of concrete by means of three-point bend tests on notched beams*. Report TVBM-3011, Lund Institute of Technology, Lund, Sweden.

[367] PIET-70 (1971). *Masonry works*. Prescriptions from Instituto Eduardo Torroja. Higher Council of Scientific Researches, CSIC, Madrid.

[368] Planas, J., Elices, M. & Guinea, G. V. (1992). Measurement of the fracture energy using three-point bend tests: Part 2—Influence of bulk energy dissipation. *Materials and Structures, 25(5)*, 305-312.

[369] Pluijm, R. van der. (1997). Non-linear behaviour of masonry under tension, *Heron, 42(1)*, 25-54.

[370] Pluijm, R. van der. (1999). Out of plane bending of masonry behaviour and strength. *PhD Thesis, Delft University of Technology, The Netherlands.*

[371] Potter, C. (2011). Seismic analysis of a typical masonry building from Barcelona's Eixample district. *MSc Thesis, Technical university of Catalonia, Spain.*

[372] Prabhu, S. (2011). Structural health monitoring of historic masonry monuments. *MSc Thesis, Clemson University, USA.*

[373] Prabhu, S. and Atamturktur, S. (2013). Selection of optimal sensor locations based on modified effective independence method: case study on a gothic revival cathedral. *Journal of Architectural Engineering, 19(4)*, 288-301.

[374] Prabhu, S., Atamturktur, S., Brosnan, D., Messier, P., & Dorrance, R. (2014). Foundation settlement analysis of Fort Sumter National Monument: Model development and predictive assessment. *Engineering Structures, 65*, 1-12.

[375] Prevosto, M. (1982). Algorithmes d'identification des caractéristiques vibratoires de structures mécaniques complexes. *Ph.D. Thesis, Université de Rennes I, France.*

[376] PROHITECH (2004-2008). *Earthquake PROtection of HIstorical Buildings by Reversible Mixed TECHnologies*. Funded by EC under the 6th Framework program grant no. INCO-CT-2004- 509119.

[377] Pusey, H. C. (2008). An historic view of shock and vibration. In *Proc. of the 26th International Modal Analysis Conference (IMAC)*, Orlando, Florida, 2-5 February.

**Q**

[378] Quelhas, B., Cantini, L., Guedes, J. M., da Porto, F. & Almeida, C. (2014). Characterization and Reinforcement of Stone Masonry Walls. In *Structural Rehabilitation of Old Buildings* (pp. 131-155). Springer Berlin Heidelberg.

**R**

[379] Rad, S. Z. (1997). Methods for updating numerical models in structural dynamics. *PhD Thesis, Imperial College of Science, Technology and Medicine, University of London, UK.*

[380] Rainieri, C., Fabbrocino, G., & Verderame, G. M. (2013). Non-destructive characterization and dynamic identification of a modern heritage building for serviceability seismic analyses. *NDT and E International, 60*, 17-31.

[381] Ramos, L. F. (2002). Experimental and numerical analysis of historical masonry structures. *MSc Thesis, University of Minho, Portugal*.

[382] Ramos, L. F. & Lourenço, P. B. (2003). Seismic analysis of the old town buildings in "Baixa Pombalina" - Lisbon, Portugal. *9th North American masonry conference.* June 1-4, Clemson, South Carolina, USA.

[383] Ramos, L. F. & Lourenço, P. B. (2004). Modeling and vulnerability of historical city centers in seismic areas: a case study in Lisbon. *Engineering structures, 26(9),* 1295-1310.

[384] Ramos, L. F. & Lourenço, P. B. (2005). Seismic analysis of one heritage compound building of the old Lisbon town. *International conference on 250th anniversary of the 1755 Lisbon earthquake*. LNEC, Lisbon, Portugal. p. 362-368.

[385] Ramos L, Casarin F, Algeri C, Lourenço PB & Modena C. (2006a). Investigation techniques carried out on the Qutb Minar, New Delhi, India. In Lourenço, P. B., Roca, P., Modena, C. & Agrawal, S. (Eds.) *Structural analysis of historical constructions*, pp. 633 – 640.

[386] Ramos L. F. (2007). Damage identification on masonry structures based on vibration signatures. *PhD Thesis, University of Minho, Portugal.*

[387] Ramos, L., Mevel, L., Lourenço, P. B., & De Roeck, G. (2008a). Dynamic monitoring of historical masonry structures for damage identification. In *Proc. of the 26th International Modal Analysis Conference (IMAC)*, Orlando, Fl, US, 4-7 February.

[388] Ramos, L.F., Lourenço, P.B, De Roeck, G, & Campos-Costa, A. (2008b). Damage identification in masonry structures with vibration measurements. In D'Ayala, D. and Fodde, E. (Eds.) *Structural Analysis of Historical Construction*. CRC Press Balkema, 311-319.

[389] Ramos, L.F., Marques, L., Lourenço, P.B., De Roeck, G. Campos-Costa, A. & Roque, J. (2010a). Monitoring historical masonry structures with operational modal analysis: two case studies. *Mechanical systems and signal processing: 24 (5)*, pp. 1291–1305.

[390] Ramos, L. F., Alaboz, M., Aguilar, R., & Lourenço, P. B. (2011). Dynamic identification and FE updating of S. Torcato Church, Portugal. *Dynamics of Civil Sturctures. Volume 4*, 71-80.

[391] Ramos, L. & Lourenço, P. B. (2011). Dynamic identification and monitoring of cultural heritage buildings. *Proc. Seismic Protection of Cultural Heritage*, October 31-November 1, Antalya, Turkey.

[392] Ramos, L. F., Manning, E., Fernandes, F., Fangueiro, R., Azenha, M., Cruz, J., & Sousa, C. (2013a). Tube-jack testing for irregular masonry walls: Prototype development and testing. *NDT and E International, 58*, 24-35.

[393] Ramos, L. F., Aguilar, R., Lourenço, P. B., & Moreira, S. (2013b). Dynamic structural health monitoring of Saint Torcato church. *Mechanical Systems and Signal Processing, 35(1)*, 1-15.

[394] Rao, S. (2005). *The finite element method in engineering*. 1st edition. Amsterdam: Elsevier/Butterworth Heinemann.

[395] Reist, P. (2013). *Signals and Systems*. Course notes. Retrieved from http://www.idsc.ethz.ch/Courses/signals_and_systems/LectureNotes/2013_SS_Le -cture8. pdf

[396] Ren, W. X. & Zong, Z. H. (2004). Output-only modal parameter identification of civil engineering structures. *Structural Engineering and Mechanics, 17(3-4)*, 429-444.

[397] Resemini S (2003). Seismic vulnerability of masonry arch railway bridges. *PhD Thesis, Università di Genova, Italy* (In Italian).

[398] RESNET (2012). *RESNET Interim guidelines for thermographic inspections of buildings.*

[399] Reynolds, P. (2008). Dynamic testing and monitoring of civil engineering structures. *Experimental Techniques, 32(6)*: 54-57.

[400] RILEM (1985). RILEM TC50-FMC. Determination of fracture energy of mortar and concrete by means of three-point bend tests on notched beams. *Materials and Structures, 18(106)*, 285–290.

[401] RILEM (1994). *RILEM TC. 76-LUM. Diagonal tensile strength tests of small wall specimens, 1991*. In RILEM, Recommendations for the Testing and Use of Constructions Materials. London: Eand FN SPON, 488–489.

[402] RILEM (2004a). *RILEM Recommendation MDT.D.4: In-situ stress tests based on the flat-jack.*

[403] RILEM (2004b). *RILEM Recommendation MDT.D.5- In-situ stress- strain behavior tests based on the flat-jack*.

[404] RISK-UE (2001-2004). *An advanced approach to earthquake risk scenarios with applications to different European towns*. Funded by EC, contract n. EVK4-CT-2000-00014.

[405] Rivera, D., Meli, R., Sánchez, R. & Orozco, B. (2008). Evaluation of the measured seismic response of the Mexico City Cathedral. *Earthquake Engineering and Structural Dynamics, 37(10)*, 1249-1268.

[406] Roca, P. & Molins, C. (1997). Dynamic load tests on masonry structures as inspection technique. *Inspection and Monitoring of the Architectural Heritage. IABSE 1997*. Italian Group of IABSE Ferrari Editrice, p. 133-140.

[407] Roca, P. (2001). Studies on the structure of Gothic cathedrals. In: Lourenço, P.B. and Roca, P. (Eds.) *Historical Constructions*, University of Minho, Guimarães, pp. 71-90.

[408] Roca, P. & González, J. L. (2001). Structure, history and morphology: The case study of the upper flying arches of Mallorca Cathedral. *UNESCO Millenium Conference*, Paris, France.

[409] Roca, P., & Lodos, J. C. (2001). Análisis estructural de catedrales góticas. *OP Ingeniería y Territorio, (56)*, 38-47.

[410] Roca, P. (2004). *Detailed description of Mallorca cathedral*. Report in the project Improving the seismic resistance of cultural heritage buildings. Funded by EU-INDIA Economic Cross Cultural Programme, contract n. ALA/95/23/2003/077-122.

[411] Roca, P., Clapés, J, Caselles, O., Vendrell, M., Giráldez, P. & Sánchez-Beitia, S. (2008). Contribution of inspection techniques to the assessment of historical structures. *International RILEM Conference*, 1-2 September, Como Lake, Italy.

[412] Roca, P., Vacas, A., Cuzzila, R., Murcia-Delso, J., & Das, A. K. (2009). Response of Gothic churches in moderate seismic Mediterranean regions. *ISCARSAH Symposium on Assessment and Strengthening of Historical Stone Masonry Constructions Subjected to Seismic Action*, Mostar, Bosnia and Herzegovina, 12th July.

[413] Roca, P., Cervera, M., Gariup, G. & Pelá, L. (2010). Structural analysis of masonry historical constructions. Classical and advanced approaches. *Archives of Computational Methods in Engineering, 17(3)*, 299-325.

[414] Roca, P., Cervera, M., Pelà, L., Clemente, R., Chiumenti, M (2012a). Structural assessment of Mallorca cathedral. *8th International Conference on Structural Analysis of Historical Construction*. 15-17 October 2012, Wrocław, Poland.

[415] Roca, P., Cervera, M., Pelà, L., Clemente, R. (2012b). Construction process numerical simulation and seismic assessment of Mallorca Cathedral. *15th International Brick and Block Masonry Conference,* 3-6 June, Florianópolis, Brazil.

[416] Roca, P., Cervera, M., Pelá, L., Clemente, R. and Chiumenti, M. (2012c). Viscoelasticity and damage model for creep behavior of historical masonry structures. *Open Civil Engineering Journal, 6*, pp.188-199.

[417] Roca, P., Cervera, M., Pelà, L., Clemente, R., & Chiumenti, M. (2013). Continuum FE models for the analysis of Mallorca Cathedral. *Engineering Structures, 46*, 653-670.

[418] Rodriguez, P. (2009). Lay-out of seismic strengthening of Mallorca cathedral, *MSc Thesis, Technical University of Catalonia, Spain.*

[419] Romao, X., Costa, A. A., Paupério, E., Rodrigues, H., Vicente, R., Varum, H., & Costa, A. (2013). Field observations and interpretation of the structural performance of constructions after the 11 May 2011 Lorca earthquake. *Engineering Failure Analysis, 34*, 670-692.

[420] Ross, R. G., (1971). Synthesis of stiffness and mass matrix from experimental vibration modes. National Aeronautic and Space Engineering and Manufacturing Meeting, *Society of Automotive Engineers*, Los Angeles, CA, pp. 2627-2635.

[421] Rossi, P.P. (1982), Analysis of mechanical characteristics of brick masonry tested by means of in situ tests. In *Proc. of the 6th International Brick and Block Masonry Conference*, 16-19 May, Rome, Italy.

[422] Rubió, J. (1912). *Lecture on the organic, mechanical and construction concepts of Mallorca Cathedral*, Anuario de la Asociación de Arquitectos de Cataluña, Barcelona, (in Spanish).

[423] Russo, S. (2013a). On the monitoring of historic Anime Sante church damaged by earthquake in L'Aquila. *Structural Control and Health Monitoring, 20 (9)*, pp. 1226--1239.

**S**

[424] Saiidi, M. & Sozen, M. A. (1981). Simple nonlinear seismic analysis of R/C structures. *Journal of the Structural Division, ASCE 107(5)*:937–51.

[425] Salas, A. (2002). Structural study of the typical bays of Mallorca cathedral. *Graduation Thesis, Technical University of Catalonia, Spain*. (in Spanish)

[426] Salawu, O. S. & Williams, C. (1995). Bridge assessment using forced-vibration testing. *Journal of Structural Engineering, 121(2)*, 161-173.

[427] Saloustros, S. (2013). Structural analysis of the church of the Poblet Monastery. *MSc Thesis, Technical university of Catalonia, Spain.*

[428] Slastan, J. A. & Foissner P. (1995). Masonry building dynamic characteristics evaluation by means of ambient vibration. In *Proc. of the 10th European Conference on Earthquake Engineering*, Vienna, Austria.

[429] Sandrolini, F., & Franzoni, E. (2006). An operative protocol for reliable measurements of moisture in porous materials of ancient buildings. *Build. Environ., 41(10)*, 1372-1380.

[430] Schlangen, E. (1993). Experimental and numerical analysis of fracture processes in concrete. *Heron, 38 (2).*

[431] SeisGram2K Seismogram Viewer v5.3.4X16 (10th Aug. 2009) (BETA) Copyright © 2000-2009 Anthony Lomax (www.alomax.net).

[432] Sena-Cruz, J., Ferreira, R. M., Ramos, L. F., Fernandes, F., Miranda, T., & Castro, F. (2013). Luiz Bandeira bridge: assessment of a historical reinforced concrete (RC) bridge. *International Journal of Architectural Heritage, 7(6)*, 628-652.

[433] Sepe, V., Speranza, E. & Viskovic, A. (2008). A method for large-scale vulnerability assessment of historic towers. *Structural Control and Health Monitoring, 15(3)*, 389-415.

[434] SEVERES (2010-2012). *Seismic vulnerability of old masony buildings*. Funded by Portuguese Foundation for Science and Technology, contract n. PTDC/ECM/100872/2008, www.severes.org.

[435] Sezen, H. & Dogangun, A. (2012). Seismic performance of historical and monumental structures. In Sezen, H (Eds.) *Earthquake Engineering*.

[436] Sharma, G (2014). *Digital signal processing*. Course notes. Retrieved from nptel.ac.in/courses/Webcourse-contents/IIT-KANPUR/Digi_Sigi_Pro/ui/TOC.htm.

[437] Shih, C.Y., Tsuei, Y.G., Allemang, R.J. & Brown, D.L. (1988b). Complex mode indicator function and its application to spatial domain parameter estimation. *Mechanical Systems and Signal Processing 2 (4)*, 367–377.

[438] Sigmund, V. A. & Herman, K., (1998). Dynamic characteristics as indicators of structural integrity. *ABSE Colloquium, IABSE Report Volume 77*. Berlin

[439] Sidhu, J. & Ewins, D. J (1984). Correlation of finite element and modal test studies of a practical structure. In *Proc. of 2nd International Modal Analysis Conference (IMAC)*, Orlando, Florida, pp. 756-762.

[440] Silva, B., Dalla Benetta, M., Da Porto, F. & Modena, C. (2014a). Experimental assessment of in-plane behaviour of three-leaf stone masonry walls. *Construction and Building Materials, 53*, 149-161.

[441] Silva, B., Pigouni, A., Valluzzi, M. & Modena, C. (2014b). Calibration of analytical formulations predicting compressive strength in consolidated three-leaf masonry walls. *Construction and Building Materials, 64*, 28-38.

[442] Silva, V. C., Lourenço, P.B., Ramos, L.F., & Mesquita, C.G. (2001). Accounting for the "block effect" in structural interventions in Lisbon's old "Pombaline" downtown buildings. In: Lourenço, P.B. and Roca, P. (Eds.) *Historical Constructions*, University of Minho, Guimarães, pp. 943-952.

[443] Sinha, J. K. (2005). On standardization of calibration procedure for accelerometer. *Journal of Sound and Vibration, 286(1)*, 417-427.

[444] Smith, S. W. (2002). *The scientist and engineer's guide to digital signal processing*. San Diego, Calif.: California Technical Pub.

[445] SMOOHS (2008-2011). *Smart monitoring of historic structures*. Funded by EC under the 7th Framework program, grant agreement n. 212939. www.smoohs.eu.

[446] Sorrentino, L., Liberatore, L., Decanini, L. D., & Liberatore, D. (2013). The performance of churches in the 2012 Emilia earthquakes. *Bulletin of Earthquake Engineering*, 1-33.

[447] Stuart-Watson, D. (2006). A simple force feedback accelerometer based on a tuning fork displacement sensor. PhD Thesis, University of Cape Town, South-Africa.

[448] Sydenham, P. H. & Thorn, R. (2005). *Handbook of measuring system design*. Chichester, England: Wiley.

**T**

[449] Tapan, M., Comert, M., Demir, C., Sayan, Y., Orakcal, K., & Ilki, A. (2013). Failures of structures during the October 23, 2011 Tabanlı (Van) and November 9, 2011 Edremit (Van) earthquakes in Turkey. *Engineering Failure Analysis, 34*, 606-628.

[450] Tavukçuoğlu, A., Akevren, S. & Grinzato, E. (2010). In situ examination of structural cracks at historic masonry structures by quantitative infrared thermography and ultrasonic testing. *Journal of Modern Optics, 57(18)*, 1779.

[451] Themelis, S. (2008). Pushover analysis for seismic assessment and design of structures. *PhD Thesis, Heriot-Watt University, UK.*

[452] Tolles, E. L., Kimbro, E. E. & Ginell, W. S. (2003). *Planning and engineering guidelines for the seismic retrofitting of historic adobe structures*. Getty Publications.

[453] Trifunac, M.D. (1970a). *Ambient Vibration Test of a 39-Story Steel Frame Building. Report EERL 70-02*, Earthq. Eng. Res. Lab., Calif. Institute of Tech., Pasadena, California, U.S.A.

[454] Trifunac, M.D. (1970b). Wind and Microtremors Induced Vibrations of a 22-Story Steel Frame Building. Report. EERL 70-011, Earthq. Eng. Res. Lab., Calif. Institute of Tech., Pasadena, California, U.S.A.

[455] Trifunac, M.D. (1972). "Comparison between Ambient and Forced Vibration Experiments, *Earthquake Eng. and Structural Dynamics, Vol. 1*, pp. 133-150.

[456] Trujillo, A. (2009). Stability analysis of Famagusta Churches: Saint George of the Latins. *MSc Thesis, University of Minho, Portugal.*

[457] Tso, W. K. & Moghadam, A. S. (1998). Pushover procedure for seismic analysis of buildings. Progress in Structural Engineering and Materials, 1(3), 337-344.

[458] Turk, A. M. & Cosgun, C. (2012). Seismic behaviour and retrofit of historic masonry minaret. *Gradevinar, 64(1)*, pp. 39–45.

[459] Turk, A. M. (2013). Seismic response analysis of masonry minaret and possible strengthening by fiber reinforced cementitious matrix (FRCM) materials. *Advances in Materials Science and Engineering, vol. 2013*.

[460] Tzenov, L. & Dimova, S. (1992). Experimental Study of the Church 'Sveta Sofia'. In *Proc. of 10th World Conference on Earthquake Engineering*, Madrid, 19-24 July, pp. 3403-3408.

**U**

[461] Underwood, M. & Keller, T. (2008a). Testing civil structures using multiple shaker excitation techniques. *Sound and Vibration, 42(4)*, 10-15.

[462] Underwood, M. & Keller, T. (2008b). Some applications for the testing of civil structures using multiple shaker excitation techniques. In *Proc. of 26th International Modal Analysis Conference (IMAC)*, Orlando, Florida, 2-5 February.

**V**

[463] Vacas, A. (2009). Análisis sísmico de las catedrales Góticas mediante el método del espectro de la capacidad. *Graduation Thesis, Technical University of Catalonia, Spain.*

[464] Van Overschee, P. & De Moor, B. (1996). *Subspace Identification for Linear Systems*, Kluwer Academic Publishers, Leuven, Belgium.

[465] Verhaegen, M., & Verdult, V. (2007). *Filtering and system identification: a least squares approach*. Cambridge university press.

[466] Vermariën, H., McConnell, E. & Li, Y (1999). Reading/recording devices. In Webster, J. G. (Ed-in-Chief), *The Measurement, Instrumentation, and Sensors Handbook*. Boca Raton, Florida: CRC Press LLC.

[467] Vestroni F., Beolchini G. C., Antonacci E. & Modena C., (1996). Identification of dynamic characteristics of masonry buildings from forced vibration tests. In *Proc. of the 11th World Conference on Earthquake Engineering*, Acapulco, México.

[468] Vidic, T., Fajfar, P. & Fischinger, M. (1994), Consistent inelastic design spectra: strength and displacement. *Earthquake Engineering and Structural Dynamics, 23,* 502-521.

[469] Vijayakumar, A. & Venkatesh babu, D.L. (2011). A Survey of Methodologies for Seismic Evaluation of Building. *Canadian Journal on Environmental, Construction and Civil Engineering: 2(5)*, 50-55.

[470] Villegas, L., lombillo, I. & lópez, F. (2009). The importance of the previous studies in the interventions of refurbishment: a practical case, the major seminar of Comillas (Cantabria, Spain). *The First International Conference on Research in Construction*, 24-26 June, Madrid, Spain.

[471] Votsis, R. A., Kyriakides, N., Chrysostomou, C. Z., Tantele, E. & Demetriou, T. (2012). Ambient vibration testing of two masonry monuments in Cyprus. *Soil Dynamics and Earthquake Engineering, 43*, 58-68.

[472] Votsis, R. A., Kyriakides, N., Tantele, E. & Chrysostomou, C. Z. (2013). Effect of damage on the dynamic characteristics of St. Nicholas cathedral in Cyprus. In *Proc. of ECCOMAS - Conference on Computational Methods in Structural Dynamics and Earthquake Engineering*, Kos Island, Greece, 12-14 June.

**W**

[473] Walker, N. & Nowicki, A. N. (2005). *Infrared Thermography Handbook*. The British Institute of Non-Destructive Testing.

[474] Walter, P. L. (1997). The history of the accelerometer. *Sound and Vibration, 31(3)*, 16-23.

[475] Walter, P. L. (1999). Review: Fifty years plus of accelerometer history for shock and vibration (1940–1996). *Shock and Vibration, 6(4)*, 197-207.

[476] Walter, P. L. (2002). *A history of the origin and evolution of modal transducers*. In SPIE proceedings series. Society of Photo-Optical Instrumentation Engineers.

[477] Ward, H.S. & Crawford, R. (1966). Wind Induced Vibrations and Building Modes. M. *Seism. Soc. Amer., Vol. 50*, pp. 793-813.

[478] Wilson, J. (1999a). A practical approach to vibration detection and measurement. Part 1: physical principles and detection techniques. *Sensors Magazine, 16(2)*.

**X**

[479] Xavier, P. V., & Patrick, O. M. (2001). *Infrared and Thermal Testing For Conservation of Historical Buildings*. ASNT Nondestructive Testing Handbook.

**Z**

[480] Zhang, L., Brincker, R. & Andersen, P. (2005). An overview of operational modal analysis: major development and issues. *1st International Operational Modal Analysis Conference (IOMAC)*, 26-27 April, Copenhagen, Denmark.

[481] Zienkiewicz, O. C. & Taylor, R. L. (2000). *The Finite Element Method*, 5th Edition, Butterworth Heinemann, Oxford.